Metabolic engineering of yeast for production of cyclopropane fatty acids and growth on novel carbon feedstocks

Wei Jiang

M.E. (Biological Engineering)

B.S. (Biological Science)

A thesis submitted for the *degree of Doctor of Philosophy* at

Monash University in 2021

Department of Chemical and Biological Engineering

Copyright notice

This page is intentionally blank

Abstract

Cyclopropane fatty acids (CFAs) as a high-value chemical have a wide range of potential applications, such as lubricants, protective coatings, plastics, and cosmetics due to their unique characteristics. Although in nature many organisms can produce CFAs at various concentrations, they are not suitable as high-efficiency production hosts. While CFAs can be naturally produced in the platform organism *Escherichia coli*, CFAs are not accumulated at high concentrations in lipid storages. Therefore, the challenge is to engineer a suitable cell factory to produce CFAs. Yeasts like S*accharomyces cerevisiae* and *Yarrowia lipolytica* are more effective hosts for lipid production because the synthetic steps and routes of fatty acids in yeast are shorter and more direct, which can convert carbon substrates to fatty acids and fatty acid derivatives more efficiently and they store fatty acids in triacylglycerols. In order to design an effective metabolic engineering strategy for heterologous CFAs production by yeast, CFAs metabolism in yeast was deeply studied. The location of CFAs biosynthesis in yeast was studied and the relationship between *E. coli cfa* synthase and yeast membranes was revealed. The effect of expression of *E. coli cfa* synthase on the composition of yeast membranes was also investigated. In addition, the substrates of *E. coli cfa* synthase in yeast were also identified. Based on this knowledge, a metabolic engineering strategy that redirected CFAs flux toward triacylglycerols to increase CFAs turnover was proposed and applied in *S. cerevisiae* and *Y. lipolytica*, which included overcoming substrate limitations for cyclopropane-fatty-acyl-phospholipid synthase, CFAs turnover to triacylglycerols and preventing the degradation of triacylglycerols.

Furthermore, to broaden the carbon feedstock base for yeast from agriculture-based sugars to non-food derived C1 compounds, a pathway for engineering methanol utilisation was designed and introduced into *Y. lipolytica*. Compared with traditional carbon sources like

glucose and glycerol, methanol diversifies the choices of feedstock for culturing, reduces the requirement for culture media sterilisation and can take advantage of the surplus of methane/methanol arising from shale oil mining. Also, it has good availability for biomanufacturing and richer energy. Here, a strategy of rational design was initiated *in silico* to select appropriate methanol assimilation pathway genes from methylotrophic yeast and bacteria, these were tested under various metabolic engineering approaches in *Y. lipolytica* to assimilate methanol as a carbon source. Finally, methanol utilisation as an auxiliary carbon source (with yeast extract) for growth and bioproduction was demonstrated in engineered *Y. lipolytica* via ^{13}C tracer analysis from ^{13}C-methanol substrate.

Declaration

This thesis is an original work of my research and contains no material which has been accepted for the award of any other degree or diploma at any university or equivalent institution and that, to the best of my knowledge and belief, this thesis contains no material previously published or written by another person, except where due reference is made in the text of the thesis.

Signature: ..Wei Jiang...

Print Name: Wei Jiang…….

Date: 18/11/2021…….

Publications during enrolment

Published or submitted articles (included in this thesis)

1. Wei Jiang, David Hernández Villamor, Huadong Peng, Jian Chen, Long Liu, Victoria Haritos, Rodrigo Ledesma-Amaro*. (2021). Metabolic Engineering Strategies to enable microbial utilization of C1 feedstocks. Nature Chemical Biology, 17, 845–855 https://doi.org/10.1038/s41589-021-00836-0

2. Wei Jiang, Huadong Peng, Rodrigo Ledesma-Amaro, Victoria Haritos*. (2021). Metabolic Engineering of Yeast for Enhanced Natural and Exotic Fatty Acid Production. Emerging Technologies for Biorefineries, Biofuels, and Value-Added Commodities, Springer: 207-228. https://doi.org/10.1007/978-3-030-65584-6_9

Acknowledgments

Choosing metabolic engineering as the research direction of my Ph.D. was a coincidence. Throughout close to four years of continuous studying, I gradually understood the importance of this research field, and now find that I have a keen interest in this research field. I am really glad I had the opportunity to work in this field that is closely related to people's lives and can impact the future of our planet. Although my Ph.D. was not even 4 years log, this time has been very fulfilling. I have gained a lot.

First, I would like to express my deep gratitude to my supervisor Professor Victoria Haritos, who always offered unconditional help and support during times of difficulty and despair. Regardless of the problem at hand, whether personal or technical, she is always there with an attentive ear and thoughtful advice. I attribute everything from my personal growth, current research ability and Ph.D. accomplishments to her. I consider myself to be very lucky for being her student, her everlasting effect will resonate with me for many years to come. Thank you, Victoria.

I would like to also thank my co-supervisor Dr. Rodrigo Ledesma Amaro. I'm extremely grateful for being given the opportunity by him to move to the UK and be part of his lab at Imperial College London. The experience of working there helped expand my intellectual horizon and allowed me to experience different kinds of research for the first time. Also, with the outbreak of the COVID-19 pandemic, I was not able to return to Australia due to closed borders. Because of his support and help, I can finish my Ph.D. project at Imperial College London. It's all thanks to him.

I would also like to thank my co-supervisor Dr. Lizhong He for his guidance and help during my first year of Ph.D. at Monash. Asides from being a great mentor, he gave me a lot of useful advice on experiment design and development.

Of course, this goes without saying. I would like to thank my husband Huadong Peng and my parents for their constant encouragement throughout my Ph.D.

I'm really thankful for my friends Alicia Graham and Mohamed Almarei. They allowed me to value the importance of friendship during hardship.

In addition, I would like to thank Jingjing Liu and Lucas Coppens for their contributions to my project.

And also, I would like to thank all Haritos group members and Ledesma Amaro group members for the great time we had together.

Finally, I would like to thank the postgraduate scholarships (MGS & MIPRS) and graduate research international travel award (GRITA) from Monash University for sponsoring me during this Ph.D.

List of Abbreviations

ACS, acetyl-CoA synthetase
Adh, alcohol dehydrogenase
AdoMet, S-adenosylmethionine (
AtDGAT1, diacylglycerol acyltransferase from *Arabidopsis thaliana*
AtLACS: long-chain acyl-CoA synthetase from *Arabidopsis thaliana*,
Aox, alcohol oxidase
Cat, catalase
CBB, Calvin Benson–Bassham cycle
CFA, cyclopropane fatty acid
Das, dihydroxyacetone synthase
Dak, dihydroxyacetone kinase
DAG, diacylglycerol
DC/HB, dicarboxylate/4-hydroxybutyrate cycle,
DHA, dihydroxyacetone
DHAP, dihydroxyacetone phosphate
DuLACS, long-chain acyl-CoA synthetase from *Durio zibethinus*
DGA, diacylglycerol acyltransferase
E4P, erythrose-4-phosphate
FA, fatty acid
FadD: fatty acyl-CoA synthetase from *Sinorhizobium meliloti*,
FAEEs, fatty acid ethyl esters
Fba, bisphosphatase
FBP1, Fructose-1,6-bisphosphatase
Fdh, formate dehydrogenase
F_6P, fructose 6-phosphate
$F_{1,6}P$, fructose 1,6-bisphosphate
Fld, formaldehyde dehydrogenase
G3P, glyceraldehyde 3-phosphate
GC-FID, gas chromatography with flame ionisation
gpd1: glycerol-3-phosphate dehydrogenase
H6P, Hexulose 6-phosphate
Hps, 3-hexulose-6-phosphate synthase
HPLC, High-performance liquid chromatography
3-HP, 3-hydroxypropionate bicycle,
Mdh, methanol dehydrogenases
MMOs, methane monooxygenases
OD, optical density
Ole: Δ9 Fatty acid desaturase,
Sam2: S-adenosylmethionine synthase
PA, phosphatidic acid
PC, phosphatidylcholine
PE, phosphatidylethanolamine
Pfk, 6-phosphofructokinase
Phi, 6-phosphate-3-hexuloisomerase
PI, phosphatidylinositol
PL, phospholipid
PPP, pentose phosphate pathway
PS, phosphatidylserine

RA, ricinoleic acid
rGlyP, the reductive glycine pathway
Rki1-2, Ribose-5-phosphate ketol-isomerase
rTCA, reductive tricarboxylic acid cycle
RuMP, ribulose-5 phosphate
R5P, ribose 5-phosphate
Ru5P, fructose ribulose 5-phosphate
SCFAs, short-chain fatty acids
S1,7BP, sedoheptulose-1,7-bisphosphate
S7P, sedoheptulose-7-phosphate
TAG, triacylglycerol
Tkl, transketolase
UFAs, unsaturated fatty acids
XuMP, xylulose monophosphate
Xu5P, xylulose 5-phosphate
Δare1&Δare2: the deletion of acyl-CoA sterol acyltransferase
Δtgl3: the deletion of triglyceride lipase 3,
Δtgl4: the deletion of triglyceride lipase 4
Δpox1: the deletion of fatty-acyl coenzyme A oxidase,

Outline

Table List

Figure List

This page is intentionally blank

CHAPTER 1

INTRODUCTION

This page is intentionally blank

Chapter 1. Introduction

1.1 Introduction and background

The economic, environmental and social sustainability problems caused by the dependency on petroleum have motivated a global shift to affordable, reliable, sustainable, and modern energy sources (Zhang et al., 2011). Facing the drawbacks such as the greenhouse effect and environmental pollution brought by traditional industrial patterns, building resilient infrastructure and promoting inclusive and sustainable industrialization is imperative. Replacement of crude oil-derived fuels and chemicals by the production of biofuels and bioproducts can be an effective strategy to reduce pollution and carbon dioxide emissions (Fortman et al., 2008). In particular, a useful feedstock for biofuels and bioproducts is lipids, consisting mainly of triacylglycerols, as they have high energy density and are readily converted to mono-alkyl esters for use as a diesel substitute. While lipids have excellent commercial utility, they are relatively expensive and in short supply, as there are important applications for lipids in food processing and oleochemicals manufacture. In 2018, the natural fatty acid global market was valued at nearly $13.5 billion and is expected to reach $17.5 billion in 2023 with a compound annual growth rate (CAGR) of 5.4% (Publishing, 2019) (BCC Research LLC, 2019). Therefore, new sources of cost-effective lipids for the production of fuels and chemicals will be in increasingly high demand.

Lipids produced by microbes have huge potential to satisfy the growing demand for bio-based energy-dense hydrocarbons and related natural products (Karmee et al., 2015), especially where their production is based on non-food carbon sources such as lignocellulosic sugars or byproduct streams from biorefineries. Recent advances in microbial metabolic engineering and process technologies have brought us closer to cost-effective yields and diversity of oleaginous products that can support this growing market (Zhou et al., 2018).

Compared with the ubiquitous bacterium *E. coli*, yeasts like *S. cerevisiae* and *Y. lipolytica* are more effective hosts for lipid production because the synthetic steps and routes of fatty acids in yeast are shorter and more direct, which can convert carbon substrates to fatty acids and fatty acids derivative more efficiently (Runguphan & Keasling, 2014; Zhang et al., 2011). Furthermore, yeasts have well-developed mechanisms for enhanced lipid storage within the cell. *S. cerevisiae* is a widely used industrial yeast due to its robustness and good tolerance of harsh industrial conditions (Hong & Nielsen, 2012) and its long history of use in large-scale fermentation to produce ethanol and beverages (Mussatto et al., 2010). The oleaginous yeast *Y. lipolytica* has also had wide use in biotechnology and has several advantages over *S. cerevisiae* in that it naturally stores substantially more lipid within the cell and utilises a broad range of low-cost feedstocks such as glycerol. The yeast holds Generally Recognized as Safe (GRAS) status for the production of citric acid and has been explored for the production of sugar derivatives and nonnative lipid products such as β-carotene and lycopene (Abdel-Mawgoud et al., 2018; Carly et al., 2017; Janek et al., 2017; Kamzolova & Morgunov, 2017; Kildegaard et al., 2017; Ma et al., 2019; Rymowicz et al., 2009).

Another active area of research is in the production of exotic fatty acids and derivatives in yeasts as feedstocks in the production of fine chemicals, medicines, detergents and soaps, lubricants, cosmetics, and skincare products (Liu et al., 2014). These lipids are not naturally present in yeast but are produced through the introduction of genes sourced from other organisms. Therefore, how to construct the efficient heterologous yeast expression system for the production of these exotic fatty acids is the biggest challenge. However, with the development of biotechnology, the challenge can be overcome by advanced synthetic biology tools and effective metabolic strategies. In the first part of our project, we focus on cyclopropane fatty acids (CFAs) as a kind of high-value exotic fatty acids. It has been demonstrated that they and their derivatives have an extensive industrial application, such as

lubricants, protective coatings, plastics, inks, cosmetics, etc. (Bao et al., 2003; Carlsson et al., 2011; Yu et al., 2011). However, the natural production of this unique fatty acid is still quite low, which limits the industrial application of CFAs. Therefore, we will study the mechanism of CFAs synthesis in yeast and attempt to build a suitable microorganism cell factory for CFAs.

Besides the production of biofuels and bioproducts as a promising alternative energy source for petroleum, one carbon (C1) compounds are also a sustainable non-food feedstock for biomanufacturing due to their natural abundance, flexible production processes, and availability as an industrial by-product (Dürre & Eikmanns, 2015; Pfeifenschneider et al., 2017; Strong et al., 2015). Currently, C1 compounds as a feedstock for microbial growth mainly contain carbon monoxide (CO), carbon dioxide (CO2), methane, methanol, formate, and formic acid (Dürre & Eikmanns, 2015; Quayle, 1972).

Although in nature, some native microorganisms can metabolise and grow on C1 compounds as carbon source or energy source, their C1 compound utilisation efficiency is low and product categories they can produce are limited. Also, metabolic regulation and synthetic biology tools for engineering native microorganisms are mostly immature. Therefore, C1 compounds-based native microorganisms cannot meet the requirement of industrial biomanufacturing (Wang et al., 2020; Zhang et al., 2018). The development of synthetic microorganisms based on C1 compounds as a carbon source can provide a potential microbial cell conversion platform to allow the synthesis of value-added chemicals using C1 compounds as a feedstock, which open the door of opportunity to reimagine industrial biomanufacturing away from the dependence on sugar-containing source towards waste and by-products such as greenhouse gases (GHG). However, this emerging field is full of challenges. For example, the function of C1 metabolic pathways imported into industrial

platform organisms like yeasts is much lower than in the original host. Besides, maximising productivity also confronts many difficulties.

In second part of our project, we designed and employed metabolic engineering and synthetic biology strategies to improve the production of exotic, valuable lipids and for the utilisation of methanol as a carbon source in yeasts, including *S. cerevisiae* and *Y. lipolytica*.

1.2 Scope of research

This thesis investigated strategies for cyclopropane fatty acids (CFAs) biosynthesis in yeast *S. cerevisiae* and *Y. lipolytica* and engineering of the yeast *Y. lipolytica* to utilise methanol which is a novel feedstock for this organism.

S. cerevisiae is a mature platform microorganism with abundant synthetic biology tools, which can be easily manipulated whereas *Y. lipolytica* is an oleaginous yeast that can accumulate a large number of lipids. To take advantage of the characteristics of different yeasts, *S. cerevisiae* was selected as a model organism to study CFAs biosynthesis. By contrast, *Y. lipolytica* was adopted as a host to construct the microbial cell factory for CFAs production. To design an effective metabolic engineering strategy for the production of CFAs by yeast, the initial step was to deduce the mechanism of cyclopropane-fatty-acyl-phospholipid synthase in yeast, which provided an important reference for studying other exotic fatty acids in yeast.

In addition, in this thesis, the yeast *Y. lipolytica* was engineered to utilise the C1 compound methanol as the carbon source for the growth and production of the higher-value product. The thesis is not just about shifting the feedstock of microorganisms from the traditional carbohydrate source to a waste source to support the reduction of dependence on fossil energy and pollution reduction but also to provide a potential microbial methanol conversion platform for high-value industrially relevant chemicals

1.3 Research objectives

The first aim of this thesis is to rationally design and implement a metabolic engineering strategy to enhance the production of exotic fatty acids in yeast. The second aim is to enable yeast to utilise methanol as a carbon source for the growth and production of higher value products via metabolic engineering and synthetic biology approaches. These aims were achieved through the following specific objectives:

(1) determine substrates and the location of action of heterologous cyclopropane-fatty-acyl-phospholipid synthase expressed in yeast

(2) Redirect cyclopropane fatty acid flux toward triacylglycerol by lipid pathway engineering

(3) Transfer the metabolic engineering strategy for CFAs production from *S. cerevisiae* into *Y. lipolytica*

(4) Select and heterologously express essential methanol utilisation genes in *Y. lipolytica*

(5) Determine methanol utilisation in engineered *Y. lipolytica* by growth tests and isotopic tracer/mass spectrometry

(6) Measure the production of higher-value products in engineered *Y. lipolytica* based on methanol as a carbon source

1.4 Thesis Outline

This Ph.D. thesis contains 6 chapters including three experimental research chapters.

Chapter 1: Introduction

The first chapter provides a background to this Ph.D. project including the global and local drivers for sustainable manufacturing and important factors, such as target products and

feedstocks. The research background, research scope, project aims and objectives, and an outline of the thesis are described in this chapter.

Chapter 2 Literature review

This chapter critically reviews the recent progress of exotic cyclopropane fatty acids production in organisms and the engineering of synthetic C1-based microorganisms. Firstly, it introduces the physical and chemical properties and biosynthesis mechanism of CFAs and the recent progress and challenges of engineering organisms to produce CFAs. The progress of engineering similar exotic fatty acids and alcohols production in yeast is also covered in brief. Alternative carbon feedstocks for microbes that allow more sustainable industrial platforms - C1 compounds such as methanol can be feedstocks for microorganisms are reviewed. This includes native pathways of methanol utilisation by microorganisms and strategies for constructing synthetic methanol-based microorganisms.

Chapter 3 Redirection of cyclopropane fatty acids flux toward triacylglycerol to increase cyclopropane fatty acids turnover in *S. cerevisiae*.

This chapter examines heterologous biosynthesis of CFAs in *S. cerevisiae* including substrates and location of catalysis. It was determined via overexpression of key genes enabling the transformations that both unsaturated fatty acids and S-adenosylmethionine are substrates for CFAs biosynthesis in yeast. Also, the majority of CFAs remained in phospholipids as determined by positional analysis of CFAs in phospholipids and subcellular localisation of cyclopropane-fatty-acyl-phospholipid synthase. Based on this knowledge, a metabolic engineering strategy that increased the turnover of CFAs from membranes and redirected CFAs flux toward triacylglycerols was proposed and applied in *S. cerevisiae*. This included overcoming substrate limitations of cyclopropane-fatty-acyl-phospholipid synthase, improved CFAs turnover to triacylglycerols, and blocking the degradation of triacylglycerols

and fatty acids. Finally, CFAs yield was increased by around 2.5-fold compared with the strain only expressing *E. coli cfa*.

Chapter 4 Transferral of the CFAs metabolic engineering strategy developed for *Saccharomyces cerevisiae* to *Yarrowia lipolytica*

Y. lipolytica is an oleaginous yeast, which is potentially an excellent host for exotic fatty acids production. Therefore, in this chapter, the metabolic engineering strategy developed to improve CFAs flux toward triacylglycerols in *S. cerevisiae* (Chapter 3) was transferred into *Y. lipolytica*. This was achieved by expressing the most impactful genes from Chapter 3 in an enhanced background in *Y. lipolytica*. While transferring the strategy from *S. cerevisiae* did not result in the same level of CFAs increase in *Y. lipolytica*, several likely causes were identified for future research.

Chapter 5 Engineering methanol assimilation in *Y. lipolytica* for high value bioproduction

In this chapter, *Y. lipolytica* was engineered to utilise methanol as feedstocks for growth and the production of high-value products. Based on the methanol assimilation pathway in native methylotrophy, essential genes were selected and expressed in *Y. lipolytica* to construct a methanol assimilation pathway. To further improve the efficiency of methanol utilisation, the non-oxidative pentose phosphate pathway was enhanced, and two rounds of adaptive laboratory evolution (ALE) were applied. Assessment of growth and ^{13}C isotope tracer studies were used to evaluate methanol utilisation efficiency. In addition, a gene cassette for resveratrol production was introduced into *Y. lipolytica*. Finally, ^{13}C incorporation into resveratrol was demonstrated that engineered *Y. lipolytica* strains have the capability to assimilate methanol into industrially relevant chemicals.

Chapter 6 Conclusion and outlook

This chapter provides a concise summary of the findings of the experimental chapter based on the objectives of different projects. This section also discusses existing problems and challenges in the experimental approach and potential directions for future work.

1.5 Reference

Abdel-Mawgoud, A.M., Markham, K.A., Palmer, C.M., Liu, N., Stephanopoulos, G., Alper, H.S. 2018. Metabolic engineering in the host Yarrowia lipolytica. *Metabolic engineering*, **50**, 192-208.

Bao, X., Thelen, J.J., Bonaventure, G., Ohlrogge, J.B. 2003. Characterization of Cyclopropane Fatty-acid Synthase fromSterculia foetida. *Journal of Biological Chemistry*, **278**(15), 12846-12853.

Carlsson, A.S., Yilmaz, J.L., Green, A.G., Stymne, S., Hofvander, P. 2011. Replacing fossil oil with fresh oil–with what and for what? *European Journal of Lipid Science and Technology*, **113**(7), 812-831.

Carly, F., Vandermies, M., Telek, S., Steels, S., Thomas, S., Nicaud, J.-M., Fickers, P. 2017. Enhancing erythritol productivity in Yarrowia lipolytica using metabolic engineering. *Metabolic engineering*, **42**, 19-24.

Dürre, P., Eikmanns, B.J. 2015. C1-carbon sources for chemical and fuel production by microbial gas fermentation. *Current opinion in biotechnology*, **35**, 63-72.

Fortman, J., Chhabra, S., Mukhopadhyay, A., Chou, H., Lee, T.S., Steen, E., Keasling, J.D. 2008. Biofuel alternatives to ethanol: pumping the microbial well. *Trends in biotechnology*, **26**(7), 375-381.

Hong, K.-K., Nielsen, J. 2012. Metabolic engineering of Saccharomyces cerevisiae: a key cell factory platform for future biorefineries. *Cellular and Molecular Life Sciences*, **69**(16), 2671-2690.

Janek, T., Dobrowolski, A., Biegalska, A., Mirończuk, A.M. 2017. Characterization of erythrose reductase from Yarrowia lipolytica and its influence on erythritol synthesis. *Microbial cell factories*, **16**(1), 118.

Kamzolova, S.V., Morgunov, I.G. 2017. Metabolic peculiarities of the citric acid overproduction from glucose in yeasts Yarrowia lipolytica. *Bioresource technology*, **243**, 433-440.

Karmee, S.K., Linardi, D., Lee, J., Lin, C.S.K. 2015. Conversion of lipid from food waste to biodiesel. *Waste management*, **41**, 169-173.

Kildegaard, K.R., Adiego-Pérez, B., Belda, D.D., Khangura, J.K., Holkenbrink, C., Borodina, I. 2017. Engineering of Yarrowia lipolytica for production of astaxanthin. *Synthetic and systems biotechnology*, **2**(4), 287-294.

Liu, R., Zhu, F., Lu, L., Fu, A., Lu, J., Deng, Z., Liu, T. 2014. Metabolic engineering of fatty acyl-ACP reductase-dependent pathway to improve fatty alcohol production in Escherichia coli. *Metabolic engineering*, **22**, 10-21.

Ma, T., Shi, B., Ye, Z., Li, X., Liu, M., Chen, Y., Xia, J., Nielsen, J., Deng, Z., Liu, T. 2019. Lipid engineering combined with systematic metabolic engineering of Saccharomyces cerevisiae for high-yield production of lycopene. *Metabolic Engineering*, **52**, 134-142.

Mussatto, S.I., Dragone, G., Guimarães, P.M., Silva, J.P.A., Carneiro, L.M., Roberto, I.C., Vicente, A., Domingues, L., Teixeira, J.A. 2010. Technological trends, global market, and challenges of bio-ethanol production. *Biotechnology advances*, **28**(6), 817-830.

Pfeifenschneider, J., Brautaset, T., Wendisch, V.F. 2017. Methanol as carbon substrate in the bio-economy: Metabolic engineering of aerobic methylotrophic bacteria for production of value-added chemicals. *Biofuels, Bioproducts and Biorefining*, **11**(4), 719-731.

Publishing, B. 2019. Oleochemical Fatty Acids: Global Markets to 2023, Industry report.

Quayle, J. 1972. The metabolism of one-carbon compounds by micro-organisms. in: *Advances in microbial physiology*, Vol. 7, Elsevier, pp. 119-203.

Runguphan, W., Keasling, J.D. 2014. Metabolic engineering of Saccharomyces cerevisiae for production of fatty acid-derived biofuels and chemicals. *Metabolic Engineering*, **21**, 103-113.

Rymowicz, W., Rywińska, A., Marcinkiewicz, M. 2009. High-yield production of erythritol from raw glycerol in fed-batch cultures of Yarrowia lipolytica. *Biotechnology Letters*, **31**(3), 377-380.

Strong, P.J., Xie, S., Clarke, W.P. 2015. Methane as a resource: can the methanotrophs add value? *Environmental science & technology*, **49**(7), 4001-4018.

Wang, Y., Fan, L., Tuyishime, P., Zheng, P., Sun, J. 2020. Synthetic Methylotrophy: A Practical Solution for Methanol-Based Biomanufacturing. *Trends in Biotechnology*.

Yu, X.-H., Rawat, R., Shanklin, J. 2011. Characterization and analysis of the cotton cyclopropane fatty acid synthase family and their contribution to cyclopropane fatty acid synthesis. *BMC plant biology*, **11**(1), 1-10.

Zhang, F., Rodriguez, S., Keasling, J.D. 2011. Metabolic engineering of microbial pathways for advanced biofuels production. *Current opinion in biotechnology*, **22**(6), 775-783.

Zhang, W., Song, M., Yang, Q., Dai, Z., Zhang, S., Xin, F., Dong, W., Ma, J., Jiang, M. 2018. Current advance in bioconversion of methanol to chemicals. *Biotechnology for biofuels*, **11**(1), 260.

Zhou, Y.J., Kerkhoven, E.J., Nielsen, J. 2018. Barriers and opportunities in bio-based production of hydrocarbons. *Nature Energy*.

CHAPTER 2

LITERATURE REVIEW

This page is intentionally blank

[1]Chapter 2 Literature review

2.1. Synthesis of fatty acids and storage as TAGs in yeasts

2.1.1 Standard fatty acids

The fatty acid (FA) and lipid biosynthesis pathways in yeast have been thoroughly studied (Henry et al., 2012). As Fig 2.1 shows, there are three main steps in lipid production: FA biosynthesis, lipid accumulation, and lipid sequestration (Liang & Jiang, 2013).

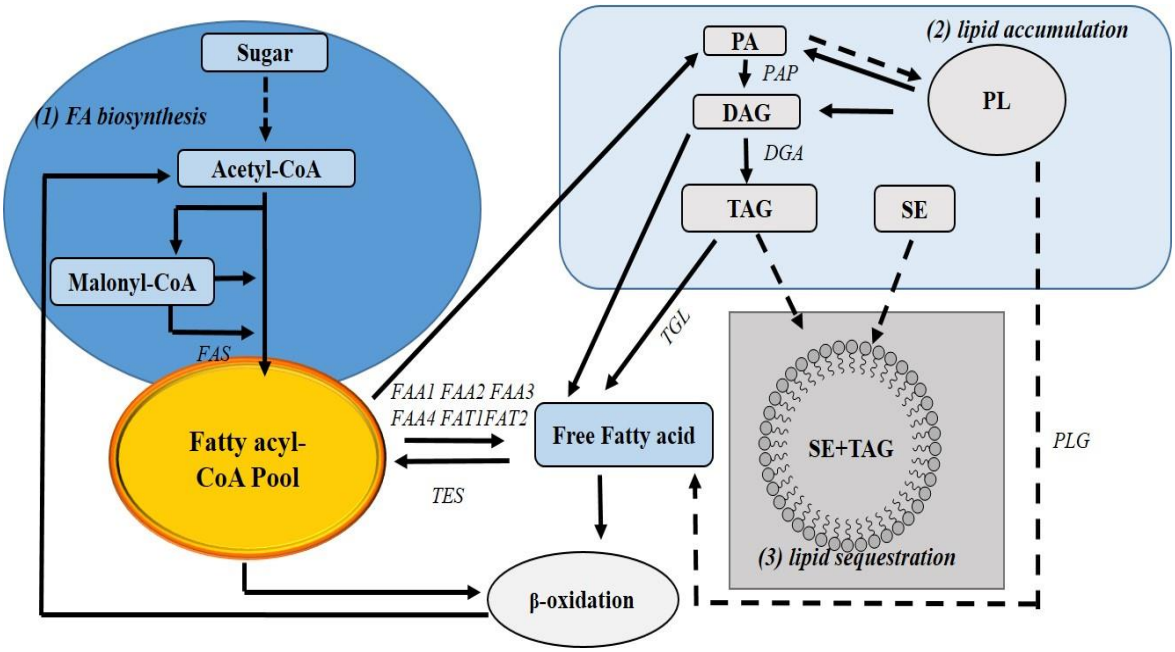

Fig 2. 1 Lipid production pathway in the yeast *S. cerevisiae*

In FA synthesis, acetyl-CoA and bicarbonate form malonyl-CoA. And then varieties of acyl-CoA can be synthesised from the condensation of acetyl-CoA and malonyl-CoA. The subsequent step is lipid accumulation, where both membrane lipids and neutral lipids are synthesized from acyl-CoA. Phospholipids (PLs) take up the majority of membrane lipids. During the de novo synthesis of PL, phosphatidic acid (PA) acts as an intermediate, whose precursor lyso-PA (LPA) is generated from glycerol-3-phosphate (G3P). Subsequently, PA

[1] Chapter 2 includes extracts of my published works namely a book chapter 'Metabolic Engineering of Yeast for Enhanced Natural and Exotic Fatty Acid Production' and a review paper entitled 'Metabolic Engineering Strategies to enable microbial utilization of C1 feedstocks'.

can be converted into phosphatidylcholine (PC), phosphatidylethanolamine (PE), phosphatidylinositol (PI), and phosphatidylserine (PS) under the action of the related enzyme. Besides PA contributing to PL synthesis, PA also can be cleaved to form diacylglycerol that can enter the lipid storage pathway once further esterified with a further FA. Neutral lipids: triacylglycerols (TAGs) and steryl esters (SE) stored in storage organelles called lipid droplets acting as depots for FA to be released as energy, membrane repair, and to sequester sterols (Chae et al., 2012; Klug & Daum, 2014; Toke & Martin, 1996; Zweytick et al., 2000).

In general, standard lipid production in yeast can be enhanced through multiple mechanisms (1) increasing FA biosynthesis, for example, by enhancing pools of precursors acetyl-CoA and malonyl-CoA; (2) reducing the consumption of FA or lipid by blocking degradation pathways such as β-oxidation; (3) providing the sufficient co-factor of fatty acid synthesis such as NADPH; (4) reducing the toxicity of high levels of FA by secreting free FA into culture media or sequestering nascent lipids within lipid droplet (Peng et al., 2018a; Pfleger et al., 2015; Yan & Pfleger, 2020). These strategies applied in *S. cerevisiae* and *Y. lipolytica* have effectively increased lipid production (Ferreira et al., 2018; Wasylenko et al., 2015).

2.1.2 Exotic fatty acids

Besides standard fatty acids, the research in the production of exotic fatty acids and derivatives such as fatty alcohols and esters, and unusual fatty acids such as those with modifications to fatty acid chain length, polyunsaturation, or added functional groups by yeasts is another active area. These fatty acids are usually challenging to produce in yeast because they are not naturally present in yeast but are produced through the introduction of genes sourced from other organisms. Therefore, the production of these fatty acids requires specialized metabolic engineering strategies.

2.1.2.1 Short/medium-chain fatty acids, Fatty acid esters and alcohols, and ricinoleic fatty acids

Short-chain fatty acids (SCFAs), where the carbon chain length is 10, or less are important industrial products as they can be used as gasoline and jet fuel precursors and intermediates in the synthesis of alkenes (Peralta-Yahya et al., 2012). Producing SCFAs in common biotechnological organisms is challenging as they do not natively produce short-chain fatty acids but prefer chain length range between C14-C18 as these are primarily precursors for the formation of cellular membranes to support cell homeostasis (Beld et al., 2015). Beyond the challenge of producing substantial SCFAs within the cells, the potential cytotoxicity due to SCFAs' capacity to damage cell membranes needs to be addressed (Jarboe et al., 2013). The first challenge is that the acyl carrier protein (ACP) and a phosphopantetheine transferase (PPT) are too large for the natural fatty acid synthase (FAS) of *S. cerevisiae* to passively diffuse into for elongation (Lomakin et al., 2007; Mootz et al., 2001; White et al., 2005). Also, the size of the short chain thioesterases (TE) cleaving the elongating fatty acid is more than 9 kDa (Buchbinder et al., 1995; Dehesh et al., 1996). To overcome these issues, FAS and TEs from different microorganisms were expressed to replace the native ones in yeast (Leber et al., 2016; Leber & Da Silva, 2014). Also, the endogenous FAS was engineered to meet the requirement of the generation of short-chain fatty acids (Xu et al., 2016; Zhu et al., 2020).

Fatty acid ethyl esters (FAEEs) are an attractive diesel oil alternative with high energy density and low toxicity to the production host (Zhou et al., 2014). Acyl-CoAs formed within the cell can be condensed by wax ester synthase/acyl-CoA: diacylglycerol acyltransferase with ethanol to synthesize FAEEs. To improve FAEEs yield, the pathway for the intermediate acyl-CoA is enhanced by metabolic engineering. Shi et al. screened five wax ester synthases for FAEEs biosynthesis; a candidate obtained from *Marinobacter hydrocarbonoclasticus* gave 6.3 mg/L FAEEs titer (Shi et al., 2012). With the integration of

this wax synthetase into the *S. cerevisiae* genome, FAEEs yield improved to 34 mg/L (Shi et al., 2014). In addition, reducing competition for acyl-CoA from non-lipid pathways was shown to improve FAEEs productivity (Valle-Rodríguez et al., 2014). As NADPH and acetyl-CoA are required to synthesize acyl-CoA, increasing the flux of acetyl-CoA and NADPH, can improve the pool of acyl-CoA. (Starai et al., 2005). The overexpression of acetyl coenzyme A carboxylase (ACC1) also contributed to the accumulation of acetyl-CoA, whereby FAEEs production reached 8.2 mg/L (Shi et al., 2012). *Y. lipolytica* has also been developed as a host for FAEEs production by similar metabolic engineering strategies. (Gao et al., 2018). Fatty alcohols have applications in detergents, medicine, cosmetics, and biofuels (Beller et al., 2015). In yeast, fatty alcohol can be obtained by the reduction of a fatty aldehyde intermediate or directly synthesized by fatty acyl-CoA that undergoes reduction via the action of a bi-functional fatty acyl-CoA reductase (Willis et al., 2011). The expression of fatty acyl-CoA reductase from the mouse in *S. cerevisiae* resulted in 47.4 mg/L of fatty alcohols (Sangwallek et al., 2013). To further improve fatty alcohol yield, a mouse fatty acid reductase MmFar1p (NADPH-dependent) with high activity was expressed in *S. cerevisiae*. The final strain containing 11 genetic modifications than the parent BY4741 strain, produced 1.2 g/L fatty alcohols in shake flasks from glucose (d'Espaux et al., 2017).

Ricinoleic acid (RA) accounts for around 90% of the total fatty acid in castor seeds (Yamamoto et al., 2008). Because of its specific structure, RA can be a substrate for double bond and hydroxyl-group reactions and therefore, an important natural raw material for the chemical industry (Mander & Liu, 2010). RA and its derivatives have broad commercial applications, including food, textile, paper, plastics, perfumes, cosmetics, paints, inks and lubricants, and biofuels (Kılıç et al., 2013; Ogunniyi, 2006). Although RA is the major component of castor seeds, the castor plant has many serious challenges in its production. In addition, the process of extracting RA from the castor seeds is complicated (Ledesma-Amaro

& Nicaud, 2016). To date, RA biosynthesis has been most successful in *Y. lipolytica* although a major challenge is that the hydroxylated ricinoleic acid is formed at the *sn*-2 position of phosphatidylcholine (PC) in the endoplasmic reticulum (ER) when the Δ12 hydroxylase (Fah12) from castor is expressed. As *Y. lipolytica* accumulates high amounts of oleic acid, the substrate for Fah12, it provides a direct precursor for RA synthesis. Up to now, the best RA yield achieved is 43% of total fatty acid and over 60 mg/g of dry cell weight in small-scale cultures and up to 12 g/L and 60% of total lipids when supplemented with 24 g/L of oleic acid at 10-L bioreactor scale (Béopoulos et al., 2014).

2.1.2.2 Cyclopropane fatty acids (CFAs)

Among a broad array of naturally produced fatty acids and lipids, there are high-value products such as cyclopropane fatty acids with unique and desirable properties for industry.

Structures, chemical and physical properties of CFAs

CFAs can be accumulated in plants and bacteria, where the FA chain contains a 3-membered carbocyclic ring (Badami & Patil, 1980; Ralaimanarivo et al., 1982; Vickery, 1980). Cyclopropane ring in a compound can act as a chemically stable moiety, it can increase lipophilicity and has an orientation that can be different from open-chain orthologues (Wessjohann et al., 2003). Compared with an in-chain methyl group, cyclopropane is relatively smaller, and its exo-carbon is twisted laterally, which leads cyclopropanes to form a rigid structure and have reduced conformational flexibility (Wessjohann et al., 2003). Owing to the specific angle strain, non-ideal bonding angles, torsional strain and the rigidity of small ring locking confirmation, the structure of the 3-carbon ring can result in a high strain (de Meijere, 1979).

The compounds with the representative structures of cyclopropane are found mostly in the natural product of the terpenoids and steroids, amino acids and alkaloids, polyketides, fatty

acids, and so on (Wessjohann et al., 2003). With these attributes, CFAs are potentially valuable as industrial chemical feedstocks and their synthesis has attracted interest. Due to the unique characteristic of cyclopropane, this kind of unusual fatty acid is easily opened by hydrogenation, which can produce a methyl branched-chain fatty acid combining chemical and physical properties of unsaturated fatty acid with oxidative stabilities of saturated fatty acids (Gontier et al., 2008). These chemical and physical properties give CFAs and their derivatives high-potential application as lubricants, cosmetics, plastics, paints, dyes, polymers, and coatings (Bao et al., 2002; Carlsson et al., 2011; Yu et al., 2011b).

Biosynthesis of CFAs

Biosynthetic mechanism of CFAs

In general, the formation of CFAs catalysed by *cfa* synthase requires precursor fatty acids and C_1 donors as shown in Fig 2.2. There are three forms of CFAs found in bacterial membrane lipids: *cis*-9,10 -methylene hexadecanoic acid, *cis*-11,12-methylene octadecanoic acid (lactobacillic acid), and *cis*-9,10-methylene octadecanoic acid (also called dihydrosterculic acid). However, these CFAs with *cis* cyclopropane rings are only found in some organisms with the relevant precursor unsaturated fatty acids (UFAs), that is, palmitoleic (*cis*-9-hexadecenoic acid), *cis*-vaccenic (*cis*-11-octadecenoic acid), and oleic (*cis*-9-octadecenoic acid) acids, respectively (Cronan Jr et al., 1974). What's more, conversion of UFAs to CFAs occurs at a particular period of growth of bacteria, and during their synthesis, the corresponding UFAs will decrease (Law, 1971). To date, enzyme characterisation studies have demonstrated that the corresponding UFAs are the substrates for CFAs synthesis.

CFAs formation requires S-adenosylmethionine (AdoMet) as the C_1 unit- methylene donor. O'Leary and William adopted auxotrophic mutants of *Enterobacter aerogenes* to verify the function of AdoMet in this process. Because the growth of auxotrophic mutants was dependent on exogenous AdoMet, the radiolabeled CFAs could be produced after feeding

[*methyl*-^{14}C] AdoMet, while feeding non-radioactive L-methionine, the CFAs with the isotopic label was not diluted (O'Leary, 1962). In 1979, Cronan et al. adopted wild-type phage T3, which can produce AdoMet hydrolase to destroy AdoMet, to infect *E. coli*, which hindered CFAs synthesis in vivo, while the mutant of phage T3 without hydrolyase infected *E. coli*, CFAs were normally synthesised (Cronan et al., 1979). Also, they demonstrated that AdoMet was an essential requirement for CFAs synthesis in vitro with cell-free systems and AdoMet analogs could cause an inhibitory effect on the reaction (Taylor & Cronan Jr, 1979; Taylor et al., 1981). All the results demonstrated that AdoMet is the other substrate of CFAs synthesis.

In addition, *cfa* synthase is the key enzyme in the synthesis of CFAs; it catalyses the addition reaction between the UFA and AdoMet, which results in the methylene group adding across the carbon-carbon double bond of UFAs to form CFAs (Grogan & Cronan, 1997a).

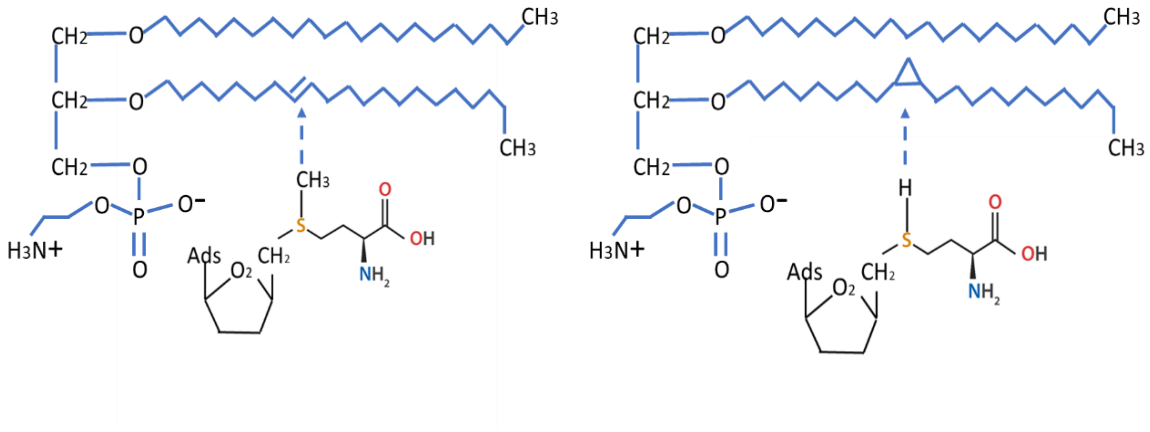

Fig 2.2 The formation process of CFAs catalysed by *cfa* synthase (Grogan & Cronan, 1997a)

The structure and function of *cfa* synthase

The *cfa* synthase from *E. coli* is the typical enzyme that cyclopropanates unsaturated fatty acids. In the crystal form and solution, the enzyme is always dimeric and each subunit has a small N-domain and a larger C-domain. The N-domain is mainly composed of 6 α-helices and 2 short β-strands which formed a hairpin. In the N-domain, the first 13 residues are

disordered, while the residues from 100 to 120 constitute a linker to the C-domain. A large β-sheet exists in the center of the C-domain, which is composed of seven strands and α-helices packed against each face of the sheet. The N-terminal region folds into a specific domain, which associates tightly with the catalytic domain (Hari et al., 2018).

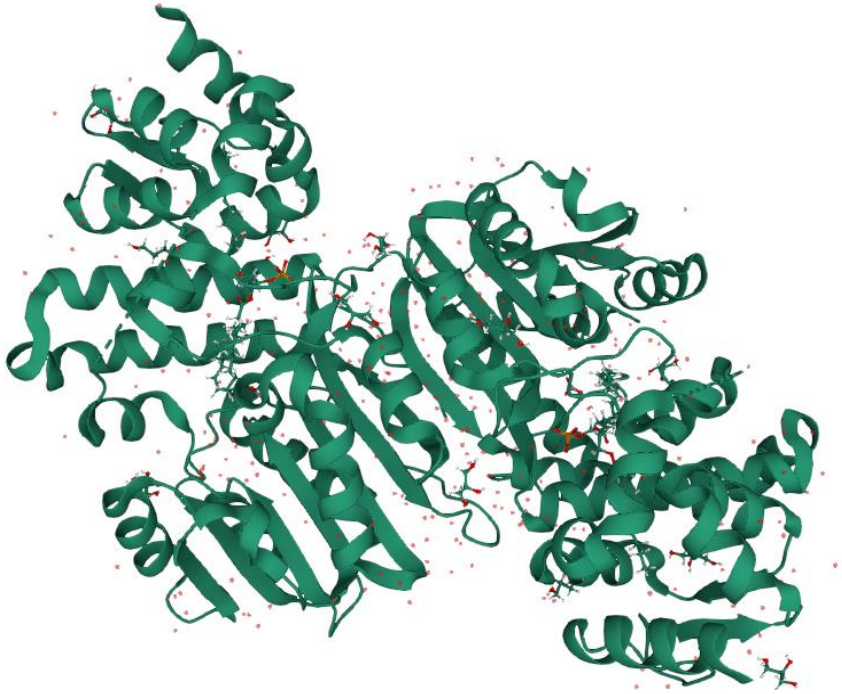

Fig 2.3-Crystal Structure of *E. coli cfa* Synthase obtained from the Protein Data Bank as accession 6BQC.

There is a large pocket within the N-domain which utilises the hydrophobic property of the pocket to bind one arm of a fatty acid. Furthermore, the interaction between the N-domain and catalytic domain is essential for ***cfa*** synthase to function. If the linker between the N- and C-domains is cleaved or lengthened, the enzyme activity is reduced. The linker between the N- and C-domains can act as a hinge; in the open form, it binds the substrate and closes for catalysis. After a catalytic cycle, it opens again to release the product (Hari et al., 2018).

cfa synthase is a soluble enzyme, but it works on unsaturated lipids in the inner and outer leaflets of the bilayer membrane of *E. coli* (Grogan & Cronan, 1997a; Taylor & Cronan Jr,

1979). The lipid in the outer leaflet could be converted by *cfa* synthase where the enzyme enters the membrane but as it lacks a hydrophobic surface and is indeed quite polar, this is not the likely route. It has been identified that the lipid can be flipped from the outer to the inner leaflet or vice versa (McConnell & Kornberg, 1971; Sharom, 2011), which is the explanation for how *cfa* synthase modifies the lipid in both leaflets. A simple model (Fig 2.4) is used to show how *cfa* synthase acts on a fatty acid chain in the bilayer membrane: the N-domain of one subunit is responsible for tethering the enzyme to the lipid surface, at the same time, a phospholipid from the lipid surface is extracted by the other subunit, then the double bond is converted to cyclopropane. The tethering subunit not only generates electrostatic contact with the membrane but also can interact with one arm of a fatty acid that has flipped out from the membrane (Hari et al., 2018).

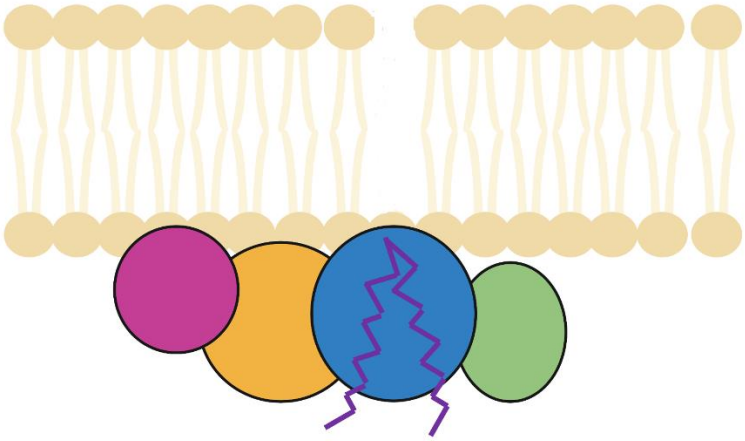

Fig 2.4 A model of action of *cfa* synthase. One subunit (pink/yellow) of the dimer of cfa synthase binds to the lipid bilayer and positions the other subunit (green and blue) for catalysis. N-Domains are colored in pink and green, and C-domains are colored in pink and blue (Hari et al., 2018).

The distribution of CFAs

In general, CFAs can be catalytically synthesised in bacteria (Barry Iii et al., 1998) (Grogan & Cronan, 1997b), some fungi (Law, 1971), plants (Bao et al., 2002; Bao et al., 2003), and parasites (Rahman et al., 1988). CFAs are the main component of the phospholipids in many species of bacteria, including gram-positive and gram-negative genera comprising strict anaerobes, aerotolerant anaerobes, facultative anaerobes, microaerophiles, and obligate aerobes. While some bacteria still lack CFAs, usually due to the precursor of CFAs being absent. For example, CFAs cannot be detected in the membrane of many thermophilic bacterial and gram-positive bacteria and are lacking in *Archaea* (Grogan & Cronan, 1997b). CFAs have also been found in some fungi like *Coprinopsis cinerea*. Liu et al. have proved that a kind of protein existing in *C. cinerea* was homologous to bacterial cyclopropane fatty acid synthase, and the product was CFAs (Liu et al., 2005). Apart from bacteria and fungi, CFAs have been detected in plants from certain gymnosperms, *Malvaceae, Sterculiaceae, Bombaceae, Tilaceae*, *Gnetaceae,* and other *Sapindales* (Badami & Patil, 1980; Christie, 1970; Vickery et al., 1984; Vickery, 1980; Yu et al., 2011b). Moreover, CFAs were also found in some protozoa, sponges, and millipedes (Carballeira et al., 2007; Oyola et al., 2012; Van der Horst et al., 1972). CFAs have not been detected in any yeasts to date.

The presence of CFAs in the membrane of bacteria can change the fluidity of lipid bilayers. Thus, the resistance of bacteria to the extreme environment can be increased, particularly in the heat, stressful and acidic environments (Chang & Cronan, 1999; Chen & Gänzle, 2016). Although it was found that these organisms can naturally produce CFAs, they cannot be developed as a host microorganism for CFAs production, because most of the organisms are non-domesticated and lack genetic manipulation tools. Even where CFAs are naturally produced in platform organisms such as *E. coli*, these bacteria do not synthesis storage lipids, hence cannot accumulate CFA in TAGs.

Heterologous production of CFAs

Up to now, microbial cell factories for CFAs production including both *S. cerevisiae* and *Y. lipolytica* have made some progress but there has been considerable research undertaken to engineer plants. John Shanklin's group explored genetically modified plant seeds as potential biofactories of CFAs by a series of experiments. In 2011, they identified three genes GhCPS1, GhCPS2, and GhCPS3 which can encode cyclopropane synthase in cotton. The difference in the expression of these three genes was revealed by gene transcript. Compared with GhCPS2 and GhCPS3, GhCPS1 was more active in yeast and kept a similar activity when expressed in plant and yeast systems, respectively, which showed that GhCPS1 could be a strong candidate gene for CFAs accumulation (Yu et al., 2011a). Subsequently, in 2014, Shanklin et al. introduced the *E. coli cfa* synthase gene into the seeds of fad2fae1 knock-out *Arabidopsis*, which resulted in CFAs content increased significantly to 9.1% in the seed. After coexpression of a lysophosphatidic acid acyltransferase from *Sterculia foetida* (SfLPAT), the accumulation of CFAs could reach up to 35%. However, the high content of CFAs negatively affected seed morphology, size, and oil accumulation. Finally, the seed germination and establishment reduced a lot, and even the seed could not grow (Yu et al., 2014). Compared with *Arabidopsis*, *Camelina* featured better biocompatibility with *cfa* synthase and SfLPAT, and was not as impacted in germination and seedling growth. However, more CFAs accumulated in the membrane lipids than in storage lipid, which could further indicate a bottleneck in the transfer of CFAs from the membrane to lipid stores (Yu et al., 2018).

Litchi chinensis is a typical plant that can produce CFAs in the seed oil and accounts for more than 40 mol % total fatty acids in the oil. Shockey et al. screened several genes from an early period, middle period, later period of CFAs biosynthesis and triacylglycerol assembly in *Litchi*, respectively. Finally, it was found that type-1 and type-2 diacylglycerol acyltransferases played a significant role in the accumulation of CFAs in TAGs via transgenic expression in yeast and model plant seeds (Shockey et al., 2018).

Besides plants, a cyanobacterium was also adopted to study the CFAs biosynthesis. After introducing the *E. coli cfa* gene into *Synechocystis*, CFAs yield reached ~30% of total fatty acid. However, the CFAs yield could further improve with the help of sn-2-specific desaturase (desC2). Regarding physiological changes of *Synechocystis*, the growth was affected by the presence of the *cfa* gene and the *desC2* gene at low temperature, but photosynthesis and respiration were not altered obviously (Machida et al., 2016). Cyanobacteria do not accumulate storage lipids and the majority of the CFAs was present on membrane lipids.

Peng et al. (2018) expressed the *E. coli cfa* gene in *S. cerevisiae* that had been engineered for higher fatty acids (FA) biosynthesis, lipid production, and sequestration. *tgl3*, encoding triglyceride lipase 3, the main enzyme responsible for hydrolysing CFAs from TAGs was deleted to block CFAs loss from the lipid droplet. The highest CFAs yield was 12 mg/g dry cell weight (DCW) which was 4-fold above the strain expressing *E. coli cfa* gene only and up to 68.3 mg/L in a two-stage bioprocess (Peng et al., 2019; Peng et al., 2018b). *Y. lipolytica* has also been engineered for the production of CFAs. *E. coli cfa* was the preferred candidate from among a range of *cfa* genes screened from bacteria and selected plants for expression as it provided good yield and resulted in both C17 and C19 cyclopropane products (Czerwiec et al., 2019). Blocking β-oxidation by knocking out *PEX10* and *MFE1*, overexpression of the native diacylglycerol acyl transferase *dga1*, increasing the genomic copy number of the *E. coli cfa* gene were successful strategies to produce cyclopropane fatty acids in *Y. lipolytica* (Markham & Alper, 2018). A further strain was constructed by mutating regulatory protein encoded by MGA2 paired with *dga1* overexpression and *cfa* expression, which produced 200 mg/L of C19:0 CFAs in small-scale fermentation. Moreover, more than 3 g/L of C19:0 CFAs was achieved in bioreactor fermentation, which accounted for up to 32.7% of total lipids (Markham & Alper, 2018).

According to the literature review, although constructing the yeast as the cell factory for CFAs production has been made some progress, CFAs metabolism in yeast is still unclear, which limits effective metabolic engineering proposed to further improve CFAs yield. Up to now, the location of *cfa* synthase actions when expressed in yeast has not been revealed and therefore where the majority of CFAs is formed. Also, in the yeast system, the substrate of CFA synthase is required to be further identified and its quantity optimised to improve the production of CFAs. In conclusion, an effective metabolic engineering and synthetic biology strategy can be proposed to utilise yeast as an ideal cell factory for CFAs, which will open the possibilities of industrial application of cyclopropane fatty acid.

2.2 Carbon feedstocks for industrial bioproduction by yeast

2.2.1 Sugar-based feedstocks

Sugars are the most common carbon source for yeast to support their living and growth. In general, yeasts are able to utilise a great diversity of sugars, such as glucose, galactose, sucrose, maltose, and melibiose, and their enzymatic pathways for the specific utilisation of these sugar compounds have been well characterized (Turcotte et al., 2009). However, these sugars are mainly from food and agriculture products, which results in competition with food industries and agriculture. In addition, a consequence of expanding bioproduction need to expand agricultural production and processing to deliver sugar feedstocks, which result in land clearing and degradation. Therefore, the exploitation of alternative feedstocks to replace sugars as the carbon source for yeast is imperative (Gokarn et al., 2007; Naik et al., 2010).

2.2.2 C1-based feedstocks

Recently, one-carbon (C1) compounds have been drawing attention as an alternative sustainable non-food feedstock for industrial yeast production due to their natural abundance, flexible production processes, and availability as industrial by-products (Dürre & Eikmanns,

2015; Pfeifenschneider et al., 2017; Strong et al., 2015). C1 feedstocks are formic acid/formate (COOH), carbon dioxide (CO_2), carbon monoxide (CO), methane (CH_4), and methanol (CH_3OH) and have been variously investigated as feedstocks in biotechnology.

2.2.2.1 CO_2, CO, CH_4, and formate

CO_2 is a common industrial waste gas, whose release into the earth's atmosphere is causing an increasingly serious greenhouse effect (Flessa et al., 2002; Song, 2006). In nature, CO_2 can be used as the carbon source for autotrophic organisms, which can fix CO_2 from the environment (Ducat & Silver, 2012; Fuchs, 2011; Hu et al., 2019). To date, several pathways have been identified in autotrophs to fix CO_2, which includes Calvin Benson–Bassham (CBB) cycle, reductive tricarboxylic acid (rTCA) cycle, the dicarboxylate/4-hydroxybutyrate (DC/HB) cycle, 3-hydroxypropionate (3-HP) bicycle, the Wood-Ljungdahl pathway (WLP) and the reductive glycine pathway (rGlyP) (Jiang et al., 2021). Based on knowledge of the natural pathways, heterotrophic microorganisms such as *E. coli* and yeast have been engineered to utilise CO_2 to various degrees including autotrophy. In 2019, the first synthetic autotrophic prokaryotic (*E. coli*) and eukaryotic (*Pichia pastoris*) cells were constructed (Gassler et al., 2020; Gleizer et al., 2019a).

Carbon monoxide (CO) is an important industrial waste gas (Liew et al., 2016; Williams et al., 1986) While it is highly toxic to mammals, a number of bacteria and archaea in nature are able to utilise CO as a primary carbon and energy source by a natural evolution (Oelgeschläger & Rother, 2008), and are known as carboxydotrophs (Meyer & Schlegel, 1983). Besides the aerobic condition, some carboxydotrophs can metabolise CO under anaerobic conditions such as acetogens, methanogens, and sulfate-reducing bacteria (SRB). The first step of CO metabolism is oxidation in the presence of water, producing CO_2 and reducting power H^+ (Oelgeschläger & Rother, 2008). Anaerobic carboxydotrophs usually

adopt the Wood-Ljungdahl pathway (WLP) to metabolize CO, while aerobes prefer Calvin-Benson-Bassham (CBB) cycle (King & Weber, 2007; Ragsdale & Pierce, 2008). However, so far, reconstructing the WLP in a heterologous host to utilise CO is still a big challenge.

Methane is readily available – it is the principal component of natural/shale gas and biogas- and is important to reduce emissions to the atmosphere as it can more effectively promote global warming than CO_2 (Howarth, 2015). In methanotrophs, microorganisms that can utilise methane for carbon and energy, methane is oxidised to methanol as the first step of methane assimilation catalysed by methane monooxygenases (MMOs) (Semrau et al., 2010). Methane is attractive from the viewpoint of the degree of reduction per carbon of methane reaches eight, thus it harbours more available electrons that can be used to improve the product yields (Whitaker et al., 2015). Although researchers in synthetic biology and metabolic engineering have done a lot of attempts to engineer synthetic methanotrophs, the heterologous expression of MMOs with full activity is still a considerable challenge. In a recent advance, catalytic MMO domains from the methanotroph *Methylococcus capsulatus* were assembled on the apoferritin scaffold, then expressed in *E. coli*, finally reaching activity similar to the native enzyme complex MMOs (Kim et al., 2019).

Formate has many advantages because it is completely water-miscible and easily stored and transported, which suggests it could support higher microbial bioproduction. The relatively high price of formate has made it less desirable as a potential industrial feedstock. Few examples proposed to use formate as an auxiliary feedstock to supplement cells with reducing power (Babel, 2009; Gleizer et al., 2019b). In native formatotrophs, there are several different pathways involved in formate dissimilation, which include the CBB cycle, the WLP, the RuMP cycle, the serine cycle, and the rGlyP [31,93,94]. So far, synthetic formatotrophs has been made great progress. In 2020, the first *E. coli* cell to solely grow on formate as a carbon source was achieved (Kim et al., 2020).

2.2.2.2 Methanol

Methanol is another abundant C1 resource in nature and can be utilised by native methanotrophs as the sole carbon source under either aerobic or anaerobic conditions (Bowman, 2006; Hanson & Hanson, 1996). Methanol is commonly produced by intermediate syngas from natural gas and other renewable resources like biogas or the hydrogenation of CO_2 (Bertau et al., 2014; Du et al., 2016). Also, compared with glucose, methanol is more reduced with the degree of reduction per carbon at 6, while that of glucose is only four.

Native pathways of methanol utilisation

Methylotrophic yeasts

Methanol can be utilised by methylotrophic prokaryotes and eukaryotes for growth in nature (Yurimoto et al., 2011; Zhang et al., 2018). Commonly, native methylotrophic prokaryotes can use various C1-compounds such as methane, methanol, and methylamine as a carbon source, but only methanol can be utilised by methylotrophic eukaryotes. Although methylamine can be metabolised in some methylotrophic eukaryotes, just as a nitrogen source rather than a carbon source (Taubert et al., 2017; van der Klei et al., 2006). Whereas native methylotrophic eukaryotes are confined to four yeast genera *Hansenula, Pichia, Candida,* and *Torulopsis* (Hazeu et al., 1972; Tani et al., 1978). In these methylotrophic yeasts, the expression of genes involved in the methanol utilisation pathway is tightly regulated by strong methanol-inducible promoters, whereas glucose or ethanol can highly repress these promoters (Hartner & Glieder, 2006).

All methylotrophic yeasts share the common methanol utilisation pathway (MUT pathway) as shown in Fig 2.5 (Yurimoto et al., 2002). When the yeast cell takes in methanol, oxidisation of methanol is the first step of methanol metabolism by methanol oxidase Mox

(*Hansenula polymorpha*) (Ledeboer et al., 1985) or alcohol oxidase Aox (*Pichia pastoris*) (Cregg et al., 1989; Nakagawa et al., 1999) or Aod (*Candida boidinii*) (Sakai & Tani, 1992) with molecular O_2 as an electron acceptor. Formaldehyde and hydrogen peroxide (H_2O_2) are the products of this oxidation reaction, both of which have strong toxic effects on cells (Yurimoto et al., 2011). Subsequently, the toxic H_2O_2 is decomposed into oxygen and water by catalase (Cat). While formaldehyde as a key central intermediate can be metabolised by either the dissimilation pathway or the assimilation pathway.

Since there are no carbon-carbon bonds in methanol, these yeast cells utilizing methanol as the sole carbon source have to convert methanol to carbon-carbon bonds for the synthesis of cellular constituents by an assimilatory metabolic pathway, condensing C_1 of methanol and a C_5 of sugar to two C3 molecules (Yurimoto et al., 2002). In the assimilation pathway, firstly formaldehyde is converted by dihydroxyacetone synthase (Das) to form dihydroxyacetone (DHA) and glyceraldehyde 3-phosphate (G3P). In the initial methanol metabolism, the key enzymes Aox or Aod or Mox, Cat, and Das are compartmentalised into peroxisomes and the corresponding reactions take place in peroxisome (van der Klei et al., 2006). Whereas DHAS and DHA need to transfer from the peroxisome to the cytosol for further steps to assimilation. In the cytosol, dihydroxyacetone phosphate (DHAP) is generated via the phosphorylation of DHA under the action of dihydroxyacetone kinase (Dak). Subsequently, fructose bisphosphatase (Fba) catalyses both DHAP and GAP for the formation of fructose 1,6-bisphosphate ($F_{1,6}P$), as the precursor of fructose 6-phosphate (F_6P). Then, the rearrangement reactions of the pentose phosphate (PPP) cycle convert F_6P to Xu_5P. All methanol assimilation steps occur within the peroxisomes delivering G3P to the cytosol whereby one-third of the total derived from methanol is used to create cell biomass and energy (Rußmayer et al., 2015).

Formaldehyde can be dissimilated via glutathione-dependent pathways. It begins with the emergence of S-hydroxymethyl glutathione (GS-CH_2OH) via formaldehyde spontaneously combining with glutathione, which occurs in peroxisomes. Whereas the enzymes involved in the following consecutive oxidation reactions of GS-CH_2OH are located in the cytosol. Firstly, GS-CH_2OH is oxidised to S-formylglutathione (GS-CHO) catalysed by GSH-dependent formaldehyde dehydrogenase (Fld) with the help of NAD^+. The second reaction is the hydrolysis of GS-CHO to GSH and formate under the action of S-formylglutathione hydrolase (Fgh). Eventually, formate is further broken down into CO_2 by NAD^+-linked formate dehydrogenase (Fdh) and generates NADH. Furthermore, methylformate synthesis is another way to detoxify formaldehyde, which is catalysed by alcohol dehydrogenase (Adh) located in the cytosol (Yurimoto et al., 2004). In methylotrophic yeasts, the metabolism of formaldehyde including its generation, assimilation, and dissimilation is primarily limited to peroxisomes, which effectively prevents formaldehyde diffusing into the cytosol and avoids the toxic effects of formaldehyde on cellular macromolecules (Purdue & Lazarow, 2001).

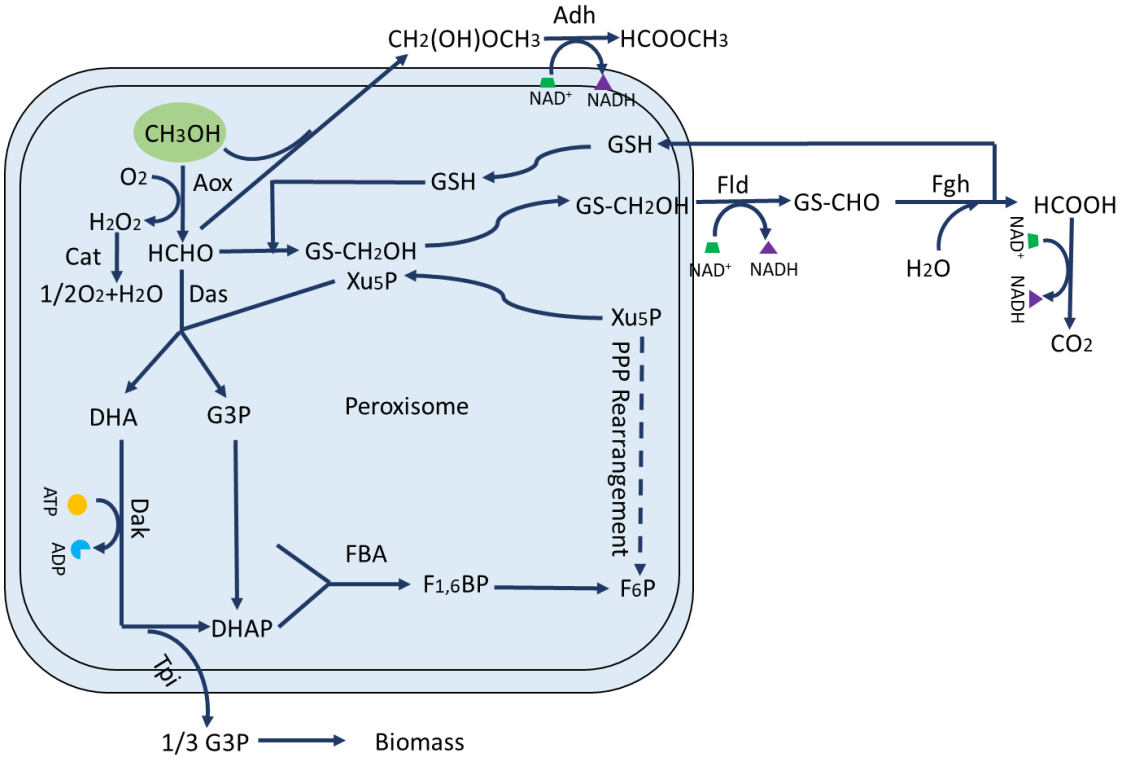

Fig 2.5 Methanol assimilation and dissimilation pathways in native methylotrophic yeasts, F1,6BP: fructose 1,6-bisphosphate, Xu5P: xylulose 5-phosphate, G3P: glyceraldehyde 3-phosphate, DHAP: dihydroxyacetone phosphate, DHA: dihydroxyacetone, GS-CH2OH: S-hydroxymethyl glutathione, GSH: glutathione, Aox: alcohol oxidase, Cat: catalase, Fld: formaldehyde dehydrogenase, Fgh: S-formylglutathione hydrolase, Fdh: formate dehydrogenase, Das: dihydroxyacetone synthase, Tpi: triosephosphate isomerase, Dak: dihydroxyacetone kinase, Fba: fructose 1,6-bisphosphate aldolase.

Methyltrophic prokaryotes

Assimilation pathways for methanol

In methylotrophic prokaryotes, the oxidation of methanol to formaldehyde is also the first step of methanol metabolism catalysed by methanol dehydrogenases (Mdh) (Lee et al., 2020; Zhang et al., 2017). There are three types of Mdh according to their dependent electron acceptor, pyrroloquinoline quinone (PQQ)-dependent methanol dehydrogenase, nicotinamide adenine dinucleotide (NAD)-dependent methanol dehydrogenase, and O_2-dependent alcohol oxidase. Generally, PQQ-dependent methanol dehydrogenase and NAD-dependent methanol dehydrogenase mainly exist in gram-negative methylotrophs and thermophilic gram-positive methylotrophs, respectively. While only eukaryotic methylotrophs harbour O_2-dependent alcohol oxidase. PQQ prosthetic group as catalytic center passes electrons from methanol oxidation to cytochrome c_L, then the electrons are further delivered to the cytochrome c oxidase, eventually to oxygen (Anthony, 2004; Whitaker et al., 2015), which makes a connection between redox reactions and the respiratory chain (Matsushita et al., 1997). In addition, PQQ-dependent methanol dehydrogenase is confined to aerobic conditions, because the molecular oxygen is required for PQQ biosynthesis (Velterop et al., 1995). Whereas NAD^+ as the cofactor of NAD-dependent methanol dehydrogenase is responsible for providing electrons in the process of oxidation of methanol, along with the generation of

NADH. Also, aerobic and anaerobic conditions do not affect the application of NAD^+-dependent methanol dehydrogenase (Zhang et al., 2017). As has been mentioned in methanol metabolism of eukaryotic methylotrophs, O_2-dependent methanol dehydrogenase is a peroxisomal enzyme, while PQQ-dependent methanol dehydrogenase and NAD^+-dependent methanol dehydrogenase are located in the periplasm and cytosol, respectively (Keltjens et al., 2014; Lee et al., 2020).

Subsequently, formaldehyde generated from the oxidation of methanol is quickly assimilated or dissimilated due to high toxicity caused by its non-specific reaction to protein and nucleic acids (Yurimoto et al., 2005). The assimilation pathways convert methanol to biomass, by which methylotrophs are capable of growing on methanol (Pfeifenschneider et al., 2017). Two formaldehyde assimilation pathways in methylotrophic bacteria are the ribulose monophosphate pathway (RuMP) and the serine pathway. For the RuMP pathway, as Fig 2.6 shows, formaldehyde is fixed with the participation of ribulose-5 phosphate (RuMP) via two consecutive reactions catalysed by 3-hexulose-6-phosphate synthase (Hps) and 6-phosphate-3-hexuloisomerase (Phi), which finally generate fructose 6-phosphate (F_6P) (Kato et al., 2006; Orita et al., 2007).

F_6P can enter into the EMP pathway, the Entner-Doudoroff (ED) pathway, or the PPP pathway (Whitaker et al., 2015) (Fig 2.6). F_6P turns into fructose 1,6-bisphosphate ($F\text{-}_{1,6}\text{-BP}$) in the EMP pathway, while it is converted to 6-phosphogluconate (6PG) via the ED pathway. Then in the EMP pathway, $F\text{-}_{1,6}\text{-BP}$ is successively cleaved to dihydroxyacetone phosphate (DHAP) and glyceraldehyde 3-phosphate (G3P) under the action of fructose-bisphosphate aldolase (Fba). By comparison, in the ED pathway, 6PG is transformed into 2-keto-3-deoxy-6-phosphogluconate (KDPG), then G3P is formed by KDPG aldolase cleaving KDPG in the ED pathway, along with pyruvate as another product and the generation of one NADH. In the last reaction of the RuMP cycle, the ribulose-5-phosphate (Ru5P) is generated from 6PG.

Besides, the PPP pathway can also reform Ru5P either via transaldolase or via sedoheptulose 1,7-bisphosphatase (Sbp17) (Pfeifenschneider et al., 2017).

Formaldehyde can be also assimilated via the serine pathway coupled with the ethyl-malonyl-CoA (EMC) pathway or the glyoxylate shunt in methylotrophic bacteria. Firstly, formaldehyde is converted to methylene tetrahydrofolate (methylene-H_4F), then methylene-H_4F as an intermediate enters into the serine cycle (Fig 2.6). Two routes are used to convert formaldehyde to methylene-H_4F. Formaldehyde can spontaneously condense with H_4F to form methylene-H_4F with consuming ATP (Kallen & Jencks, 1966). Besides, tetrahydromethanopterin (H_4MPT)-dependent enzymes can catalyse formaldehyde to formate, next, H_4F-dependent enzymes further catalyse formate to methylene-H_4F, which is the main route. In the serine cycle, firstly, methylene-H_4F and glycine as the substrate of serine-hydroxymethyltransferase (Shmt) are condensed into serine. Glycine can be reproduced via the serine cycle. Subsequently, the serine is converted to phosphoenolpyruvate (PEP) via the continuous four-step reaction. PEP as the substrate of phosphoenolpyruvate carboxylase is catalysed to oxaloacetate, along with fixing CO_2. Then, the key intermediate malate is formed, which can connect the different metabolic pathways. In the serine cycle, oxaloacetate is converted to malate by methanol dehydrogenase. While malate dehydrogenase reversibly catalyse malate to form oxaloacetate via the citric acid (TCA) cycle (Lindén et al., 2016). In addition, isocitrate as one intermediate of the TCA cycle can be also broken down into succinate and glyoxylate through the glyoxylate shunt in the effect of Isocitrate lyase. In the next reaction, glyoxylate is converted to malatebymalate synthase with the participation of acetyl-CoA (Ahn et al., 2016). The next reaction in the serine cycle is the generation of malyl-CoA from malateby malate thiokinase. Then malyl-CoA is cleaved to acetyl-CoA and glyoxylate (Okubo et al., 2010). In the last step of the serine cycle, glycine regenerated from glyoxylate is recycled to serine. Whereas, the acetyl-CoA enters into the EMC pathway,

eventually, glyoxylate is re-produced via several series of reactions in the EMC pathway (Peyraud et al., 2009).

Dissimilation pathways for methanol

Formaldehyde can be dissimilated to CO_2, which is a common pathway in organisms since there are various demethylation reactions in vivo to produce formaldehyde (Yurimoto et al., 2005). H_4F-mediated and tetrahydromethanopterin (H_4MPT)-mediated pathways are commonly found in methylotrophic and non-methylotrophic organisms. The initial formaldehyde oxidation reaction of the H_4F-mediated pathway is the same as that of formaldehyde assimilation via the serine cycle, which forms methylene-H_4F by the formaldehyde spontaneously condensing with H_4F. Although the formation of methylene-H_4MPT is also spontaneous, the formaldehyde activating enzyme (Fae) can accelerate this reaction (Hagemeier et al., 2000). Eventually, methylene-H_4F is oxidized to formate via the H_4F-mediated pathway or H_4MPT-mediated pathway. In the last step, formate is oxidized to CO_2 by formate dehydrogenase (Fdh) and produces NADH. During the H_4F-mediated pathway, NADPH is primarily generated. While the H_4MPT-mediated pathway can produce both NADH and NADPH (Lee et al., 2016).

Intriguingly, all conversions are reversible in the H_4F-mediated pathway. Hence, it is inferred that besides the direct condensation of formaldehyde with H_4F can form methylene-H_4F, the combination of the H_4MPT and H_4F-mediated pathway can also generate methylene-H_4F, which synthesize the methylene-H_4MPT firstly, then converts to formate via the H_4MPT-mediated pathway, finally forms methylene-H_4F through the reverse route of H_4F- mediated pathway, which shows H_4MPT-mediated pathway may participate in both of the formaldehyde assimilation and dissimilation pathway (Marx et al., 2005).

Besides this route, methylotrophic bacteria can also adopt glutathione-dependent pathways for formaldehyde dissimilation (Lee et al., 2002). However, glutathione cannot be produced in several Gram-positive bacteria. These gram-positive bacteria use mycothiol (MSH) to replace glutathione (Duine, 1999). For the mycothiol-dependent pathway, in the first step, mycothiol, like glutathione, spontaneously condenses with formaldehyde to form an S-hydroxymethyl mycothiol (MS-CH_2OH). Then mycothiol-dependent formaldehyde dehydrogenase (MD-FalDH) oxidises MS-CH_2OH to S-formylmycothiol (MS-CHO), which is subsequently hydrolysed to formate, at last, converted to CO_2 (Newton & Fahey, 2002). In addition, it was found that bacillithiol can be used as a thiol cofactor for formaldehyde oxidation in *B. methanolicus*, which is inferred that bacillithiol-dependent formaldehyde oxidation help cells respond to a surge of methanol content (Müller et al., 2015).

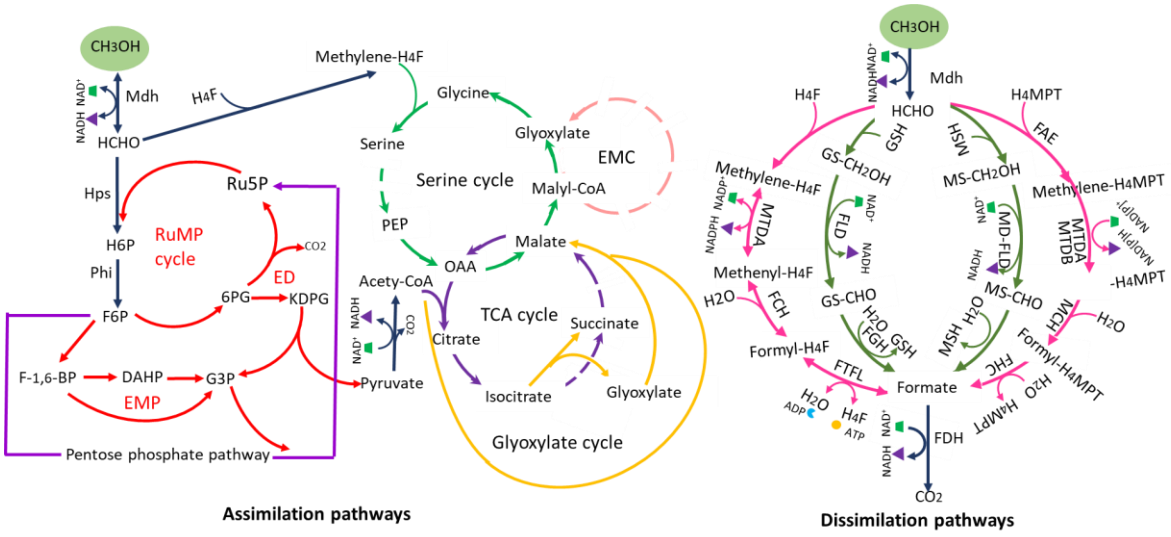

Fig 2.6 Methanol assimilation (Left) and dissimilation (Right) in native methylotrophic prokaryotes. H6P: Hexulose 6-phosphate, F_6P: fructose 6-phosphate, $F_{1,6}P$: fructose 1,6-bisphosphate, Ru5P: ribulose 5-phosphate, DHAP: dihydroxyacetone phosphate, DHA: dihydroxyacetone, GS-CH_2OH: S-hydroxymethyl glutathione, KDPG: 2-keto-3-deoxy-6-phosphogluconate, 6PG: 6-phosphogluconate, H_4F: tetrahydrofolate, H4MPT:

tetrahydromethanopterin, GSH: glutathione, Bacillithiol MSH: mycothiol, MS-CH_2OH: S-hydroxymethyl mycothiol, Methylene-H_4MPT: methylene-Tetrahydromethanopterin, Methylene-H4F: methylene-Tetrahydrofolate, Mdh : methanol dehydrogenase, Hps: 3-hexulose-6-phosphate synthase; Phi: 6-phospho-3-hexuloisomerase, Fdh, formate dehydrogenase.

Methanol-based synthetic organisms

Towards synthetic methylotrophic prokaryotes

Although some natural methylotrophic organisms have been discovered, which are able to utilise methanol as the sole carbon and energy source for growth, the predictability of growth, the chemical range produced by these organisms, and the conversion efficiency of carbon to products is limited and genetic tools their manipulation are lacking (Fei et al., 2014; Whitaker et al., 2015)Therefore, engineering non-methylotrophic organisms for C1 utilisation as energy and carbon source has become an emerging focus of metabolic engineering (Bennett et al., 2018b). Especially, platform organisms such as *E. coli* and *S. cerevisiae* have been already extensively engineered for various chemical productions with outstanding industrial growth (Müller et al., 2015), which have more potential to realise the conversion to value-added products.

Recently, engineering *E. coli* as a synthetic methylotrophy has made some progress. In 2015, Müller et al. built a stoichiometric genome-scale *E. coli* model (Feist et al., 2007) integrating reactions NAD^+-dependent Mdh, PQQ-dependent Mdh, and their associated cytochrome c oxidase, Hps, and Phi used for the establishment of RuMP cycle, and serine glyoxylate aminotransferase, malate thiokinase and malyl-CoA lyase used for the establishment of the serine cycle. They adopted flux balance analysis (FBA) and set maximal biomass yield as a constraint parameter with methanol or glucose as the carbon source. Also, the uptake rate of

methanol was set at the same as that of glucose. The model indicated methanol can be efficiently metabolised in synthetic methylotrophic *E. coli,* which preferred NAD^+-dependent Mdh for methanol oxidation to formaldehyde rather than PQQ-dependent Mdh. And the RuMP cycle was used for biomass accumulation instead of the serine cycle. Based on the result of the *in-silico* modelling and in order to make an appropriate choice for different enzymes, Mdh and alcohol dehydrogenase activities from different microorganisms were tested with or without the activator protein Act in a cell-free extract of *E. coli* and in vivo measured in *E. coli* cell suspensions. Finally, it was found that Mdh2 from *B. methanolicus* MGA3 with Act performed best during the enzyme activity test in vitro. In addition, the concentration of formaldehyde production was highest in vivo in the effect of Mdh2 from *B. methanolicus* MGA3 in vivo, while Act has no impact in vivo. Müller et al. also tested Hps and Phi activity from different organisms and the enzyme activity after fusion of Hps and Phi in vitro and in vivo. However, the artificial fusion of Hps and Phi didn't have any positive effect. In order to test the ability of Hps and Phi for formaldehyde detoxification, the natural GSH-dependent dissimilation pathway was blocked by deleting the *frmA* gene encoding formaldehyde dehydrogenase A. In vitro, the activities of Hps and Phi from *B. methanolicus MGA3* were highest while was relatively low in vivo based on formaldehyde consumption. And ribose supplementation could increase their activities. ^{13}C label incorporation experiment detected hexose 6-phosphates containing 6 label carbons, which showed these molecules could pass the entire RuMP cycle several times. Therefore, methanol assimilation could be established by Mdh, Hps, and Phi, despite the only achievement of roughly 40% ^{13}C carbon labelling fraction (Fig 2.7A) (Müller et al., 2015).

Price et al. (2016) further improved methanol utilisation by the scaffoldless engineered enzyme assembly (Fig 2.7B). They found that a small amount of H6P was detected with the ratio of Mdh3 to Hps from *B. methanolicus* at 1:1 in vitro, while H6P obviously improved

with the ratio increasing up to 10. However, a high ratio commonly can cause a serious cellular burden in vivo, which can be overcome by the supramolecular enzyme complex. To avoid large and disordered structures for multimeric enzymes assembly caused by the protein scaffolding approach, a scaffoldless self-assembly approach was adopted to assemble Hps and Phi to the base Mdh3 at different ratios. Thereinto, SH3, the Src homology 3 domain from the adaptor protein CRK, was used for clustering three multimeric enzymes. Compared with the non-assembled Mdh and Hps, the level of H6P catalysed by assembled Mdh and Hps at 1:1 was around 35-fold higher. The 1:5 ratio can further increase H6P by twice. In addition, the H6P level in the effect of SH3-enzyme fusion was better than that of the Mdh-His6-Hps assembly. When the bifunctional Hps-Phi was fused with Mdh3, there was a 50-fold improvement in the conversion of methanol to F_6P. To prevent the reduction reaction of formaldehyde toward methanol, the Lactate dehydrogenase (Ldh) was added to establish NADH Sink for NADH consumption, which gave rise to a 2-fold increase in methanol oxidation and F_6P production. Finally, this supramolecular enzyme complex was tested in *E. coli*. The result demonstrated formate as the product of methanol dissimilation could be increased by 8-fold. However, the overall methanol conversion efficiency was still relatively low (Price et al., 2016).

In the prior studies, the RuMP cycle was the only pathway to metabolise formaldehyde in this engineered *E. coli*, which is limited by the regeneration of Ru5P. Hence, artificial linear methanol assimilation was firstly constructed in *E. coli* by introducing Mdh and Fls (formolase), converting three formaldehydes to dihydroxyacetone (DHA) via the carboligation reaction (Fig 2.7C). After adaptive evolution, the final engineered strain could consume 2 g/L methanol consistent with a ^{13}C-methanol-labelling experiment, which demonstrated methanol was incorporated into cellular biomass (Wang et al., 2017).

Subsequently, an Mdh from *B. stearothermophilus* and the RuMP pathway from *B. methanolicus* were selected to express in the *E. coli* ΔfrmA strain. Compared with cultures in yeast extract only as a substrate for engineered *E. coli*, methanol as an auxiliary carbon source with 1 g/L yeast extract resulted in a 30% increase in biomass. Besides, based on the results, it was inferred that Mdh from *B. stearothermophilus* can oxidise methanol more quickly to a concentration below the toxicity threshold. In addition, ^{13}C-labelling demonstrated that the carbon from methanol was utilised in product naringenin synthesis, and the product titer was improved where methanol was a co-substrate, albeit at a low percentage of methanol incorporation into naringenin (Whitaker et al., 2017).

Gonzalez et al. (2018) further found that yeast extract as a co-substrate could lead to 17% incorporation in glycogen and 30% labelling in F_6P by ^{13}C tracer, as the representative of biomass components and intracellular metabolites, respectively. Interestingly, ^{13}C-glucose as co-substrate with yeast extract resulted in less than 3% label. High-level label incorporation was found in some amino acids where yeast extract was co-substrate. Since yeast extract mainly consists of amino acids, it was inferred that it was able to act as a regulatory mechanism. In order to verify this hypothesis, twenty-five potential co-substrates including the amino acids, sugars, and organic acids were assessed. Based on the result of the growth and incorporation of ^{13}C-methanol into biomass components, threonine performed best in assisting ^{13}C-methanol assimilation in yeast. The leucine-responsive protein (Lrp) regulates the threonine degradation pathway; compared with the base stains, the Lrp knockout strain significantly increased the biomass concentration and ^{13}C-labelling in glycogen and RNA in the yeast provided with ^{13}C-methanol (Fig 2.7D). Therefore, a strategy to knock out Lrp with co-utilisation of methanol and threonine could be used to improve methanol utilisation efficiency (Gonzalez et al., 2018).

Subsequently, an *E. coli* strain showing methanol auxotrophy was constructed via either deleting *Rpe* coding ribulose-phosphate 3-epimerase or *RpiAB* coding ribose-5-phosphate isomerase A and B, which could not grow on ribose or xylose minimal medium, unless methanol was supplemented with xylose or ribose (Fig 2.7E). Combined with adaptive laboratory evolution, the rate of methanol consumption could reach 0.17 ± 0.006 (h^{-1}) at an approximately 1:1 molar ratio of methanol/xylose as co-substrate in this engineered strain. Additionally, labelled carbon derived from methanol was found in 43% and 71% of ethanol and 1-butanol products via ^{13}C tracer (Chen et al., 2018).

In the same year, Meyer et al. (2018) achieved the methanol-essential growth of *E. coli* with gluconate as a co-substrate (Fig 2.7F). Based on reaction knockout analysis of methanol essentiality *in silico*, the phosphogluconate dehydratase (Edd) and ribose-5-phosphate isomerases (RpiAB) were deleted for the accumulation of ribulose 5-phosphate as the formaldehyde acceptor. Edd and RpiAB deletion redirected 6-phosphogluconate formed by the phosphorylation of gluconate towards ribulose 5-phosphate instead of entering into the Entner-Doudoroff pathway and prevented the conversation of ribulose 5-phosphate to ribose 5-phosphate. Meanwhile, the NAD^+-dependent malate dehydrogenase (Maldh) was deleted to lower TCA cycle activity, which decreased NADH production, thus a high NAD+/NADH ratio to promote the oxidation of methanol, which was consistent with the mutation in the N- and C terminal domain of DNA-binding transcriptional repressor/nicotinamide *NadR* involving in the NAD^+ salvage pathway after a long-term evolution, which weakened the function of repressing NAD^+. Eventually, the best engineered *E. coli* strain after ALE could reach a growth of OD600nm 1.34 ± 0.03, which was 31 ± 4% higher than the wild type strain (Meyer et al., 2018).

Woolston et al. (2018) made an effort to further drive methanol assimilation by enhancing formaldehyde consumption (Fig 2.7G). They verified Ru5P was a primary limitation to

formaldehyde assimilation by supplementing xylose as the auxiliary carbon source to methanol, resulting in a dramatic decrease of formaldehyde in the engineered *E. coli* strains harbouring Mdh, Hps, and Phi. Xylose was converted to ribulose 5-phosphate (Ru5P) through the pentose phosphate pathway, and this acted as the co-substrate of Hps to promote formaldehyde assimilation. Interestingly, the *E. coli* strain expressing only Mdh produced less formaldehyde with the xylose supplement, which was likely caused by the inhibiting effect of increased NADH during xylose metabolism on Mdh. Thereby, to avoid this negative effect of xylose supplement, based on analysis of the genome-scale model of *E. coli* utilising methanol as the sole carbon source, iodoacetate (IA) was used to block the lower glycolysis to improve the generation of Ru5P, leading to a dramatic increase in the intermediates G3P, DHAP, and FBP while F_6P and Ru5P didn't change significantly. Hence GlpX (gluconeogenic FBPase) was expressed to catalyse the dephosphorylation of FBP to F_6P, resulting in a 6.4 ± 2.1 and 4.0 ± 1.2-fold increase in F_6P and Ru5P, respectively. Besides, it was verified that GlpX had SBPase activity, suggesting the regeneration of Ru5P was also likely through the SBPase variant of the RuMP pathway. In addition, the kinetic isotope effect associated with deuterated methanol demonstrated Mdh kinetically restrained overall pathway flux (Woolston et al., 2018).

Recently, a novel methanol assimilation route that mixes and matches methylotrophic enzymes from different organisms was designed through *in silico* modelling. Among 266 pathway variants constructed using different combinations of Mdh and Das, an Mdh from *A. gerneri* expressed as a hybridised version with a codon-optimized Das from *P. angusta* led to the highest incorporation of methanol carbon into the muti-carbon compound, PEP, at 22% (Fig 2.7H). The strain harbouring the hybrid Mdh/Das was grown on xylose with or without methanol supplement and had native *frmA* (formaldehyde dehydrogenase) and *frmB* (S-formylglutathione hydrolase) genes deleted and *fsaB* (fructose-6-phosphate aldolase isoform

B), *gldA* (glycerol dehydrogenase), and *tktA* (transketolase isoforms A) overexpressed. Finally, higher ^{13}C-methanol incorporation in measured central metabolites was obtained, which showed methanol assimilation was further improved by these modifications (De Simone et al., 2020). In addition, an alternative strategy of heterologous expression of the PPP pathway from *B methanolicus* coupled with deletion of phosphoglucose isomerase (Pgi), rerouted glucose catabolism through the PPP rather than via glycolysis and enhanced Ru5P generation in cells grown on methanol and glucose (Fig 2.7I) (Bennett et al., 2018a).

In recent years, *Corynebacterium glutamicum*, a highly productive microorganism for biotechnological amino acids production, has also been engineered as a synthetic methylotroph. *C. glutamicum* cannot utilise methanol as a carbon source for biomass production but it can be dissimilated to CO_2 via native enzymes: alcohol dehydrogenase (AdhA*)* which oxidises methanol to formaldehyde, MSH-dependent formaldehyde dehydrogenase (AdhE*)*, or acetaldehyde dehydrogenase (Ald*)* which catalyses its conversion to formate which is decomposed into CO_2 by formate dehydrogenase (Fdh*)* (Witthoff et al., 2013). While leaving the methanol dissimilation pathway intact as a "safety valve", a pathway for methanol assimilation was introduced into C. *glutamicum* through the recombinant expression of Hps and Phi sourced from *B. subtilis* or *B. methanolicus*. Combining these with Mdh-Act expression gave rise to a 3-fold increase in methanol oxidation rate and a higher OD compared with the non-engineered control strain. Unexpectedly, while the methylotroph bacterium *M. gastri* has a close relationship to *C. glutamicum*, the Hps and Phi from *M. gastri* didn't show functional activity in *C. glutamicum*. As 78% of the consumed methanol in this strain was oxidised to CO_2, the 'safety valve' was removed via knockout of *ald* and *adhE* genes. Nevertheless, the compensation of Mdh-Act and Hps-Phi didn't rescue the reduced methanol consumption rate, the retarded growth, and lower final cell dry weight (Witthoff et al., 2015). Meanwhile, in a *C. glutamicum* strain with

ΔaldΔfdh dual knockout and expressing Mdh sourced from *B. methanolicus*, Hps, and Phi from *B. subtilis*, methanol was demonstrated as the feedstock for the production of non-native cadaverine through ^{13}C labelling (Leßmeier et al., 2015). Furthermore, based on the RuMP-based methanol assimilation pathway, the construction of xylose utilisation pathway for generating the formaldehyde accepter Ru5P combined with knockout *rpiB* (ribose phosphate isomerase), preventing the conversion of Ru5P and R5P and enabling *ΔaldΔadhE C. glutamicum* strains to grow on methanol and xylose as co-substrates.

ALE improved methanol utilisation in engineered *C. glutamicum*. Two rounds of ALE improved the co-metabolized average mole ratio of methanol to xylose as to 3.81:1 and methanol uptake rate during exponential growth up to 0.86 mmol/gCDW h. The biomass yield of the best performing strain from the co-substrates methanol and xylose could reach 0.16 gCDW/g. Of further note, the accumulation of extracellular glutamate during culturing on methanol/xylose illustrated the useful products that could be synthesised via the methanol assimilation pathway (Tuyishime et al., 2018). In addition, tolerance engineering played a big role in constructing a superior synthetic methylotrophic *C. glutamicum*, which increased growth rate, methanol consumption, and methanol-based biosynthesis. Transcriptome analysis revealed that glycolysis and NAD^+-dependent malate dehydrogenase (Madh) was down-regulated after methanol tolerance engineering, while part of the TCA cycle, some amino acid biosynthesis, oxidative phosphorylation, ribosome biosynthesis was enhanced. The mutation in O-acetyl-L-homoserine sulfhydrylase *Cgl0653* (MetY) and methanol-induced membrane-bound transporter *Cgl0833* provide the evidence to speculate the toxic mechanism of methanol. Methanol brought stress to the membrane-bound protein Cgl0833 as methanol is analogous to methanethiol, methanol mistaken for methanethiol took part in enzymatic reaction in the effect of O-acetyl-L-homoserine sulfhydrylase *Cgl0833*, resulting in the formation of some dysfunctional proteins (Wang et al., 2020).

Towards synthetic methylotrophic eukaryotes

Besides *E. coli* and *C. glutamicum*, synthetic methylotrophy has been attempted in non-methylotrophic eukaryotes such as yeast *S. cerevisiae* and *Y. lipolytica*. In 2017, two different methanol assimilation pathways originating from prokaryote *B. methanolicus* and *B. subtilis* and eukaryote *P. pastoris* were separately introduced into *S. cerevisiae*. To avoid the instability of recombinants caused by the loss of plasmids, all the genes were integrated into the chromosome. The methanol consumption rate of the recombinant *S. cerevisiae* expressing *P. pastoris* methanol-pathway genes reached 2.35 g/L in the presence of yeast extract, the central metabolite pyruvate was also detected in the recombinant strains in the presence of methanol, while no methanol consumption or cell growth was observed in *S. cerevisiae* expressing methanol pathway genes from *B. methanolicus* and *B. subtilis* (Dai et al., 2017).

Besides the bacterial and yeast methanol assimilation pathway, a hybrid pathway was designed by mixing bacterial methanol oxidation with yeast formaldehyde assimilation genes in *S. cerevisiae (*Espinosa et al., 2020*)*. Because methanol oxidation and the first step of formaldehyde assimilation occur in peroxisomes of *P. pastoris*, enzymes involved in the yeast methanol assimilation pathway were targeted to the peroxisome and compared with those produced in the cytosol. Peroxisome-targeting of enzymes resulted in subtle yeast growth on solid 1% but no growth on solid 2% methanol medium whereas yeast expressing the hybrid or bacterial pathways showed growth on solid 2% methanol medium.

When naturally methylotrophic yeast *P. pastoris* grows on the methanol, a massive proliferation of peroxisomes can occur, providing an important site for the initial reactions of methanol metabolism (Sibirny, 2016) whereas, in *S. cerevisiae*, peroxisome proliferation has been observed as a result of some specific stresses such as fatty acid oxidation and therefore may not be sufficiently proliferative to be effective for methanol metabolism. Enhancing the

pentose phosphate pathway flux in *S. cerevisiae* by overexpressing transketolase (*tkl1*) or transaldolase (*tal1*) slightly improved the growth of the recombinant strain expressing the bacterial methanol assimilation pathway (Espinosa et al., 2019).

While *S. cerevisiae* has always been considered a non-methylotrophic yeast, ^{13}C-labelled metabolites were detected in a wild-type strain incubated with ^{13}C-methanol as a carbon source, which demonstrated a native methanol assimilation pathway existed in *S. cerevisiae*. *sfa1*, identified as the first gene of the native formaldehyde detoxification pathway in *S. cerevisiae*, was overexpressed and promoted growth of strains with the hybrid pathway and bacterial methanol pathways on solid 2% and 4% methanol medium, and their growth in liquid medium containing methanol. ^{13}C-Methanol was found to be assimilated through a central metabolic pathway in engineered *S. cerevisiae* strain, and growth was ~OD600 0.4 with yeast extract as co-substrate. Whole-genome sequencing of wild type following 230 rounds of ALE revealed a truncated transcription factor YGR067C. The reverse engineering of this mutation into wild type confirmed the role of this factor in optimising growth on methanol. Combining metabolomics, transcriptomics, and proteomics analysis, it was inferred that the mutation in YGR067C decreased the expression of gluconeogenesis, TCA cycle, and glyoxylate cycle, leading metabolic flux towards methanol assimilation. Furthermore, Adh2 (alcohol dehydrogenase 2) and Cat8, a transcription factor involved in de-repressing 414 genes, played a regulatory role in methanol assimilation (Espinosa et al., 2020).

Based on the sequence of formaldehyde dehydrogenase (Fld) in *S. cerevisiae*, the orthologue in *Y. lipolytica* was identified and deleted which caused reduced tolerance to formaldehyde. As methanol was converted into formaldehyde in the *Y. lipolytica Δfld* strain, the result suggested this was catalysed by endogenous alcohol dehydrogenases in *Y. lipolytica*. The expression of *hps* from *B. methanolicus* restored the formaldehyde tolerance caused by the

deletion of *fld* and *Phi* was also introduced to construct the RuMP pathway. Nevertheless, methanol was not utilised in this strain including in the presence of glycerol or yeast extract as co-substrates (Vartiainen et al., 2019).

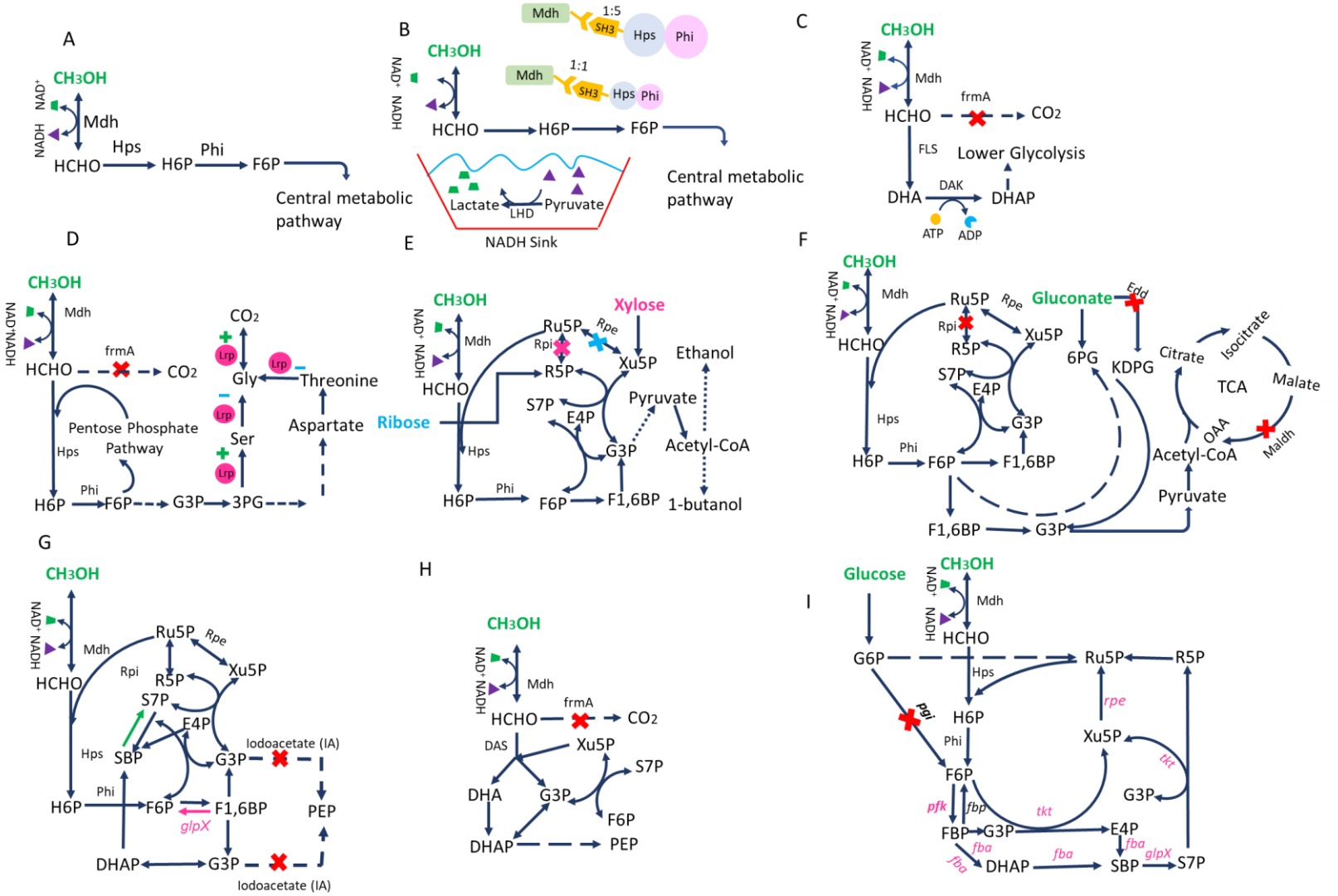
A
CH3OH
NAD+
NADH
Mdh
HCHO
Hps
H6P
Phi
F6P
Central metabolic pathway
B
Mdh
1:5
SH3
Hps
Phi
CH3OH
NAD+ NADH
Mdh
1:1
SH3
Hps
Phi
HCHO
H6P
F6P
Central metabolic pathway
Lactate
LHD
Pyruvate
NADH Sink
C
CH3OH
NAD+ NADH
Mdh
HCHO
frmA
CO2
FLS
Lower Glycolysis
DHA
DAK
DHAP
ATP
ADP
D
CH3OH
NAD+NADH
Mdh
HCHO
frmA
CO2
Gly
Lrp
Threonine
Pentose Phosphate Pathway
Ser
Aspartate
Hps
Phi
H6P
F6P
G3P
3PG
E
CH3OH
NAD+ NADH
Mdh
Xylose
Ru5P
Rpe
Rpi
Xu5P
Ethanol
HCHO
R5P
S7P
E4P
Pyruvate
Ribose
Hps
G3P
Acetyl-CoA
H6P
Phi
F6P
F1,6BP
1-butanol
F
CH3OH
NAD+ NADH
Mdh
Ru5P
Rpe
Gluconate
Edd
HCHO
Rpi
Xu5P
6PG
KDPG
Citrate
Isocitrate
R5P
S7P
E4P
TCA
Malate
Hps
G3P
OAA
Maldh
Phi
H6P
F6P
F1,6BP
Acetyl-CoA
Pyruvate
F1,6BP
G3P
G
CH3OH
NAD+ NADH
Mdh
Ru5P
Rpe
HCHO
Rpi
Xu5P
R5P
S7P
E4P
Hps
SBP
G3P
Iodoacetate (IA)
H6P
Phi
F6P
F1,6BP
PEP
glpX
DHAP
G3P
Iodoacetate (IA)
H
CH3OH
NAD+ NADH
Mdh
HCHO
frmA
CO2
DAS
Xu5P
S7P
DHA
G3P
F6P
DHAP
PEP
I
Glucose
CH3OH
NAD+
NADH
Mdh
HCHO
G6P
Ru5P
R5P
Hps
pgi
H6P
rpe
Phi
Xu5P
tkt
F6P
G3P
pfk
fbp
tkt
FBP
G3P
E4P
fba
fba
fba
glpX
DHAP
SBP
S7P

Fig 2.7 Typical metabolic engineering strategy applied to the construction of synthetic methylotrophic *E. coli*. (A) the basic strategy of overexpression of MDH and key RuMP pathway. (B) the strategy of multifunctional enzyme complex. (C) the strategy of the linear methanol assimilation pathway. (D) the strategy of co-utilisation of threonine with methanol and deletion of leucine-responsive regulatory protein. (E) the strategy of synthetic methanol auxotrophy of *E. coli*. (F) the strategy of co-utilisation of gluconate with methanol and deletion of phosphogluconate dehydratase (G) the strategy of improving formaldehyde consumption to drive methanol assimilation. (H) the strategy of the hybrid methanol assimilation pathway. (I) the strategy of expression of heterologous non-oxidative pentose phosphate pathway and phosphoglucose isomerase deletion.

2.2.3 Reference

Ahn, S., Jung, J., Jang, I.-A., Madsen, E.L., Park, W. 2016. Role of glyoxylate shunt in oxidative stress response. *Journal of Biological Chemistry*, **291**(22), 11928-11938.

Anthony, C. 2004. The quinoprotein dehydrogenases for methanol and glucose. *Archives of biochemistry and biophysics*, **428**(1), 2-9.

Babel, W. 2009. The auxiliary substrate concept: from simple considerations to heuristically valuable knowledge. *Engineering in Life Sciences*, **9**(4), 285-290.

Badami, R., Patil, K.B. 1980. Structure and occurrence of unusual fatty acids in minor seed oils. *Progress in lipid research*, **19**(3-4), 119-153.

Bao, X., Katz, S., Pollard, M., Ohlrogge, J. 2002. Carbocyclic fatty acids in plants: biochemical and molecular genetic characterization of cyclopropane fatty acid synthesis of Sterculia foetida. *Proceedings of the National Academy of Sciences*, **99**(10), 7172-7177.

Bao, X., Thelen, J.J., Bonaventure, G., Ohlrogge, J.B. 2003. Characterization of Cyclopropane Fatty-acid Synthase fromSterculia foetida. *Journal of Biological Chemistry*, **278**(15), 12846-12853.

Barry Iii, C.E., Lee, R.E., Mdluli, K., Sampson, A.E., Schroeder, B.G., Slayden, R.A., Yuan, Y. 1998. Mycolic acids: structure, biosynthesis and physiological functions. *Progress in lipid research*, **37**(2-3), 143-179.

Beld, J., Lee, D.J., Burkart, M.D. 2015. Fatty acid biosynthesis revisited: structure elucidation and metabolic engineering. *Molecular BioSystems*, **11**(1), 38-59.

Beller, H.R., Lee, T.S., Katz, L. 2015. Natural products as biofuels and bio-based chemicals: fatty acids and isoprenoids. *Natural product reports*, **32**(10), 1508-1526.

Bennett, R.K., Gonzalez, J.E., Whitaker, W.B., Antoniewicz, M.R., Papoutsakis, E.T. 2018a. Expression of heterologous non-oxidative pentose phosphate pathway from Bacillus methanolicus and phosphoglucose isomerase deletion improves methanol assimilation and metabolite production by a synthetic Escherichia coli methylotroph. *Metabolic engineering*, **45**, 75-85.

Bennett, R.K., Steinberg, L.M., Chen, W., Papoutsakis, E.T. 2018b. Engineering the bioconversion of methane and methanol to fuels and chemicals in native and synthetic methylotrophs. *Current opinion in biotechnology*, **50**, 81-93.

Béopoulos, A., Verbeke, J., Bordes, F., Guicherd, M., Bressy, M., Marty, A., Nicaud, J.-M. 2014. Metabolic engineering for ricinoleic acid production in the oleaginous yeast Yarrowia lipolytica. *Applied microbiology and biotechnology*, **98**(1), 251-262.

Bertau, M., Offermanns, H., Plass, L., Schmidt, F., Wernicke, H.-J. 2014. *Methanol: the basic chemical and energy feedstock of the future*. Springer.

Bossio, D.A., Scow, K. 1998. Impacts of carbon and flooding on soil microbial communities: phospholipid fatty acid profiles and substrate utilization patterns. *Microbial ecology*, **35**(3-4), 265-278.

Bowman, J. 2006. The methanotrophs—the families Methylococcaceae and Methylocystaceae. *The prokaryotes*, **5**, 266-289.

Buchbinder, J.L., Witkowski, A., Smith, S., Fletterick, R.J. 1995. Crystallization and preliminary diffraction studies of thioesterase II from rat mammary gland. *Proteins: Structure, Function, and Bioinformatics*, **22**(1), 73-75.

Carballeira, N.M., Montano, N., Vicente, J., Rodriguez, A.D. 2007. Novel cyclopropane fatty acids from the phospholipids of the Caribbean sponge Pseudospongosorites suberitoides. *Lipids*, **42**(6), 519-524.

Carlsson, A.S., Yilmaz, J.L., Green, A.G., Stymne, S., Hofvander, P. 2011. Replacing fossil oil with fresh oil–with what and for what? *European Journal of Lipid Science and Technology*, **113**(7), 812-831.

Chae, M., Han, G.-S., Carman, G.M. 2012. The Saccharomyces cerevisiae Actin Patch Protein App1p Is a Phosphatidate Phosphatase Enzyme*♦. *Journal of Biological Chemistry*, **287**(48), 40186-40196.

Chang, Y.Y., Cronan, J.E. 1999. Membrane cyclopropane fatty acid content is a major factor in acid resistance of Escherichia coli. *Molecular microbiology*, **33**(2), 249-259.

Chen, C.-T., Chen, F.Y.-H., Bogorad, I.W., Wu, T.-Y., Zhang, R., Lee, A.S., Liao, J.C. 2018. Synthetic methanol auxotrophy of Escherichia coli for methanol-dependent growth and production. *Metabolic engineering*, **49**, 257-266.

Chen, Y.Y., Gänzle, M.G. 2016. Influence of cyclopropane fatty acids on heat, high pressure, acid and oxidative resistance in Escherichia coli. *International journal of food microbiology*, **222**, 16-22.

Christie, W.W. 1970. Cyclopropane and cyclopropene fatty acids. *Topics in lipid chemistry*, **1**, 1-49.

Cregg, J.M., Madden, K., Barringer, K., Thill, G., Stillman, C. 1989. Functional characterization of the two alcohol oxidase genes from the yeast Pichia pastoris. *Molecular and cellular biology*, **9**(3), 1316-1323.

Cronan, J., Reed, R., Taylor, F., Jackson, M. 1979. Properties and biosynthesis of cyclopropane fatty acids in Escherichia coli. *Journal of bacteriology*, **138**(1), 118-121.

Cronan Jr, J.E., Nunn, W.D., Batchelor, J.G. 1974. Studies on the biosynthesis of cyclopropane fatty acids in Escherichia coli. *Biochimica et Biophysica Acta (BBA)-Lipids and Lipid Metabolism*, **348**(1), 63-75.

Czerwiec, Q., Idrissitaghki, A., Imatoukene, N., Nonus, M., Thomasset, B., Nicaud, J.M., Rossignol, T. 2019. Optimization of cyclopropane fatty acids production in Yarrowia lipolytica. *Yeast*, **36**(3), 143-151.

d'Espaux, L., Ghosh, A., Runguphan, W., Wehrs, M., Xu, F., Konzock, O., Dev, I., Nhan, M., Gin, J., Apel, A.R. 2017. Engineering high-level production of fatty alcohols by Saccharomyces cerevisiae from lignocellulosic feedstocks. *Metabolic engineering*, **42**, 115-125.

Dai, Z., Gu, H., Zhang, S., Xin, F., Zhang, W., Dong, W., Ma, J., Jia, H., Jiang, M. 2017. Metabolic construction strategies for direct methanol utilization in Saccharomyces cerevisiae. *Bioresource technology*, **245**, 1407-1412.

de Meijere, A. 1979. Bonding properties of cyclopropane and their chemical consequences. *Angewandte Chemie International Edition in English*, **18**(11), 809-826.

De Simone, A., C. M. Vicente, C. Peiro, L. Gales, F. Bellvert, B. Enjalbert and S. Heux (2020). "Mixing and matching methylotrophic enzymes to design a novel methanol utilization pathway in E. coli." Metabolic Engineering 61: 315-325.

Dehesh, K., Edwards, P., Hayes, T., Cranmer, A.M., Fillatti, J. 1996. Two novel thioesterases are key determinants of the bimodal distribution of acyl chain length of Cuphea palustris seed oil. *Plant Physiology*, **110**(1), 203-210.

Du, X.L., Jiang, Z., Su, D.S., Wang, J.Q. 2016. Research progress on the indirect hydrogenation of carbon dioxide to methanol. *ChemSusChem*, **9**(4), 322-332.

Ducat, D.C., Silver, P.A. 2012. Improving carbon fixation pathways. *Current opinion in chemical biology*, **16**(3-4), 337-344.

Duine, J.A. 1999. Thiols in formaldehyde dissimilation and detoxification. *Biofactors*, **10**(2-3), 201-206.

Dürre, P., Eikmanns, B.J. 2015. C1-carbon sources for chemical and fuel production by microbial gas fermentation. *Current opinion in biotechnology*, **35**, 63-72.

Espinosa, M.I., Gonzalez-Garcia, R.A., Valgepea, K., Plan, M., Scott, C., Pretorius, I.S., Marcellin, E., Paulsen, I.T., Williams, T.C. 2020. Engineering and Evolution of Methanol Assimilation in Saccharomyces cerevisiae. *bioRxiv*, 717942.

Espinosa, M.I., Valgepea, K., Gonzalez-Garcia, R.A., Scott, C., Pretorius, I.S., Marcellin, E., Paulsen, I.T., Williams, T. 2019. Native and synthetic methanol assimilation in Saccharomyces cerevisiae. *bioRxiv*, 717942.

Fei, Q., Guarnieri, M.T., Tao, L., Laurens, L.M., Dowe, N., Pienkos, P.T. 2014. Bioconversion of natural gas to liquid fuel: opportunities and challenges. *Biotechnology advances*, **32**(3), 596-614.

Feist, A.M., Henry, C.S., Reed, J.L., Krummenacker, M., Joyce, A.R., Karp, P.D., Broadbelt, L.J., Hatzimanikatis, V., Palsson, B.Ø. 2007. A genome-scale metabolic reconstruction for Escherichia coli K-12 MG1655 that accounts for 1260 ORFs and thermodynamic information. *Molecular systems biology*, **3**(1).

Ferreira, R., Teixeira, P.G., Gossing, M., David, F., Siewers, V., Nielsen, J. 2018. Metabolic engineering of Saccharomyces cerevisiae for overproduction of triacylglycerols. *Metabolic engineering communications*, **6**, 22-27.

Flessa, H., Ruser, R., Dörsch, P., Kamp, T., Jimenez, M., Munch, J., Beese, F. 2002. Integrated evaluation of greenhouse gas emissions (CO2, CH4, N2O) from two farming systems in southern Germany. *Agriculture, Ecosystems & Environment*, **91**(1-3), 175-189.

Fuchs, G. 2011. Alternative pathways of carbon dioxide fixation: insights into the early evolution of life? *Annual review of microbiology*, **65**, 631-658.

Gao, Q., Cao, X., Huang, Y.-Y., Yang, J.-L., Chen, J., Wei, L.-J., Hua, Q. 2018. Overproduction of fatty acid ethyl esters by the oleaginous yeast Yarrowia lipolytica through metabolic engineering and process optimization. *ACS synthetic biology*, **7**(5), 1371-1380.

Gassler, T., Sauer, M., Gasser, B., Egermeier, M., Troyer, C., Causon, T., Hann, S., Mattanovich, D., Steiger, M.G. 2020. The industrial yeast Pichia pastoris is converted from a heterotroph into an autotroph capable of growth on CO 2. *Nature Biotechnology*, **38**(2), 210-216.

Gleizer, S., Ben-Nissan, R., Bar-On, Y.M., Antonovsky, N., Noor, E., Zohar, Y., Jona, G., Krieger, E., Shamshoum, M., Bar-Even, A. 2019a. Conversion of Escherichia coli to generate all biomass carbon from CO2. *Cell*, **179**(6), 1255-1263. e12.

Gleizer, S., Ben-Nissan, R., Bar-On, Y.M., Antonovsky, N., Noor, E., Zohar, Y., Jona, G., Krieger, E., Shamshoum, M., Bar-Even, A., Milo, R. 2019b. Conversion of Escherichia coli to Generate All Biomass Carbon from CO2. *Cell*, **179**(6), 1255-1263.e12.

Gokarn, R.R., Selifonova, O.V., Jessen, H.J., Gort, S.J., Selmer, T., Buckel, W. 2007. 3-Hydroxypropionic acid and other organic compounds, Google Patents.

Gontier, E., Thomasset, B., Wallington, E., Wilmer, J. 2008. Plant Cyclopropane Fatty Acid Synthase Genes and Uses Thereof, Google Patents.

Gonzalez, J.E., Bennett, R.K., Papoutsakis, E.T., Antoniewicz, M.R. 2018. Methanol assimilation in Escherichia coli is improved by co-utilization of threonine and deletion of leucine-responsive regulatory protein. *Metabolic engineering*, **45**, 67-74.

Grogan, D.W., Cronan, J.E. 1997a. Cyclopropane ring formation in membrane lipids of bacteria. *Microbiology and Molecular Biology Reviews*, **61**(4), 429-441.

Grogan, D.W., Cronan, J.E. 1997b. Cyclopropane ring formation in membrane lipids of bacteria. *Microbiol. Mol. Biol. Rev.*, **61**(4), 429-441.

Hagemeier, C.H., Chistoserdova, L., Lidstrom, M.E., Thauer, R.K., Vorholt, J.A. 2000. Characterization of a second methylene tetrahydromethanopterin dehydrogenase from Methylobacterium extorquens AM1. *European journal of biochemistry*, **267**(12), 3762-3769.

Hanson, R.S., Hanson, T.E. 1996. Methanotrophic bacteria. *Microbiological reviews*, **60**(2), 439-471.

Haque, M., Hirai, Y., Yokota, K., Mori, N., Jahan, I., Ito, H., Hotta, H., Yano, I., Kanemasa, Y., Oguma, K. 1996. Lipid profile of Helicobacter spp.: presence of cholesteryl glucoside as a characteristic feature. *Journal of bacteriology*, **178**(7), 2065-2070.

Hari, S.B., Grant, R.A., Sauer, R.T. 2018. Structural and Functional Analysis of E. coli Cyclopropane Fatty Acid Synthase. *Structure*, **26**(9), 1251-1258. e3.

Hartner, F.S., Glieder, A. 2006. Regulation of methanol utilisation pathway genes in yeasts. *Microbial Cell Factories*, **5**(1), 39.

Hazeu, W., de Bruyn, J.C., Bos, P. 1972. Methanol assimilation by yeasts. *Archiv für Mikrobiologie*, **87**(2), 185-188.

Henry, S.A., Kohlwein, S.D., Carman, G.M. 2012. Metabolism and regulation of glycerolipids in the yeast Saccharomyces cerevisiae. *Genetics*, **190**(2), 317-349.

Howarth, R.W. 2015. Methane emissions and climatic warming risk from hydraulic fracturing and shale gas development: implications for policy. *Energy and Emission Control Technologies*, **3**, 45-54.

Hu, G., Li, Y., Ye, C., Liu, L., Chen, X. 2019. Engineering microorganisms for enhanced CO2 sequestration. *Trends in biotechnology*, **37**(5), 532-547.

Jarboe, L.R., Royce, L.A., Liu, P. 2013. Understanding biocatalyst inhibition by carboxylic acids. *Frontiers in microbiology*, **4**, 272.

Jiang, W., Villamor, D.H., Peng, H., Chen, J., Liu, L., Haritos, V., Ledesma-Amaro, R. 2021. Metabolic engineering strategies to enable microbial utilization of C1 feedstocks. *Nature Chemical Biology*, **17**(8), 845-855.

Kallen, R.G., Jencks, W.P. 1966. The mechanism of the condensation of formaldehyde with tetrahydrofolic acid. *Journal of Biological Chemistry*, **241**(24), 5851-5863.

Kato, N., Yurimoto, H., Thauer, R.K. 2006. The physiological role of the ribulose monophosphate pathway in bacteria and archaea. *Bioscience, biotechnology, and biochemistry*, **70**(1), 10-21.

Keltjens, J.T., Pol, A., Reimann, J., den Camp, H.J.O. 2014. PQQ-dependent methanol dehydrogenases: rare-earth elements make a difference. *Applied microbiology and biotechnology*, **98**(14), 6163-6183.

Kılıç, M., Uzun, B.B., Pütün, E., Pütün, A.E. 2013. Optimization of biodiesel production from castor oil using factorial design. *Fuel processing technology*, **111**, 105-110.

Kim, H.J., Huh, J., Kwon, Y.W., Park, D., Yu, Y., Jang, Y.E., Lee, B.-R., Jo, E., Lee, E.J., Heo, Y. 2019. Biological conversion of methane to methanol through genetic reassembly of native catalytic domains. *Nature Catalysis*, **2**(4), 342-353.

Kim, S., Lindner, S.N., Aslan, S., Yishai, O., Wenk, S., Schann, K., Bar-Even, A. 2020. Growth of E. coli on formate and methanol via the reductive glycine pathway. *Nature Chemical Biology*, 1-8.

King, G.M., Weber, C.F. 2007. Distribution, diversity and ecology of aerobic CO-oxidizing bacteria. *Nature Reviews Microbiology*, **5**(2), 107-118.

Klug, L., Daum, G. 2014. Yeast lipid metabolism at a glance. *FEMS yeast research*, **14**(3), 369-388.

Law, J.H. 1971. Biosynthesis of cyclopropane rings. *Accounts of Chemical Research*, **4**(6), 199-203.

Leber, C., Choi, J.W., Polson, B., Da Silva, N.A. 2016. Disrupted short chain specific β-oxidation and improved synthase expression increase synthesis of short chain fatty acids in Saccharomyces cerevisiae. *Biotechnology and bioengineering*, **113**(4), 895-900.

Leber, C., Da Silva, N.A. 2014. Engineering of Saccharomyces cerevisiae for the synthesis of short chain fatty acids. *Biotechnology and bioengineering*, **111**(2), 347-358.

Lechevalier, M. 1989. Lipids in bacterial taxonomy. *Practical handbook of microbiology*, 57-67.

Ledeboer, A., Edens, L., Maat, J., Visser, C., Bos, J., Verrips, C., Janowicz, Z., Eckart, M., Roggenkamp, R., Hollenberg, C. 1985. Molecular cloning and characterization of a gene coding for methanol oxidase in Hansenula polymorpha. *Nucleic acids research*, **13**(9), 3063-3082.

Ledesma-Amaro, R., Nicaud, J.-M. 2016. Yarrowia lipolytica as a biotechnological chassis to produce usual and unusual fatty acids. *Progress in Lipid Research*, **61**, 40-50.

Lee, B., Yurimoto, H., Sakai, Y., Kato, N. 2002. Physiological role of the glutathione-dependent formaldehyde dehydrogenase in the methylotrophic yeast Candida boidinii. *MICROBIOLOGY-READING-*, **148**(9), 2697-2704.

Lee, J.-Y., Park, S.-H., Oh, S.-H., Lee, J.-J., Kwon, K.K., Kim, S.-J., Choi, M., Rha, E., Lee, H., Lee, D.-H. 2020. Discovery and Biochemical Characterization of a Methanol Dehydrogenase From Lysinibacillus xylanilyticus. *Frontiers in Bioengineering and Biotechnology*, **8**.

Lee, O.K., Hur, D.H., Nguyen, D.T.N., Lee, E.Y. 2016. Metabolic engineering of methanotrophs and its application to production of chemicals and biofuels from methane. *Biofuels, Bioproducts and Biorefining*, **10**(6), 848-863.

Leßmeier, L., Pfeifenschneider, J., Carnicer, M., Heux, S., Portais, J.-C., Wendisch, V.F. 2015. Production of carbon-13-labeled cadaverine by engineered Corynebacterium glutamicum using carbon-13-labeled methanol as co-substrate. *Applied microbiology and biotechnology*, **99**(23), 10163-10176.

Liang, M.-H., Jiang, J.-G. 2013. Advancing oleaginous microorganisms to produce lipid via metabolic engineering technology. *Progress in lipid research*, **52**(4), 395-408.

Liew, F., Martin, M.E., Tappel, R.C., Heijstra, B.D., Mihalcea, C., Köpke, M. 2016. Gas fermentation—a flexible platform for commercial scale production of low-carbon-fuels and chemicals from waste and renewable feedstocks. *Frontiers in microbiology*, **7**, 694.

Lindén, P., Keech, O., Stenlund, H., Gardeström, P., Moritz, T. 2016. Reduced mitochondrial malate dehydrogenase activity has a strong effect on photorespiratory metabolism as revealed by 13C labelling. *Journal of experimental botany*, **67**(10), 3123-3135.

Liu, Y., Srivilai, P., Loos, S., Aebi, M., Kües, U. 2005. An essential gene for fruiting body initiation in the basidiomycete Coprinopsis cinerea is homologous to bacterial cyclopropane fatty acid synthase genes. *Genetics 172(2): 873-884.*

Lomakin, I.B., Xiong, Y., Steitz, T.A. 2007. The crystal structure of yeast fatty acid synthase, a cellular machine with eight active sites working together. *Cell*, **129**(2), 319-332.

Machida, S., Shiraiwa, Y., Suzuki, I. 2016. Construction of a cyanobacterium synthesizing cyclopropane fatty acids. *Biochimica et Biophysica Acta (BBA)-Molecular and Cell Biology of Lipids*, **1861**(9), 980-987.

Mander, L., Liu, H.-W. 2010. *Comprehensive natural products II: Chemistry and Biology*. Elsevier.

Markham, K.A., Alper, H.S. 2018. Engineering Yarrowia lipolytica for the production of cyclopropanated fatty acids. *Journal of industrial microbiology & biotechnology*, **45**(10), 881-888.

Marx, C.J., Van Dien, S.J., Lidstrom, M.E. 2005. Flux analysis uncovers key role of functional redundancy in formaldehyde metabolism. *PLoS biology*, **3**(2).

Matsushita, K., Arents, J., Bader, R., Yamada, M., Adachi, O., Postma, P. 1997. Escherichia coli is unable to produce pyrroloquinoline quinone (PQQ). *Microbiology*, **143**(10), 3149-3156.

McConnell, H.M., Kornberg, R.D. 1971. Inside-outside transitions of phospholipids in vesicle membranes. *Biochemistry*, **10**(7), 1111-1120.

Meyer, F., Keller, P., Hartl, J., Gröninger, O.G., Kiefer, P., Vorholt, J.A. 2018. Methanol-essential growth of Escherichia coli. *Nature communications*, **9**(1), 1-10.

Meyer, O., Schlegel, H.G. 1983. Biology of aerobic carbon monoxide-oxidizing bacteria. *Annual review of microbiology*, **37**(1), 277-310.

Mootz, H.D., Finking, R., Marahiel, M.A. 2001. 4′-Phosphopantetheine transfer in primary and secondary metabolism of Bacillus subtilis. *Journal of Biological Chemistry*, **276**(40), 37289-37298.

Müller, J.E., Meyer, F., Litsanov, B., Kiefer, P., Potthoff, E., Heux, S., Quax, W.J., Wendisch, V.F., Brautaset, T., Portais, J.-C. 2015. Engineering Escherichia coli for methanol conversion. *Metabolic engineering*, **28**, 190-201.

Naik, S.N., Goud, V.V., Rout, P.K., Dalai, A.K. 2010. Production of first and second generation biofuels: A comprehensive review. *Renewable and Sustainable Energy Reviews*, **14**(2), 578-597.

Nakagawa, T., Mukaiyama, H., Yurimoto, H., Sakai, Y., Kato, N. 1999. Alcohol oxidase hybrid oligomers formed in vivo and in vitro. *Yeast*, **15**(12), 1223-1230.

Newton, G.L., Fahey, R.C. 2002. Mycothiol biochemistry. *Archives of microbiology*, **178**(6), 388-394.

O'Gara, J.P., Gomelsky, M., Kaplan, S. 1997. Identification and molecular genetic analysis of multiple loci contributing to high-level tellurite resistance in Rhodobacter sphaeroides 2.4. 1. *Applied and environmental microbiology*, **63**(12), 4713-4720.

O'Leary, W.M. 1962. S-adenosylmethionine in the biosynthesis of bacterial fatty acids. *Journal of bacteriology*, **84**(5), 967-972.

Oelgeschläger, E., Rother, M. 2008. Carbon monoxide-dependent energy metabolism in anaerobic bacteria and archaea. *Archives of microbiology*, **190**(3), 257-269.

Ogunniyi, D.S. 2006. Castor oil: a vital industrial raw material. *Bioresource technology*, **97**(9), 1086-1091.

Okubo, Y., Yang, S., Chistoserdova, L., Lidstrom, M.E. 2010. Alternative route for glyoxylate consumption during growth on two-carbon compounds by Methylobacterium extorquens AM1. *Journal of bacteriology*, **192**(7), 1813-1823.

Orita, I., Sakamoto, N., Kato, N., Yurimoto, H., Sakai, Y. 2007. Bifunctional enzyme fusion of 3-hexulose-6-phosphate synthase and 6-phospho-3-hexuloisomerase. *Applied microbiology and biotechnology*, **76**(2), 439-445.

Oudejans, R., van der Horst, D., Opmeer, F., Tieleman, W. 1976. On the function of cyclopropane fatty acids in millipedes (Diplopoda). *Comparative Biochemistry and Physiology Part B: Comparative Biochemistry*, **54**(2), 227-230.

Oyola, S.O., Evans, K.J., Smith, T.K., Smith, B.A., Hilley, J.D., Mottram, J.C., Kaye, P.M., Smith, D.F. 2012. Functional analysis of Leishmania cyclopropane fatty acid synthetase. *PloS one*, **7**(12), e51300.

Peng, H., He, L., Haritos, V.S. 2019. Enhanced Production of High-Value Cyclopropane Fatty Acid in Yeast Engineered for Increased Lipid Synthesis and Accumulation. *Biotechnology journal*, **14**(4), 1800487.

Peng, H., He, L., Haritos, V.S. 2018a. Metabolic engineering of lipid pathways in Saccharomyces cerevisiae and staged bioprocess for enhanced lipid production and cellular physiology. *Journal of Industrial Microbiology and Biotechnology*, **45**(8), 707-717.

Peng, H., He, L., Haritos, V.S. 2018b. Metabolic engineering of lipid pathways in Saccharomyces cerevisiae and staged bioprocess for enhanced lipid production and cellular physiology. *Journal of Industrial Microbiology & Biotechnology*, **45**(8), 707-717.

Peralta-Yahya, P.P., Zhang, F., Del Cardayre, S.B., Keasling, J.D. 2012. Microbial engineering for the production of advanced biofuels. *Nature*, **488**(7411), 320.

Peyraud, R., Kiefer, P., Christen, P., Massou, S., Portais, J.-C., Vorholt, J.A. 2009. Demonstration of the ethylmalonyl-CoA pathway by using 13C metabolomics. *Proceedings of the National Academy of Sciences*, **106**(12), 4846-4851.

Pfeifenschneider, J., Brautaset, T., Wendisch, V.F. 2017. Methanol as carbon substrate in the bio-economy: Metabolic engineering of aerobic methylotrophic bacteria for production of value-added chemicals. *Biofuels, Bioproducts and Biorefining*, **11**(4), 719-731.

Pfleger, B.F., Gossing, M., Nielsen, J. 2015. Metabolic engineering strategies for microbial synthesis of oleochemicals. *Metabolic engineering*, **29**, 1-11.

Price, J.V., Chen, L., Whitaker, W.B., Papoutsakis, E., Chen, W. 2016. Scaffoldless engineered enzyme assembly for enhanced methanol utilization. *Proceedings of the National Academy of Sciences*, **113**(45), 12691-12696.

Purdue, P.E., Lazarow, P.B. 2001. Peroxisome biogenesis. *Annual review of cell and developmental biology*, **17**(1), 701-752.

Ragsdale, S.W., Pierce, E. 2008. Acetogenesis and the Wood–Ljungdahl pathway of CO2 fixation. *Biochimica et Biophysica Acta (BBA)-Proteins and Proteomics*, **1784**(12), 1873-1898.

Rahman, M.D., Ziering, D.L., Mannarelli, S.J., Swartz, K.L., Huang, D.S., Pascal Jr, R.A. 1988. Effects of sulfur-containing analogs of stearic acid on growth and fatty acid biosynthesis in the protozoan Crithidia fasciculata. *Journal of medicinal chemistry*, **31**(8), 1656-1659.

Ralaimanarivo, A., Gaydou, E.M., Bianchini, J.P. 1982. Fatty acid composition of seed oils from sixAdansonia species with particular reference to cyclopropane and cyclopropene acids. *Lipids*, **17**(1), 1-10.

Rußmayer, H., Buchetics, M., Gruber, C., Valli, M., Grillitsch, K., Modarres, G., Guerrasio, R., Klavins, K., Neubauer, S., Drexler, H. 2015. Systems-level organization of yeast methylotrophic lifestyle. *BMC biology*, **13**(1), 1-25.

Sakai, Y., Tani, Y. 1992. Cloning and sequencing of the alcohol oxidase-encoding gene (AOD1) from the formaldehyde-producing asporogeneous methylotrophic yeast, Candida boidinii S2. *Gene*, **114**(1), 67-73.

Sangwallek, J., Kaneko, Y., Sugiyama, M., Ono, H., Bamba, T., Fukusaki, E., Harashima, S. 2013. Ketoacyl synthase domain is a major determinant for fatty acyl chain length in Saccharomyces cerevisiae. *Archives of microbiology*, **195**(12), 843-852.

Schmid, K.M., Patterson, G.W. 1988. Effects of cyclopropenoid fatty acids on fungal growth and lipid composition. *Lipids*, **23**(3), 248-252.

Semrau, J.D., DiSpirito, A.A., Yoon, S. 2010. Methanotrophs and copper. *FEMS microbiology reviews*, **34**(4), 496-531.

Sharom, F.J. 2011. Flipping and flopping—lipids on the move. *IUBMB life*, **63**(9), 736-746.

Shi, S., Valle-Rodríguez, J.O., Khoomrung, S., Siewers, V., Nielsen, J. 2012. Functional expression and characterization of five wax ester synthases in Saccharomyces cerevisiae and their utility for biodiesel production. *Biotechnology for biofuels*, **5**(1), 1-10.

Shi, S., Valle-Rodríguez, J.O., Siewers, V., Nielsen, J. 2014. Engineering of chromosomal wax ester synthase integrated Saccharomyces cerevisiae mutants for improved biosynthesis of fatty acid ethyl esters. *Biotechnology and bioengineering*, **111**(9), 1740-1747.

Shockey, J., Kuhn, D., Chen, T., Cao, H., Freeman, B., Mason, C. 2018. Cyclopropane fatty acid biosynthesis in plants: phylogenetic and biochemical analysis of Litchi Kennedy pathway and acyl editing cycle genes. *Plant cell reports*, **37**(11), 1571-1583.

Sibirny, A.A. 2016. Yeast peroxisomes: structure, functions and biotechnological opportunities. *FEMS yeast research*, **16**(4).

Song, C. 2006. Global challenges and strategies for control, conversion and utilization of CO2 for sustainable development involving energy, catalysis, adsorption and chemical processing. *Catalysis today*, **115**(1-4), 2-32.

Starai, V.J., Gardner, J.G., Escalante-Semerena, J.C. 2005. Residue Leu-641 of acetyl-CoA synthetase is critical for the acetylation of residue Lys-609 by the protein acetyltransferase enzyme of Salmonella enterica. *Journal of Biological Chemistry*, **280**(28), 26200-26205.

Strong, P.J., Xie, S., Clarke, W.P. 2015. Methane as a resource: can the methanotrophs add value? *Environmental science & technology*, **49**(7), 4001-4018.

Tani, Y., Kato, N., Yamada, H. 1978. Utilization of methanol by yeasts. in: *Advances in applied microbiology*, Vol. 24, Elsevier, pp. 165-186.

Taubert, M., Grob, C., Howat, A.M., Burns, O.J., Pratscher, J., Jehmlich, N., von Bergen, M., Richnow, H.H., Chen, Y., Murrell, J.C. 2017. Methylamine as a nitrogen source for microorganisms from a coastal marine environment. *Environmental microbiology*, **19**(6), 2246-2257.

Taylor, F.R., Cronan Jr, J.E. 1979. Cyclopropane fatty acid synthase of Escherichia coli. Stabilization, purification, and interaction with phospholipid vesicles. *Biochemistry*, **18**(15), 3292-3300.

Taylor, F.R., Grogan, D.W., Cronan Jr, J.E. 1981. [18] Cyclopropane fatty acid synthase from Escherichia coli. in: *Methods in enzymology*, Vol. 71, Elsevier, pp. 133-139.

Toke, D.A., Martin, C.E. 1996. Isolation and characterization of a gene affecting fatty acid elongation in Saccharomyces cerevisiae. *Journal of Biological Chemistry*, **271**(31), 18413-18422.

Turcotte, B., Liang, X.B., Robert, F., Soontorngun, N. 2009. Transcriptional regulation of nonfermentable carbon utilization in budding yeast. *FEMS yeast research*, **10**(1), 2-13.

Tuyishime, P., Wang, Y., Fan, L., Zhang, Q., Li, Q., Zheng, P., Sun, J., Ma, Y. 2018. Engineering Corynebacterium glutamicum for methanol-dependent growth and glutamate production. *Metabolic engineering*, **49**, 220-231.

Valle-Rodríguez, J.O., Shi, S., Siewers, V., Nielsen, J. 2014. Metabolic engineering of Saccharomyces cerevisiae for production of fatty acid ethyl esters, an advanced biofuel, by eliminating non-essential fatty acid utilization pathways. *Applied energy*, **115**, 226-232.

Van der Horst, D., Oudejans, R., Zandee, D. 1972. Occurrence of cyclopropane fatty acids in females and eggs of the millipede Graphidostreptus tumuliporus (Karsch)(Myriapoda: Diplopoda), as contrasted with their absence in the males. *Comparative Biochemistry and Physiology Part B: Biochemistry and Molecular Biology*, **41**(2), 417-423.

van der Klei, I.J., Yurimoto, H., Sakai, Y., Veenhuis, M. 2006. The significance of peroxisomes in methanol metabolism in methylotrophic yeast. *Biochimica et Biophysica Acta (BBA)-Molecular Cell Research*, **1763**(12), 1453-1462.

Vartiainen, E., Blomberg, P., Ilmén, M., Andberg, M., Toivari, M., Penttilä, M. 2019. Evaluation of synthetic formaldehyde and methanol assimilation pathways in Yarrowia lipolytica. *Fungal biology and biotechnology*, **6**(1), 27.

Velterop, J., Sellink, E., Meulenberg, J., David, S., Bulder, I., Postma, P. 1995. Synthesis of pyrroloquinoline quinone in vivo and in vitro and detection of an intermediate in the biosynthetic pathway. *Journal of bacteriology*, **177**(17), 5088-5098.

Vickery, J., Whitfield, F., Ford, G., Kennett, B. 1984. The fatty acid composition of Gymnospermae seed and leaf oils. *Journal of the American Oil Chemists' Society*, **61**(3), 573-575.

Vickery, J.R. 1980. The fatty acid composition of seed oils from ten plant families with particular reference to cyclopropene and dihydrosterculic acids. *Journal of the American Oil Chemists' Society*, **57**(2), 87-91.

Wang, X., Wang, Y., Liu, J., Li, Q., Zhang, Z., Zheng, P., Lu, F., Sun, J. 2017. Biological conversion of methanol by evolved Escherichia coli carrying a linear methanol assimilation pathway. *Bioresources and Bioprocessing*, **4**(1), 41.

Wang, Y., Fan, L., Tuyishime, P., Liu, J., Zhang, K., Gao, N., Zhang, Z., Ni, X., Feng, J., Yuan, Q. 2020. Adaptive laboratory evolution enhances methanol tolerance and conversion in engineered Corynebacterium glutamicum. *Communications biology*, **3**(1), 1-15.

Wasylenko, T.M., Ahn, W.S., Stephanopoulos, G. 2015. The oxidative pentose phosphate pathway is the primary source of NADPH for lipid overproduction from glucose in Yarrowia lipolytica. *Metabolic engineering*, **30**, 27-39.

Wessjohann, L.A., Brandt, W., Thiemann, T. 2003. Biosynthesis and metabolism of cyclopropane rings in natural compounds. *Chemical reviews*, **103**(4), 1625-1648.

Whitaker, W.B., Jones, J.A., Bennett, R.K., Gonzalez, J.E., Vernacchio, V.R., Collins, S.M., Palmer, M.A., Schmidt, S., Antoniewicz, M.R., Koffas, M.A. 2017. Engineering the biological conversion of methanol to specialty chemicals in Escherichia coli. *Metabolic engineering*, **39**, 49-59.

Whitaker, W.B., Sandoval, N.R., Bennett, R.K., Fast, A.G., Papoutsakis, E.T. 2015. Synthetic methylotrophy: engineering the production of biofuels and chemicals based on the biology of aerobic methanol utilization. *Current opinion in biotechnology*, **33**, 165-175.

White, S.W., Zheng, J., Zhang, Y.-M., Rock, C.O. 2005. The structural biology of type II fatty acid biosynthesis. *Annu. Rev. Biochem.*, **74**, 791-831.

Williams, E., Colby, J., Lyons, C., Bell, J. 1986. The bacterial utilization of synthetic gases containing carbon monoxide. *Biotechnology and Genetic Engineering Reviews*, **4**(1), 169-212.

Willis, R.M., Wahlen, B.D., Seefeldt, L.C., Barney, B.M. 2011. Characterization of a fatty acyl-CoA reductase from Marinobacter aquaeolei VT8: a bacterial enzyme catalyzing the reduction of fatty acyl-CoA to fatty alcohol. *Biochemistry*, **50**(48), 10550-10558.

Witthoff, S., Mühlroth, A., Marienhagen, J., Bott, M. 2013. C1 metabolism in Corynebacterium glutamicum: an endogenous pathway for oxidation of methanol to carbon dioxide. *Appl. Environ. Microbiol.*, **79**(22), 6974-6983.

Witthoff, S., Schmitz, K., Niedenführ, S., Nöh, K., Noack, S., Bott, M., Marienhagen, J. 2015. Metabolic engineering of Corynebacterium glutamicum for methanol metabolism. *Appl. Environ. Microbiol.*, **81**(6), 2215-2225.

Woolston, B.M., King, J.R., Reiter, M., Van Hove, B., Stephanopoulos, G. 2018. Improving formaldehyde consumption drives methanol assimilation in engineered E. coli. *Nature communications*, **9**(1), 1-12.

Xu, P., Qiao, K., Ahn, W.S., Stephanopoulos, G. 2016. Engineering Yarrowia lipolytica as a platform for synthesis of drop-in transportation fuels and oleochemicals. *Proceedings of the National Academy of Sciences*, **113**(39), 10848-10853.

Yamamoto, K., Kinoshita, A., Shibahara, A. 2008. Ricinoleic acid in common vegetable oils and oil seeds. *Lipids*, **43**(5), 457-460.

Yan, Q., Pfleger, B.F. 2020. Revisiting metabolic engineering strategies for microbial synthesis of oleochemicals. *Metabolic engineering*, **58**, 35-46.

Yu, X.-H., Prakash, R.R., Sweet, M., Shanklin, J. 2014. Coexpressing Escherichia coli cyclopropane synthase with Sterculia foetida lysophosphatidic acid acyltransferase enhances cyclopropane fatty acid accumulation. *Plant physiology*, **164**(1), 455-465.

Yu, X.-H., Rawat, R., Shanklin, J. 2011a. Characterization and analysis of the cotton cyclopropane fatty acid synthase family and their contribution to cyclopropane fatty acid synthesis. *BMC plant biology*, **11**(1), 1-10.

Yu, X.H., Cahoon, R.E., Horn, P.J., Shi, H., Prakash, R.R., Cai, Y., Hearney, M., Chapman, K.D., Cahoon, E.B., Schwender, J. 2018. Identification of bottlenecks in the accumulation of cyclic fatty acids in camelina seed oil. *Plant biotechnology journal*, **16**(4), 926-938.

Yu, X.H., Rawat, R., Shanklin, J. 2011b. Characterization and analysis of the cotton cyclopropane fatty acid synthase family and their contribution to cyclopropane fatty acid synthesis. *Bmc Plant Biology*, **11**(1), 97.

Yurimoto, H., Kato, N., Sakai, Y. 2005. Assimilation, dissimilation, and detoxification of formaldehyde, a central metabolic intermediate of methylotrophic metabolism. *The Chemical Record*, **5**(6), 367-375.

Yurimoto, H., Lee, B., Yasuda, F., Sakai, Y., Kato, N. 2004. Alcohol dehydrogenases that catalyse methyl formate synthesis participate in formaldehyde detoxification in the methylotrophic yeast Candida boidinii. *Yeast*, **21**(4), 341-350.

Yurimoto, H., Oku, M., Sakai, Y. 2011. Yeast methylotrophy: metabolism, gene regulation and peroxisome homeostasis. *International journal of microbiology*, **2011**.

Yurimoto, H., Sakai, Y., Kato, N. 2002. Methanol metabolism. *Hansenula polymorpha*, 61-75.

Zhang, W., Song, M., Yang, Q., Dai, Z., Zhang, S., Xin, F., Dong, W., Ma, J., Jiang, M. 2018. Current advance in bioconversion of methanol to chemicals. *Biotechnology for biofuels*, **11**(1), 260.

Zhang, W., Zhang, T., Wu, S., Wu, M., Xin, F., Dong, W., Ma, J., Zhang, M., Jiang, M. 2017. Guidance for engineering of synthetic methylotrophy based on methanol metabolism in methylotrophy. *RSC advances*, **7**(7), 4083-4091.

Zhou, Y.J., Buijs, N.A., Siewers, V., Nielsen, J. 2014. Fatty acid-derived biofuels and chemicals production in Saccharomyces cerevisiae. *Frontiers in bioengineering and biotechnology*, **2**, 32.

Zhu, Z., Hu, Y., Teixeira, P.G., Pereira, R., Chen, Y., Siewers, V., Nielsen, J. 2020. Multidimensional engineering of Saccharomyces cerevisiae for efficient synthesis of medium-chain fatty acids. *Nature Catalysis*, **3**(1), 64-74.

Zweytick, D., Leitner, E., Kohlwein, S.D., Yu, C., Rothblatt, J., Daum, G. 2000. Contribution of Are1p and Are2p to steryl ester synthesis in the yeast Saccharomyces cerevisiae. *European journal of biochemistry*, **267**(4), 1075-1082.

This page is intentionally blank

CHAPTER 3

REDIRECTION OF CYCLOPROPANE FATTY ACIDS FLUX TOWARD TRIACYLGLYCEROL TO INCREASE CYCLOPROPANE FATTY ACIDS TURNOVER IN *SACCHAROMYCES CEREVISIAE*

This page is intentionally blank

Chapter 3 Redirection of cyclopropane fatty acids flux toward triacylglycerols to increase cyclopropane fatty acids turnover in *Saccharomyces cerevisiae*

Abstract

In this chapter, the location of cyclopropane fatty acids (CFAs) biosynthesis in recombinant *S. cerevisiae* was studied and the relationship between *E. coli* cyclopropane-fatty-acyl-phospholipid *(cfa)* synthase and yeast membranes was revealed. The effect of the expression of *E. coli cfa* synthase on the composition of yeast membranes was also investigated. Also, the substrates of *E. coli cfa* synthase in yeast were identified. Based on this knowledge, a metabolic engineering strategy that redirected CFAs flux toward triacylglycerols to increase CFAs turnover was proposed and applied in *S. cerevisiae*, which included overcoming substrate limitations for *E. coli cfa* synthase, increasing CFAs turnover in membranes and preventing the degradation of triacylglycerols. Finally, CFAs production in TAGs was increased to 12.17 mg/g DCW, which was approx. 3-fold increase above the base strain and demonstrated the effectiveness of the redirection strategy.

3.1 Introduction

Fatty acids such as ricinoleic fatty acid (12-hydroxyoctadec-cis-9-enoic acid, C18:1-OH) and linoleic acid (18:2ω6) are widely used in the production of lubricants, plastics, protecting coating and cosmetics, etc (Jiang et al., 2021; Yu et al., 2014). Among these more specialised fatty acids, cyclopropane fatty acids (CFAs) also have the potential to become high-value products. It has been demonstrated that they and their derivatives have extensive industrial application, especially in the lubrication and oleochemical industries (Schmid, 1999), due to their unique characteristics, where the strained cyclopropane ring is easily opened by hydrogenation to produce a methyl branched-chain fatty acid with chemical and physical properties of unsaturated fatty acid and oxidative stabilities of saturated fatty acids (Gontier et al., 2008). However, the natural production of this unique fatty acid, mostly in plant oils, is quite low.

John Shanklin's group explored genetically modified *Arabidopsis thaliana* plant seeds as potential bio-factories for CFAs production. The co-expression of the *E. coli cfa* synthase gene with a lysophosphatidic acid acyltransferase from *Sterculia foetida* causes the accumulation of CFAs, which can reach up to 35% of the total fatty acid in the seed of recombinant Arabidopsis. However, seed germination and establishment reduced markedly, and most seeds could not grow (Yu et al., 2014). Subsequently, they expressed the same genes in *Camelina sativa* and showed that germination rate and seedling development were negatively impacted. Also, more CFAs accumulated in the membrane phospholipids rather than storage lipids, triglycerides, which indicated a bottleneck in the transfer of CFAs from the membrane where they are formed, to the lipid droplet (Yu et al., 2018). Shockey et al. revealed type-1 and type-2 diacylglycerol acyltransferases of *Litchi chinensis*, a plant that

naturally produces a small quantity of CFAs in seed lipids, played a significant role in the accumulation of CFAs in triacylglycerols (TAGs) (Shockey et al., 2018).

Compared with plants and other microorganisms, the yeast *Saccharomyces cerevisiae* is usually used as a reliable model organism for molecular biology, biochemistry, and eukaryotic lipid metabolism, due to the availability of mutants with lipid metabolic pathway gene deletions and the relatively easy genetic manipulation (Klug & Daum, 2014), which has already efficiently improved the yield of some standard fatty acids (Ferreira et al., 2018a; Peng et al., 2018c) and some unusual fatty acids (Huang et al., 1999; Kainou et al., 2006) with the help of metabolic engineering and synthetic biology. In our previous research, a series of engineered yeast *S. cerevisiae* strains for increased fatty acid production, which resulted in the lipid yield of 8.0% DCW (Peng et al., 2018b), were used as a base strain to produce CFAs. This increased the overall yield of CFAs but did not overcome the main bottleneck.

Although some progress has been made in the production and accumulation of CFAs in common biotechnology organisms, there are few reports of CFAs production in *S. cerevisiae*. Here, we have made progress on engineering yeast to efficiently produce CFA through a systematic study of the location of CFAs synthesis in recombinant *S. cerevisiae* expressing *cfa*, investigating the ability of native yeast enzymes to process this unusual fatty acid, and examining potential substrate limitations. Ultimately, we have developed a novel strategy that involves the cycling of fatty acids from membrane phospholipids to storage triglycerides to enrich these in CFAs (Fig 3.1).

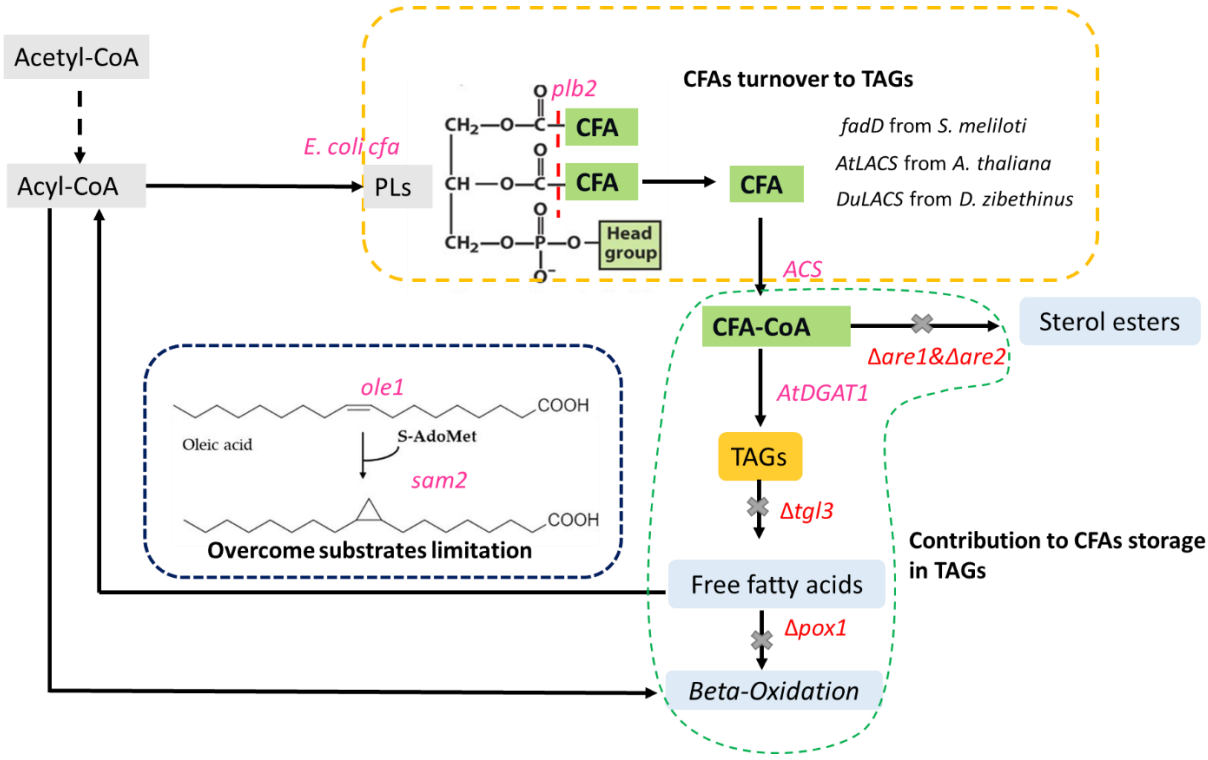

Fig 3.1 Workflow of engineered lipid pathway for efficient biosynthesis of CFA-containing triacylglycerol in *S. cerevisiae*, which contains three steps, (1) overcoming substrates limitation of *E. coli cfa* synthase by overexpressing *ole1* and *sam2*, (2) CFAs turnover to TAGs by overexpressing *plb2* to release CFAs from PLs, then CFAs in free fatty acid form is converted to CFAs-CoA by expressing ACS, (3) contributing to CFAs storage in TAGs via increasing TAGs accumulation under the effect of *AtDGAT1* and preventing TAGs degradation by deleting *tgl3* or *are1* and *are2* and *pox1*. The genes heterogeneously expressed or overexpressed in *S. cerevisiae* are shown in pink text, genes deleted are red. *ole1:* Δ9 Fatty acid desaturase, *sam2*: S-adenosylmethionine synthase, *AtDAGT1*: diacylglycerol acyltransferase from *Arabidopsis thaliana*, *fadD*: fatty acyl-CoA synthetase from *Sinorhizobium meliloti*, *AtLACS*: long-chain acyl-CoA synthetase from *Arabidopsis thaliana*, *DuLACS*: long-chain acyl-CoA synthetase from *Durio zibethinus, Δtgl3:* the deletion of triglyceride lipase 3, *Δpox1*: the deletion of fatty-acyl coenzyme A oxidase, *Δare1&Δare2*: the deletion of acyl-CoA sterol acyltransferase.

3.2 Materials and Methods

3.2.1 Yeast strains, plasmids, transformation and culture condition

The following genes: *cfa* (cyclopropane-fatty-acyl-phospholipid synthase, Accession No.: NC_000913.3) from *Escherichia coli*, *fadD* (fatty acyl-CoA synthetase, Accession No.: NC_003047.1) from *Sinorhizobium meliloti*, *DGAT1* (diacylglycerol acyltransferase), and *LACS* (Long-chain acyl-CoA synthetase)from *Arabidopsis thaliana* (Accession No.: NC_ 003071.7 and No.: NC NC_003071.7), *LACS* (Long-chain acyl-CoA synthetase) from *Durio zibethinus* (Accession XP_022770776.1), *ole1* (Δ9 Fatty acid desaturase), *plb2* (lysophospholipase 2) and *sam2* (S-adenosylmethionine synthase 2) from *S. cerevisiae* (Accession No.: NC_001139.9, No.: NC_ 001145.3 and No.: NC_ 001136.10) were used in this study. All genes were codon-optimised for *S. cerevisiae* and cloned into the into a pESC vector (Agilent, USA) under Gal1 or Gal10 promoters with different yeast markers (Ura, His, Leu). Each gene was designed with a Kozak sequence AAACA at the 5' end to increase expression (Runguphan & Keasling, 2014), were ligated into BamHI-XhoI, SpeI-BglII, and BamHI-XhoI, SpeI-BglII, respectively, to generate the expression plasmids used in this study Knockout strains were generated by deletion of genes including *tgl3* encoding triacylglycerol lipase 3, *pox1* encoding acyl-coenzyme A oxidase, *are1* encoding sterol O-acyltransferase 1, and *are2* encoding sterol O-acyltransferase 2 via CRISPR gene-editing technology. Based on the sequence of the target gene, gRNAs were designed by the CRISPR tool in Benchling. Then gRNA sequences were assembled into the gRNA expression vector by Golden Gate assembly. Meanwhile, donor DNA consisting of 500 bp arms of homology was transferred into yeast together with the CRISPR DNA to assist the homology-directed repair at the double-strand break. Finally, yeast colony PCR was used to verify the deletion of target genes. Subsequently, plasmids were transformed into *S. cerevisiae* BY4741 strains [ATCC 4040002] (MATa his3Δ1 leu2Δ0 met15Δ0 ura3Δ0) and knockout strains via the lithium acetate

transformation method. Details of the engineered strains used in this study are listed in Table 3.1.

Wild-type BY4741 was grown in yeast extract peptone dextrose (YPD) medium (10 g/L yeast extract, 20 g/L Bacteriological Peptone, and 20 g/L glucose). Transformants were selected and grown in corresponding synthetic complete minimal medium (SC medium) according to auxotrophy of the transformants, then the transformants with gene expression or knockout were verified by yeast colony PCR. The composition of the SC medium includes a 6.7 g/L yeast nitrogen base without amino acids, 20 g/L glucose, and an appropriate yeast synthetic drop-out medium supplement. The addition of galactose was used to induce gene expression. *S. cerevisiae* strains were pre-cultured in SC medium with glucose for 24 h, then seed cultures were transferred into 250 mL Erlenmeyer flasks containing 50 mL SC medium with 2% (w/v) galactose and 1% (w/v) raffinose at 0.4 initial OD600 nm, then incubated at 30°C, 250 rpm for 72 h before harvest.

Table 3.1 Strains used in this study

Strains	**Genotype and gene listing**
BY4741	Parental strain, MATa his3Δ1 leu2Δ0 met15Δ0 ura3Δ0
HBY14	*AtDGAT1-Δtgl3*
CBY4741	*Eccfa*
CBY05	*Eccfa-Δtgl3*
CBY14	*Eccfa-AtDGAT1-Δtgl3*
CBYO	*Eccfa -AtDGAT1-Scole1-Δtgl3*
CBYSAM2	*Eccfa-AtDGAT1-Scsam2-Δtgl3*
CBYO+SAM	*Eccfa-AtDGAT1-Scole1-Scsam2-Δtgl3*
CBYPOS	*Eccfa-AtDGAT1-Scole1-Scsam2-plb2-Δtgl3*
CBYPOSF	*Eccfa-AtDGAT1-Scole1-Scsam2-plb 2-fadd-Δtgl3*
CBYPOSA	*Eccfa-AtDGAT1-Scole1-Scsam2-plb 2-AtLACS-Δtgl3*
CBYPOSD	*Eccfa-AtDGAT1-Scole1-Scsam2-plb 2-DuLACS-Δtgl3*
2KO CBYPOSA	*Eccfa-AtDGAT1-Scole1-Scsam2- plb2-AtLACS-Δtgl3-Δpox1*

2KO CBYPOSD	*Eccfa-AtDGAT1-Scole1-Scsam2- plb2-DuLACS-Δtgl3-Δpox1*
2KO CBYPOSF	*Eccfa-AtDGAT1-Scole1-Scsam2-plb2-Smfadd-Δtgl3-Δpox1*
3KO CBYPOSA	*Eccfa-AtDGAT1-Scole1-Scsam2-plb2-AtLACS-Δtgl3-Δare1-Δare2*
3KO CBYPOSD	*Eccfa-AtDGAT1-Scole1-Scsam2- plb2-DuLACS-Δtgl3-Δare1-Δare2*
3KO CBYPOSF	*Eccfa-AtDGAT1-Scole1-Scsam2-plb2-Smfadd-Δtgl3-Δare1-Δare2*

3.2.2 Cell biomass measurement

Cells were collected after the fermentation in flasks, then washed with distilled water twice. Subsequently, the wet biomass was frozen at -80℃, then lyophilised under vacuum overnight. The dry biomass was weighed, then used for lipid analysis and lipid yield calculations.

3.2.3 CFAs Supplementation

CFAs (Santa Cruz Biotechnology, Inc. USA) were dissolved in ethanol at 0.5 M and added into the yeast culture medium at 100 μM final concentration with 0.01% (v/v) tergitol. Tergitol is a non-ionic surfactant, which can assist the dispersion of the CFAs in the medium. Medium containing the same concentration of tergitol and the same volume of ethanol without CFAs was used as a control (Siloto et al., 2009; Xue et al., 2013).

3.2.4Construction of *cfa-gfp*

To investigate the localisation of recombinant *E. coli cfa* expressed in yeast cells, *cfa-gfp* was constructed. The *gfp* sequence was inserted into the pESC-*cfa* plasmid at the N-terminus of *cfa* under the Gal1 promoter (Agilent, USA). A flexible linker GGGGSGGGGS was introduced between the sequence of *gfp* and *cfa*. The pEGFP-*cfa* was transformed into yeast strain HBY14 which is the strain BY4741 expressing AtDGAT1 (diacylglycerol acyltransferase from *Arabidopsis thaliana*) and deletion of triglyceride lipase 3 (*tgl3)*.

3.2.5 Confocal microscopy of yeast cells

Lipid droplets in the yeast strain HBY expressing *cfa-gfp* were stained using Bodipy 558/568 C12 (Life Technologies Australia Pty Ltd). 1 mL of yeast cells after 24 h induction culture was harvested, diluted to 0.5 OD600nm, then incubated in a shaker for 30 min with 0.5 μL Bodipy 558/568 C12 stock solution (1 μg/mL). After staining, yeast cells were washed twice with fresh medium (Suzuki et al., 2012). Mitochondria Deep Red (Life Technologies Australia Pty Ltd) was used to stain the mitochondria in the yeast strain HBY expressing *cfa-gfp*. 1 mL harvested yeast cells after 24 h induction culture were centrifuged, the supernatant was discarded, and the cell pellet was suspended in HEPES buffer. Mitochondria Deep Red stock solution (1 mM) was added to the yeast solution, which brought the final concentration of the dye to 25 nM. After incubation for 30 min, the stained cells were washed twice with HEPES buffer. Subsequently, the stained yeast cells were imaged by a Leica Microsystems SP5 confocal microscope with HCX PL APO 63×/1.4 OIL CS oil-immersion objective under the appropriate excitation lasers for the fluorophores. The images were analysed by Leica LAS X (Leica Microsystems, Inc.) microscope control software.

3.2.6 Fatty acid analysis

Yeast cells after harvest were stored at -80℃ and freeze-dried under vacuum overnight. For the total fatty acids analysis, 20 μL 10 mg/mL tridecanoic acid was added to 20 ~ 30 mg dry yeast cells as the internal standard, then converted into fatty acid methyl esters (FAMEs) via addition of 2 mL acidic methanol (methanol/hydrochloric acid/chloroform (10:1:1)) and heating at 90°C for 1 h. Once cooled, the sample was washed with 0.9% NaCl solution and extracted with 2 mL hexane. FAME were analysed by gas chromatography (GC, Agilent 7890A) fitted with a Flame Ionisation Detector (FID) as previously described (Peng et al., 2018c). GC conditions included helium as the carrier gas, and separation was achieved using a DB-Fast FAME capillary column (Agilent J&W 30 m ×0.25 mm ×0.25 μm). Injections were made in split mode (10:1), initial column temperature was 80°C for 0.5 min, then

increased at 20°C/min to 175°C, then at 10°C/min to 185°C held for 0.5 min, then heated at 7°C/ min to 230°C and held for 10 min. The injection port and flame ionisation detector were 250°C.

Fatty acids in yeast were identified by retention time in comparison with the retention times of 37 individual fatty acids in the mixed fatty acid standard (Supelco 37 Component, Sigma Aldrich). Each fatty acid was baseline-separated in the GC-FID program and individual calibration curves were generated for each component over the range 1- 40 µg/mL. CFA (as FAME) was analysed separately using a pure standard (ab144075, Abcam, Inc.) and a calibration curve was generated by analysis of this standard diluted in hexane. C17CFA and C19CFA as FAME eluted at 8.43 and 10.43 min and were clearly separated from all other 37 fatty acids. CFA concentration was calculated based on the FAME standard prepared over the same concentration range. Mass spectrometry (MS) was not used to confirm the presence of CFA as both electron impact MS and high-resolution MS cannot be used to differentiate CFA from saturated fatty acids of the same molecular weight.

3.2.7 CFAs distribution in TAGs and polar lipid fractions

The analysis of CFAs distribution in the TAGs and polar lipid was carried out according to an adapted Bligh Dyer procedure (Bligh & Dyer, 1959). Total lipids were extracted in methanol/chloroform (2:1) from 20 ~ 30 mg dry yeast cells, with 0.2 mg glyceryl tritridecanoate added as an internal standard. The mixture was vortexed for 6 min with glass beads. Subsequently, 0.5 mL chloroform and 0.5 mL Millipore H_2O were used to isolate lipid from the mixture. After centrifugation, 0.5 mL chloroform containing lipids was transferred into a clean GC vial, then dried under nitrogen gas and redissolved in chloroform. Next, thin layer chromatography (TLC) silica gel plates (L × W 20 cm × 20 cm; Sigma-Aldrich) was applied to separate lipids redissolved in chloroform and the components were separated using

hexane/diethyl ether/acetic acid (70:30:1, v/v/v) as the mobile phase. Then iodine vapour was used to visualise lipid spots. Phospholipids (PLs), TAGs, and other lipids were scraped from the corresponding region of the TLC plate, and individual samples were methylated by reacting them with magic methanol solvent at 80°C for 60 min. The resulting FAMEs were extracted into hexane and analysed by GC-FID as described above.

3.2.8 Position analysis of fatty acids in phospholipids

Total fatty acids were extracted from yeast cells, then separated by TLC as described above. PLs were scraped from the corresponding region of the TLC plate and dissolved in 0.5 ml borate buffer (0.5 M, pH 7.5, containing 0.4 mM $CaCl_2$). After sonication, 5 U of phospholipase A2 from honeybee venom (Sigma-Aldrich) was added to digest PLs plus diethyl ether (2 mL) and the mixture then vortexed for 2 h at 22°C. The ether phase was removed by evaporation, then 0.3 mL 1 M HCl was added to stop the digestion of PLs. The reaction mixture was extracted with chloroform/methanol (2:1, v/v), then dried under nitrogen gas and redissolved in chloroform. Next, the extract was separated by TLC in chloroform/methanol/ammonia/water (70:30:4:2 v/v/v/v) and lipid spots visualised using iodine vapour. Spots corresponding to released free fatty acids and lysophospholipids were located, then scraped from the plates and methylated directly as described above. Finally, the FAMEs were measured by GC-FID as described above.

3.3 Results

3.3.1 Subcellular localisation of functional *E. coli cfa* synthase heterologously expressed in *S. cerevisiae*

It has been demonstrated that the enzyme *cfa* synthase has an affinity for the lipid bilayers of the plasma membrane of *E. coli* and catalyses the methylenation of unsaturated moieties of phospholipids in the lipid bilayer the bacterium (Taylor & Cronan Jr, 1979; Wang et al.,

1992). However, there are no prior reports that describe the localisation of heterologously expressed *E. coli cfa* synthase in *S. cerevisiae* which natively lacks the gene/enzyme. In this study, the subcellular localisation of expressed *E. coli* synthase (named *Eccfas*) was investigated via confocal microscopy of cells expressing *Eccfa*-fused to green fluorescent protein at the enzyme's N-terminus.

The expressed *Eccfa-gfp* fusion protein maintained its cyclopropanation function as demonstrated by the conversion of yeast fatty acids. CFAs was generated in the HBY14 strain expressing *Eccfa-gfp* at approximately the same concentration as *Eccfa* alone, and the percentage of lipids that were composed of CFAs was also similar (Fig 3.2 A). Fluorescence from *cfa-gfp* was observed on the plasma membrane as shown in Fig 3.3 B1, C1 and the green, fluorescent signal was also visualised in other locations in recombinant yeast cells. To explore whether *cfa-gfp* was also localised to the membranes of mitochondria, the yeast strain expressing *cfa-gfp* was stained with a mitochondrial-specific stain and visualised by confocal microscopy as shown in Fig 3.3 B2. The partially or entirely overlapped fluorescent signal generated by *cfa-gfp* and mitochondrial dye indicated that cyclopropane synthase was also present on the mitochondrial membrane (Fig 3.3 B3, B4). Furthermore, *cfa-gfp* protein was also found associated with the lipid droplets; Bodipy 558/568 C12 was used to stain lipid droplets in the yeast strain expressing *cfa-gfp* as shown by the red fluorescence in Fig 3.3 C2. The overlapped fluorescence of *cfa-gfp* and the red Bodipy 558/568 C12 suggested the cyclopropane synthase also localised to the membrane of lipid droplets in Fig 3.3 C3, C4.

A

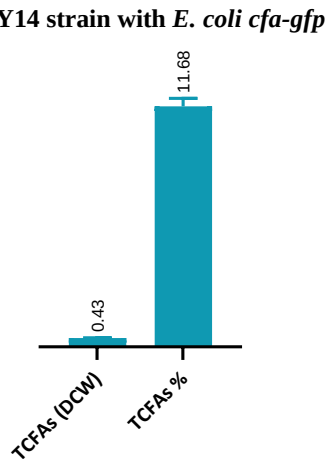
HBY14 strain with E. coli cfa-gfp
11.68
0.43
TCFAs (DCW)
TCFAs %

B

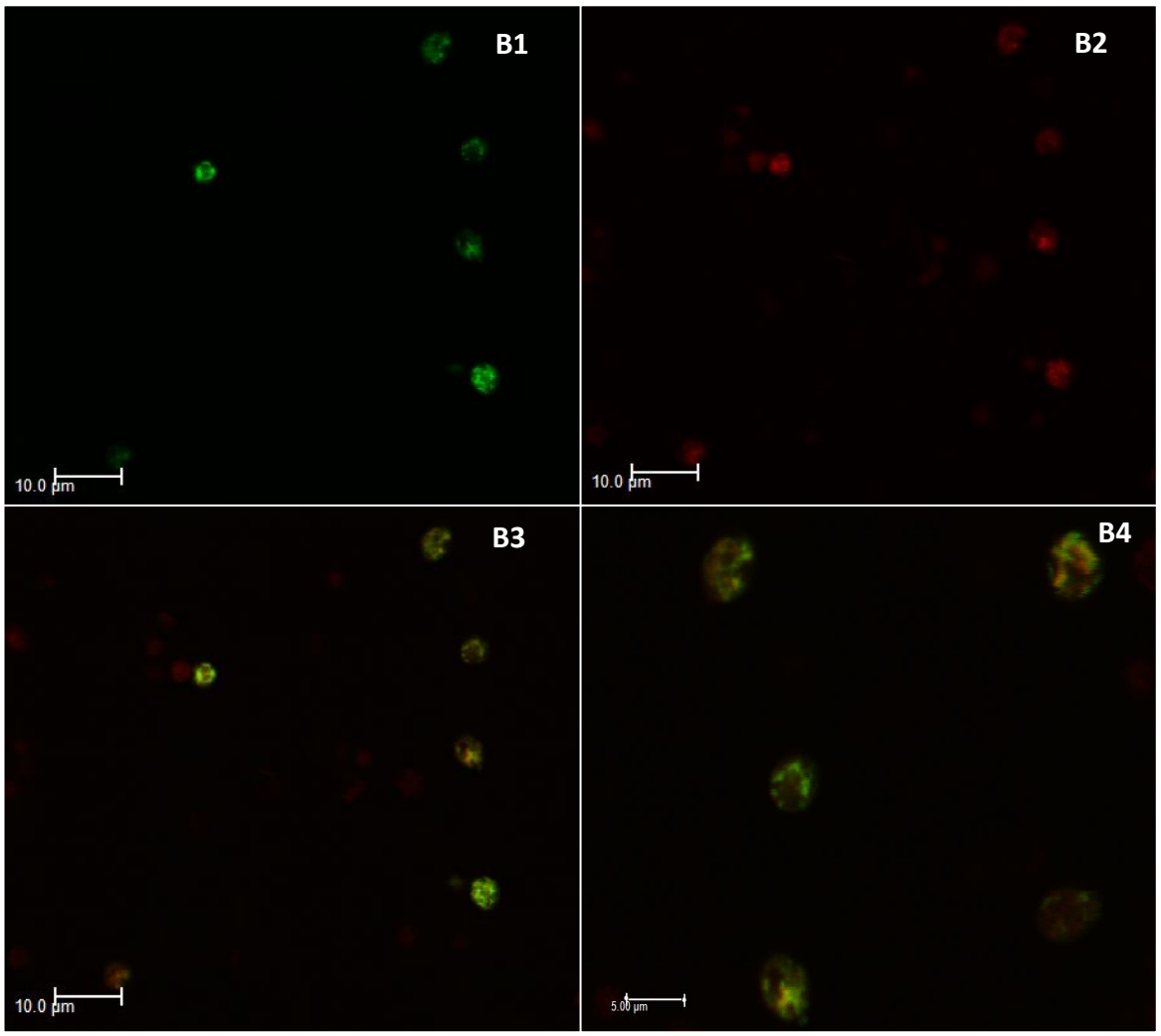
B1
10.0 µm
B2
10.0 µm
B3
10.0 µm
B4
5.00 µm

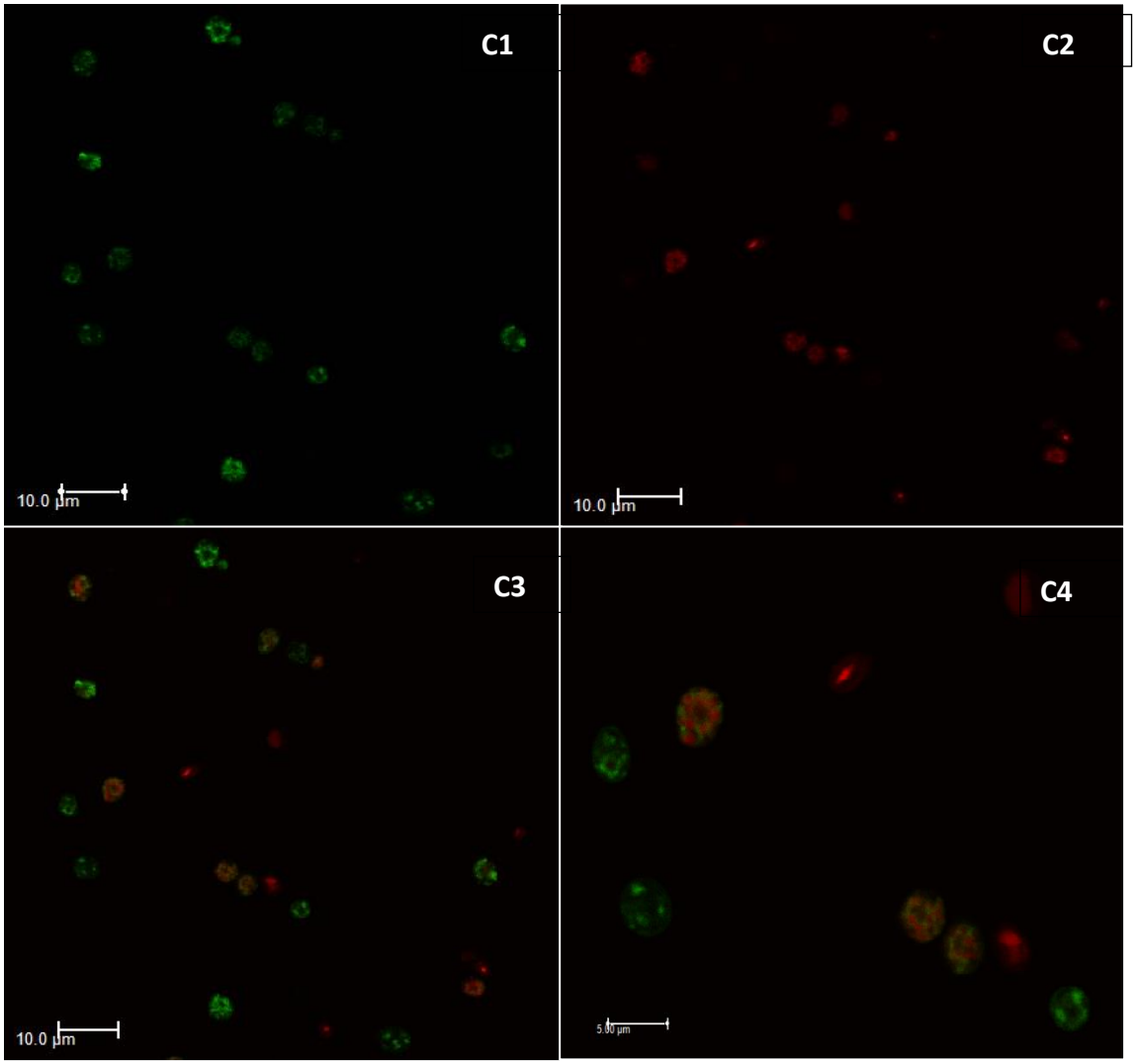

Fig 3.2 Expression and location of *Eccfa* expressed in *S. cerevisiae* (**A**) Total CFAs by weight% (DCW basis) and the percentage of CFAs in TFAs in HBY14 strain with the expression of *cfa-gfp*. Values are means of triplicate experiments ± SD, (**B1**), (**C1**) HBY yeast cells expressing the *cfa*-EGFP were imaged by confocal fluorescence microscopy, (**B2**),(**C2**) The mitochondria and lipid droplets of HBY yeast cells were stained by fluorescence dyes, Mitotracker deep red and Bodipy 558/568 C_{12}, respectively, (**B3**), (**B4**) Overlay of *cfa–gfp* and Mitotracker deep red labelled mitochondria with different magnification, (**C3**), (**C4**) Overlay of *cfa–gfp* and of Bodipy 558/568 C_{12} labelled lipid droplets at a different magnification.

.

3.3.2 Capability of yeast lipid metabolising enzymes to metabolise exogenous CFAs

Wildtype BY4741, HBY14 engineered for increased lipid production and CBY14 strain expressing *E. coli cfa* (Table 3.1) were assessed for their ability to take up and accumulate CFAs provided exogenously via the media. The fatty acid compositions of the yeasts were measured both with and without the addition of exogenous CFAs and the results are presented in Fig 3.3. CFAs were found incorporated into both TAGs and PLs in wild type BY4741 and lipid-engineered HBY14 strains after feeding CFAs (Fig 3.3 A-D). As expected, no CFAs were detected in BY4741 and HBY14 without CFAs supplement. Furthermore, in samples fed exogenously with CFAs, CFAs content in TAGs was double the content in HBY14 compared to the BY4741 strain (Fig 3.3B) whereas the CFA content in PLs in HBY14 was significantly lower than BY4741. This result can be attributed to the lipid accumulation engineering of HBY14 which promoted lipid flux towards TAGs. In addition, the percentage of CFAs of TAGs was slightly lower in HBY14 than in BY4741 strain due to the accumulation of standard fatty acids in TAGs, which accounted for the majority of the total (Fig 3.3D).

Exogenously supplied CFAs also increased internal CFAs content of PLs and TAGs in the CBY strain by more than 2- and 3-fold above the strain without CFAs supplement, respectively. Also, the content of CFAs in PLs of the CBY strain given CFAs exogenously reached 40% of the total fatty acid (Fig 3C), significantly increased from 25% of the CBY14 strain without supplementation. Taken together these results demonstrate that the native lipid metabolising enzymes of *S. cerevisiae* accepts and inserts CFAs within lipid stores within the cell, the expression of recombinant lipid metabolising enzymes such as DGAT increases CFAs content in TAGs but not preferentially above native fatty acids, and that the strain CBY14 which is engineered for production of CFAs within the cell, has extra capacity in PLs and TAGs for additional CFAs accumulation.

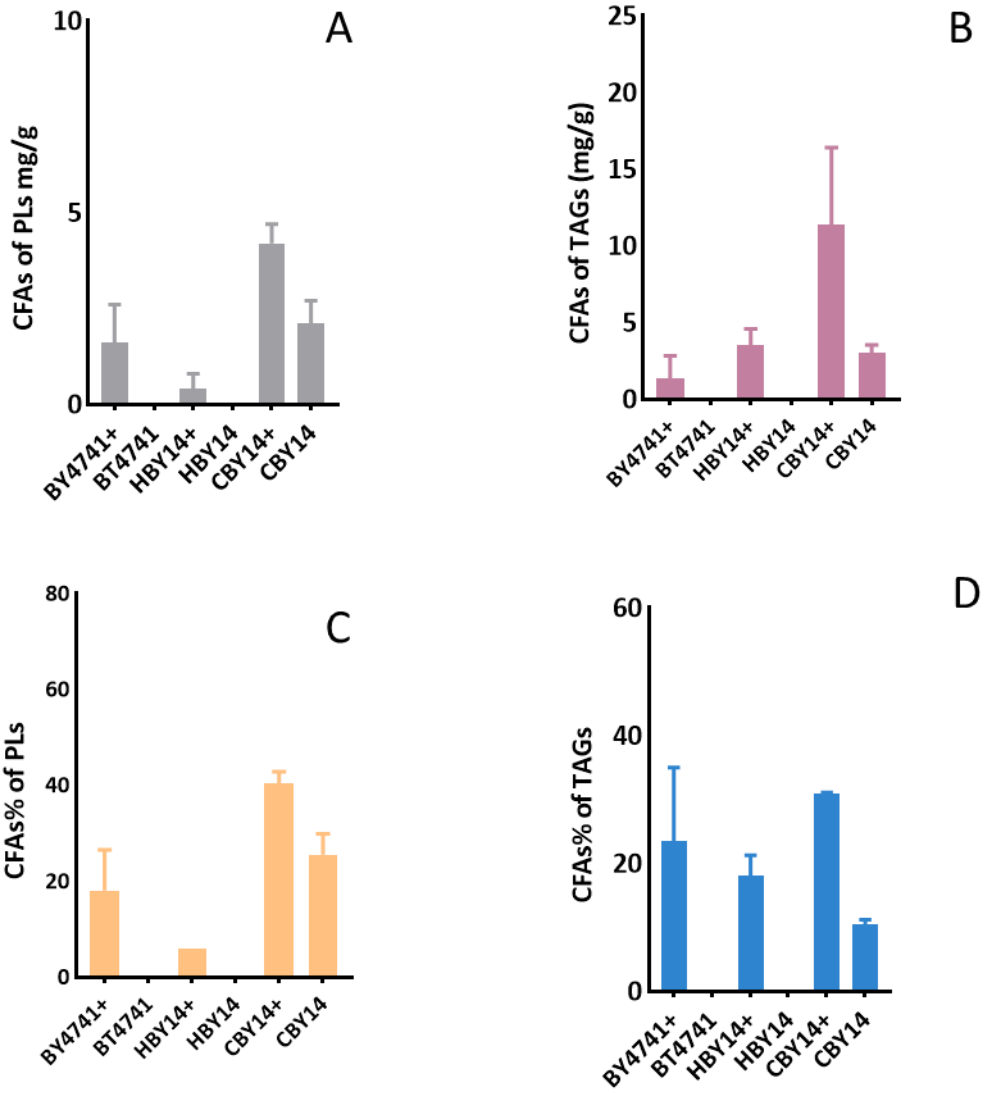

Fig 3.3 GC analysis of fatty acid composition in wild type, HBY14 and CBY14 strains with/without feeding CFAs. (**A**) CFAs of PLs (mg/g), (**B**) CFAs of TAGs (mg/g), (**C**) percentage of CFAs to total fatty acids of TAGs fraction, (**D**) percentage of CFAs to total fatty acids of PLs fraction. Values are means of triplicate experiments ± SD.

3.3.3 Compositional analysis of CFAs in PLs

In order to investigate the effect of *E. coli cfa* synthase on the composition of yeast membrane phospholipids, a compositional analysis of CFAs in PLs was carried out. Fatty acid composition of *sn-1* and *sn-2* positions of PLs in BY4741, CBY4741 and CBYO strains are summarised in Table 3.2 and the genotype of these strains are presented in Table 3.1. In the BY4741 strain, the fatty acids C16:1 and C18:1 were found in both *sn-2* and *sn-1* positions but the majority were in the *sn*-2 position, which illustrates unsaturated fatty acids (UFAs) are the main component at the *sn*-2 position, while saturated fatty acids (SFAs) take up the majority in the *sn*-1 position. After the expression of *E. coli cfa*, the UFAs in both of *sn*-1 and *sn*-2 positions were significantly reduced, to the extent of being absent in the *sn*-1 position. CFAs content was significantly higher in *sn-2* compared with *sn-1* position. When the yeast delta-9 desaturase (*Scole1*), which catalyses the formation of the initial double bond between the 9^{th} and 10^{th} carbons of both palmitoyl (16:0) and stearoyl (18:0) CoA substrate to form UFAs C16:1 and C18:1 (Bossie & Martin, 1989), was overexpressed in the strain also expressing *E coli cfa*, the CFAs content in *sn*-2 and *sn*-1 position significantly increased above the *cfa*-only strain. Concomitantly, the concentration of UFA was reduced in the *sn*-1 and *sn*-2 positions of these PLs. The effect of expression of *E. coli cfa* and *Scole1* on the fatty acids composition of PLs further demonstrates *E. coli cfa* synthase acts on the membrane systems of cells, which is consistent with the result of subcellular localisation of *E. coli cfa* synthase. In addition, it was shown that CFAs are formed in both *sn*-1 and *sn*-2 positions and that UFAs are the precursors of CFAs in yeast.

Table 3.2 Fatty acid composition at the sn-1 and sn-2 positions of yeast PLs (Data are means of triplicate experiments ± SD)

Strain	**Position in PSs**	**Percentage %** C16:1	C16:0	C18:1	C18:0	CFAs
BY4741	*sn*-2	45.65 ± 5.38	7.01 ± 3.45	40.84 ± 0.03	5.78 ± 2.93	0.00 ± 0.00
	sn-1	8.48 ± 1.04	41.85 ± 2.42	17.78 ± 3.99	31.89 ± 2.61	0.00 ± 0.00
CBY4741	*sn*-2	24.74 ± 2.47*	11.14 ± 2.39	24.05 ± 2.84*	8.17 ± 1.74	29.90 ± 1.68**
	sn-1	0.00 ± 0.00**	41.56 ± 0.60	0.00 ± 0.00*	42.24 ± 2.02	16.20 ± 2.62*
CBYO	*sn*-2	6.27 ± 5.54*	6.29 ± 3.56	10.91 ± 5.33*	5.31 ± 3.47	69.77 ± 5.88**
	sn-1	0.00 ± 0.00**	39.73 ± 3.44	0.00 ± 0.00*	33.82 ± 1.61	26.45 ± 5.05*

Notes: * Represented that the effect of factor was significant at $p < 0.05$ (Students t-test). ** Represented that the effect of factor was significant at $p < 0.01$ (t-test).

3.3.4 Overcome substrates limitation of *E. coli cfa* synthase

Based on the above results, the delta-9 desaturase (*Scole1*) was introduced into the engineered strain expressing *AtDAGT1* and deleted *tgl3*, to attempt to increase the precursor UFAs of CFAs. Besides UFAs, S-adenosylmethionine is another important substrate/cofactor for *E. coli cfa* synthase which provides a methyl group for the formation of the cyclopropane ring (Grogan & Cronan, 1997). Therefore, the S-adenosylmethionine synthase 2 (*ScSAM2*) was overexpressed in the same engineered strain to attempt to increase the availability of S-adenosylmethionine. As Fig 3.4A and B show, PLs content was relatively stable with around 1% in these engineered strains. Expression of *AtDAGT1* and deletion of *tgl3* was beneficial for the accumulation of TAGs in these strains as compared with CBY4741, Δ*tgl3* led to a significant increase in TAGs content when combined with *AtDGAT1*. When *Scole1* and *Scsam2* were expressed separately in the higher lipid-producing strain (CBY14), there was no significant improvement of TAGs or CFAs content over that strain (Fig 3.4). However, overexpression of both *Scole1 and Scsam2* in the same strain significantly increased TAGs content and CFAs amount in TAGs on a dried weight basis (Fig 3.4 B, D). As standard fatty acid content was increased alongside that of CFAs in TAGs, the percentage of CFAs as a proportion of all TAGs decreased in the CBYO+SAM2 strain (Fig 3.4 F). Interestingly, CFAs content in PLs of the CBYO+SAM2 strain was the highest among the engineered strains (Fig 3.4 E) suggesting the formation of CFAs on PLs is not the rate-limiting step and that turnover of CFAs from PLs to TAGs may be the bottleneck in achieving greater accumulation of CFAs in TAGs in these engineered *S. cerevisiae* strains.

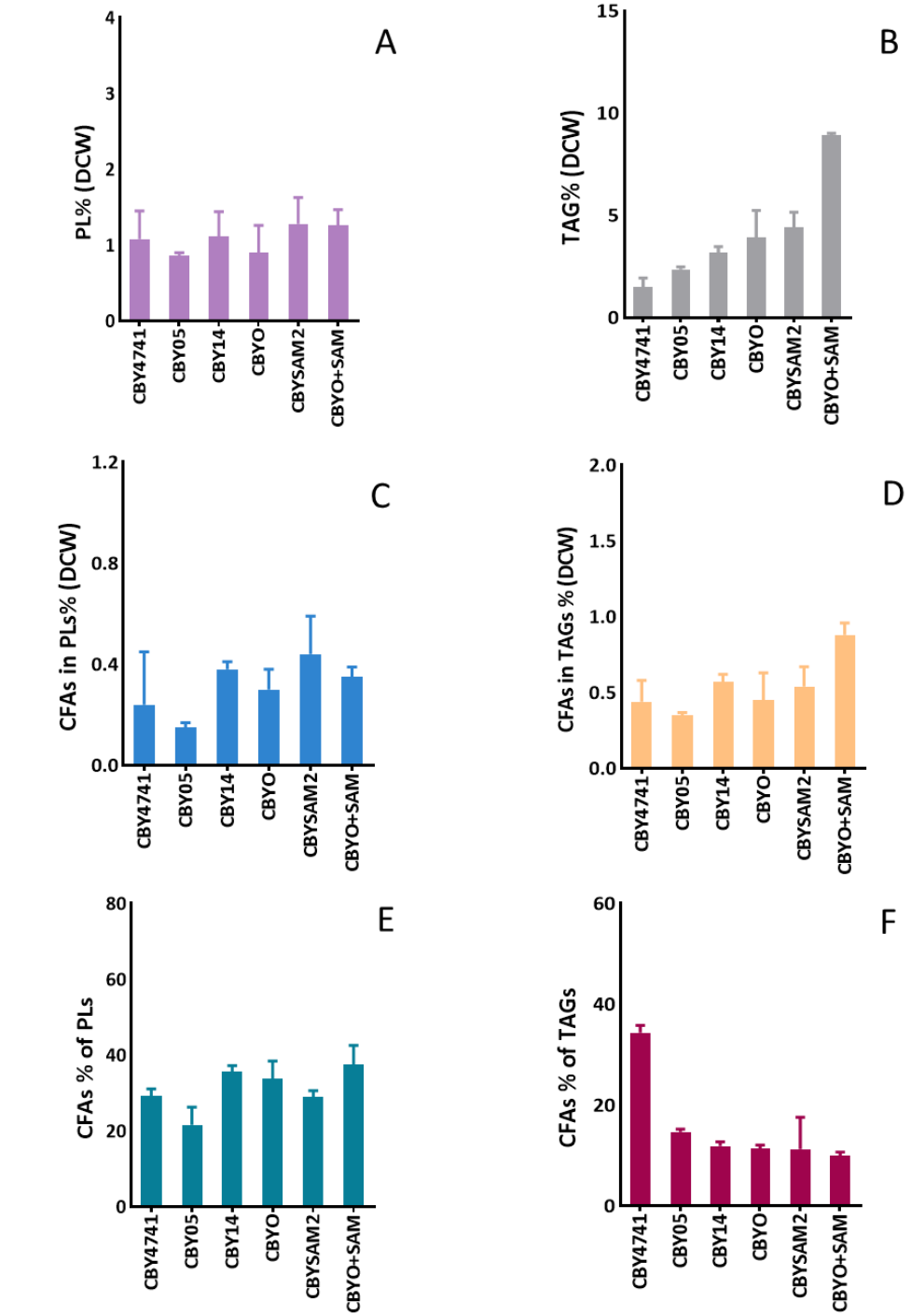

E. coli cfa	✓	✓	✓	✓	✓	✓
AtDGAT1			✓	✓	✓	✓
Scole1				✓		✓
Scsam2					✓	✓
Δtgl3		✓	✓	✓	✓	✓

E. coli cfa	✓	✓	✓	✓	✓	✓
AtDGAT1			✓	✓	✓	✓
Scole1				✓		✓
Scsam2					✓	✓
Δtgl3		✓	✓	✓	✓	✓

Fig 3.4 The effect of expression of *ole1*and *sam2* on CFAs content in lipid fractions of engineered strains. (**A**) total PLs content (mg/g), (**B**) total TAGs content (mg/g), (**C**) CFAs of PLs (mg/g), (**D**) CFAs of TAGs (mg/g), (**E**) percentage of CFAs to total fatty acids of PLs fraction, (**F**) percentage of CFAs to total fatty acids of TAGs fraction. Values are means of triplicate experiments ± SD.

Notes: * Represented that the effect of factor was significant at $p < 0.05$ (t-test).

3.3.5 CFAs turnover to TAGs

The strategy designed to enhance lipid formation and the flux of CFAs-modified fatty acids from PLs into TAGs to increase CFAs in storage lipid is shown in Fig 3.1. Firstly, the substrate pools for *E. coli cfa* synthase, unsaturated fatty acids and SAM were increased by overexpression of *Scole1* and *Scsam2*. Next, to increase the rate of transfer of CFAs from PLs to TAGs, overexpression of a native phospholipase (phospholipase B2, *Plb2*) was attempted. Then, to increase the likelihood of the free fatty acids released from the PLs by the phospholipase being incorporated into TAGs, the expression of one of a range of acyl-CoA synthases was investigated.

Phospholipase B2 (*Plb2*) cleaves the acyl chain at the *sn*-1 and *sn*-2 positions from the backbone of PL (Ferreira et al., 2018b). The overexpression of *plb2* in the strain expressing *Scole1* and *Scsam* resulted in dramatic changes; a significantly reduced amount of PLs compared to the parent strain (Fig 3.5 A) and reduced TAGs content (Fig 3.5 B). The CFAs levels were also reduced in this strain in the PLs and TAGs and this was reflected in the percentage of CFAs to standard fatty acids in both these fractions (Fig 3.4 C – F). These results indicate CFAs (and other fatty acids) were released from PLs by *Plb2* but were not increased in the TAGs fraction.

As phospholipases hydrolyse acyl chains and release free fatty acids; these products are potentially being metabolised and are not incorporated into TAGs. Therefore, to facilitate the conversion of free CFAs released from the PLs into TAGs, a range of acyl CoA synthases were introduced into the engineered strain expressing *Plb2*. The aim was to increase conversion of free CFAs to CFAs-CoA via the expression of *fadD* from *Sinorhizobium meliloti*, or *AtLACS* from *Arabidopsis thaliana* or *DuLACS* from *Durio zibethinus*. CFA-CoA would be directed to TAGs with the catalysis of *AtDGAT1* (Fig 3.1). Among the three acyl-CoA synthases, the effect of *fadD* expression was most useful. Compared with the CBYPOS strain, the expression of *fadD* tripled CFAs in TAGs on a dried weight basis (Fig 3.5D) and the CFAs proportion in TAGs increased by 10% compared with the CBYPOS strain (Fig 3.5F). *AtLACS* or *DuLACS* expression in the CBYPOS strain had similar impacts on CFAs content to *fadD* in PLs and TAGs but were less effective.

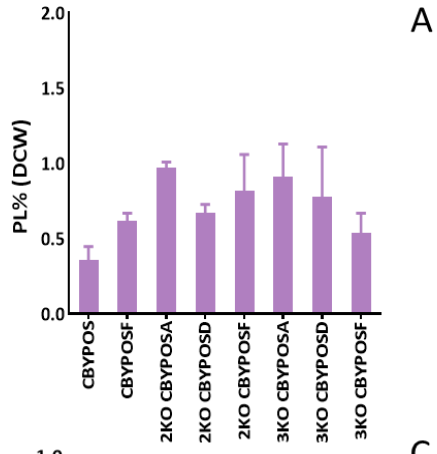

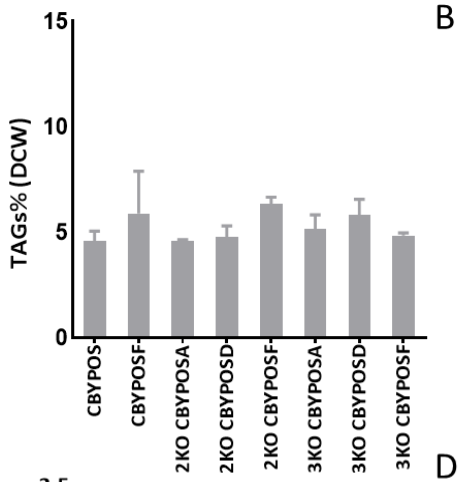

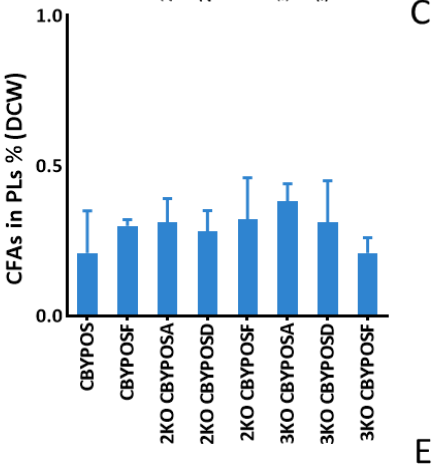

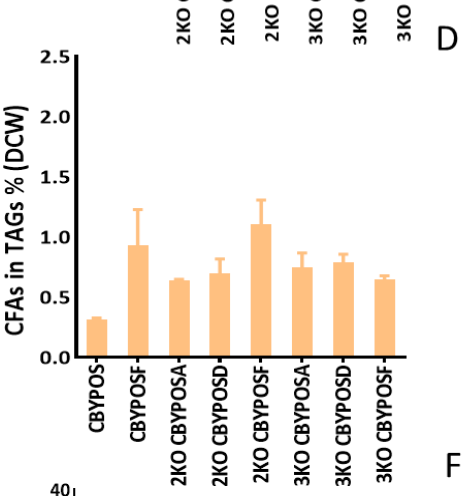

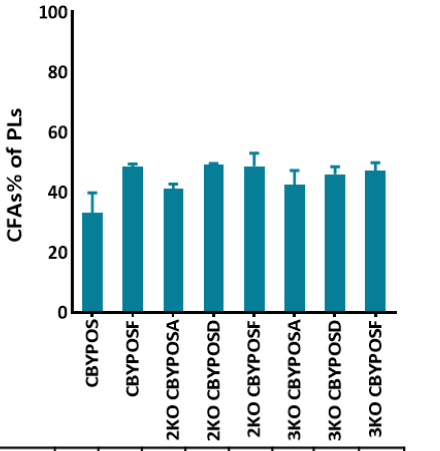

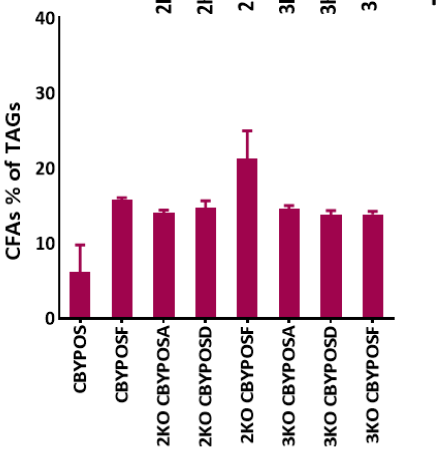

E. coli cfa-AtDGAT1-Scole1-Scsam2-Δtgl3	✓	✓	✓	✓	✓	✓	✓	✓
fadd		✓			✓			✓
DuLACS				✓			✓	
AtLACS			✓			✓		
Δpox1			✓	✓	✓			
Δare1& Δare2						✓	✓	✓

E. coli cfa-AtDGAT1-Scole1-Scsam2-Δtgl3	✓	✓	✓	✓	✓	✓	✓	✓
fadd		✓			✓			✓
DuLACS				✓			✓	
AtLACS			✓			✓		
Δpox1			✓	✓	✓			
Δare1& Δare2						✓	✓	✓

Fig 3.5 The effect of expression of *Plb2*, *fadD*, *AtLACS*, *DuLACS*, the KO of *pox1* and the KOs of *are1* and *are2* on CFAs content in lipid fractions of engineered strains. (**A**) total PLs content (mg/g), (**B**) total TAGs content (mg/g), (**C**) CFAs of PLs (mg/g), (**D**) CFAs of TAGs (mg/g), (**E**) percentage of CFAs to total fatty acids of PLs fraction, (**F**) percentage of CFAs to total fatty acids of TAGs fraction. Values are means of triplicate experiments ± SD. Notes: * Represented that the effect of the factor was significant at $p < 0.05$ (t-test). ** Represented that the effect of the factor was significant at $p < 0.01$ (t-test).

3.3.6 Blocking β-oxidation of fatty acids

To prevent consumption of fatty acids that were liberated from the membranes and to favour the increase of CFAs storage in TAGs, the β-oxidation of fatty acids was blocked by the deletion of acyl-coenzyme A oxidase *(Pox1*) in the CBYPOSF strain. This strain already has the major triglyceride lipase (*tgl3*) deleted to reduce the release of TAGs from lipid droplets and is termed 2KO. Also, to prevent acyl-CoA from forming sterol esters at the expense of TAGs, knockouts of *are1* and *are2* encoding sterol O-acyltransferases were performed. While deleting *Pox1* did not result in significantly increased TAGs content, both CFAs content in TAGs and the percentage of fatty acids that were present as CFAs in TAGs were highest in 2KOCBYPOSF strain (Fig 3.5 D, F). This result suggested that some CFA was being consumed via β-oxidation before it reached storage TAGs. CFAs production in TAGs in 2KOCBYPOSF strains reached 12.17 mg/g.

Conversely, the deletion of *are1* and *are2* did not improve the overall yield of TAGs nor increase the amount, on a dried weight basis, or on a percentage basis, of CFAs in TAGs (Fig 3.5 D, F) indicating CFAs was not being routed towards the formation of sterol esters in the CBYPOSF strain.

3.4 Discussion

Two major routes of TAGs formation are found in *S. cerevisiae* in yeast: the acyl-CoA independent pathway, and the acyl-CoA dependent pathway (Beopoulos et al., 2008; Czabany et al., 2007; Daum et al., 2007). Exogenous fatty acids supplied to yeast may be activated into the coenzyme A form, then taken via the acyl-CoA dependent route to synthesise TAGs via acylation reactions with the glycerol backbone, or alternatively to form PLs (Færgeman et al., 2001; Papanikolaou & Aggelis, 2011). Most yeast investigated to date do not produce CFAs natively. Therefore, CFAs are a new exotic fatty acid for yeasts, and it is unknown whether the native lipid pathway enzymes in yeasts, which normally handle C16 and C18 saturated and monounsaturated fatty acids, can utilise CFAs either generated intracellularly or supplied as an exogenous fatty acid in media. When supplemented as an exogenous fatty acid, CFAs provided to *S. cerevisiae* strains BY4741 and HBY14 was identified in both PLs and TAGs fractions, suggesting the endogenous yeast enzymes such as acyl-CoA synthetase can activate CFAs, and acyl transferases can esterify CFA-CoA to the glycerol backbone of TAGs. Therefore, in the case of intracellular production of CFAs, it is expected that CFAs can be incorporated into TAGs using the native CoA-dependent pathway. However, the HBY14 strain supplemented with CFAs in the media resulted in around 18% of the total fatty acids being CFAs and the majority of the fatty acids in TAGs were standard fatty acids. Therefore, selecting an acyltransferase with a preference for CFAs may improve the flux of CFAs into TAGs.

Expression of the *cfa-gfp* fusion protein in *S. cerevisiae* maintained it cyclopropanation activity as CFAs production after expressing *cfa-gfp* was consistent with that of an earlier report in the same base strain (Peng et al., 2018a), and illustrated that the function of *E. coli cfa* synthase was not affected by its fusion with GFP. Through the expression of a GFP-fused reporter protein, it was found that *E. coli cfa* synthase localised to the plasma membranes of yeast cells similarly to its known site of action when expressed natively in *E. coli (*Grogan &

Cronan Jr, 1997*)*. Labelling mitochondria and lipid droplets with fluorescent probes suggested *E. coli cfa* synthase-GFP was also present on the membranes of these organelles. As a prokaryote, *E. coli* lacks internal membranes and organelles and while *E. coli cfa* has been expressed in eukaryotes, this phenomenon has not been previously reported. Therefore, it can be concluded that *E. coli cfa* synthase acts on the membrane system of recombinant yeast cells.

Although the subcellular localisation revealed the relationship between the *E. coli cfa* synthase and yeast membrane system, how the *E. coli cfa* synthase affects the composition of membrane phospholipids is still unknown. Therefore, the compositional analysis of CFAs in PLs was carried out to investigate the change of phospholipids. Fatty acid positional analysis of the phospholipids in yeast expressing *E. coli cfa* shows CFAs were added to both positions, *sn*-1 and *sn*-2, and that UFAs were preferentially converted to CFAs in this fraction. This is advantageous for the maximising of CFAs yield in yeast as the concentration can be increased through the conversion at both PLs positions. However, it also suggests that the amount of UFA on PLs is rate-limiting for the production of CFAs. The overexpression of the Δ9-desaturase, *Scole1*, in the CFA-producing strain relieved this limit by increasing the UFA pool in the PLs of yeast and increasing the pool of SAM substrate by overexpression *Scsam2* could overcome the limitation of the substrates for *E. coli cfa* synthase. This combination greatly enhanced CFAs content in PLs and TAGs and the percentage of CFAs accounting for PLs and TAGs.

Although total CFAs content increased under the impact of *Scole1* and *Scsam2* overexpression, the PLs fraction remained rich in CFAs which are available to be transferred to storage TAGs. As the positional analysis showed CFAs occupying both positions, phospholipase B2, *plb2*, was overexpressed to release CFAs-containing acyl chains from PLs as it cleaves from both positions. No obvious impacts were observed in recombinant yeast by

expressing plb2, which accords with earlier research (Ferreira et al., 2018b). The released free fatty acids require activation to acyl-CoA forms for incorporation into TAGs and three candidates: *FadD, AtLACS* and *DuLACS* were compared for their impact on CFAs incorporation into TAGs. *FadD* encodes an acyl-coenzyme A (CoA) synthase in bacterial systems, such as *E. coli*, *Sinorhizobium meliloti* and *Pseudomonas aeruginosa*, and are responsible for the activation of exogenous long-chain fatty acids (Kang et al., 2010; Soto et al., 2002; Weimar et al., 2002). In 2011, Lo´pez-Lara et al. detected CFAs in the free fatty acid fraction of the *ΔfadD* mutant *S. meliloti* while no CFAs were found among free fatty acids of the wild type strain. As cyclopropane fatty acyl residues are esterified to membrane lipids in bacteria (Grogan & Cronan, 1997), therefore, Lo´pez-Lara's results suggested that the accumulation of CFAs in free fatty acids originated from membrane lipids. They concluded that *fadD* was required for the utilisation of endogenous fatty acids released from membrane lipids (Pech-Canul et al., 2011). Therefore, it can be inferred that *FadD* utilises CFAs when heterogeneously expressed in yeast. Compared with the activities of *AtLACS* and *DuLACS*, the effect of *FadD* was prominent.

Now having increased the likelihood of CFAs-CoA formation through the expression of *FadD*, its flux into TAGs can be improved by the expression of the diacyl acyltransferase, *AtDGAT1*, which increased cellular TAGs content. However, acyl-CoA can also be consumed by β-oxidation which is carried out in the peroxisomes of yeast. Although more CFA-CoA could be produced by expressing acyl-CoA synthase, some CFAs-CoA may be consumed via β- oxidation rather than storage in TAGs. β-Oxidation was blocked in the *FadD* strain by deletion of *pox1,* which further increased the accumulation of CFAs in TAGs. Oxidation of FA by β-oxidation in yeast can generate energy. In *S. cerevisiae,* only the gene *pox1* encoding peroxisomal acyl-CoA oxidase determines the flux through the β-oxidation (Dmochowska et al., 1990; Hiltunen et al., 2003). Therefore, deletion of *pox1* is usually an

effective approach for the enhancement of fatty acids biosynthesis. For example, Valle-Rodriguez et al' (2014) deleted *pox1* avoiding FA degradation as well as *dga1*, *lro1*, *are1*, and *are2* blocking the formation of neutral lipid whereby the engineered *S. cerevisiae* reached 1.5% intracellular free fatty acids by DCW, 5-fold higher than control (Valle-Rodríguez et al., 2014). The Nielsen group also adopted the strategy of blocking lipid degradation (*Δtgl3, 4, 5, Δpox1, Δpxa1*) to increase TAGs accumulation in *S. cerevisiae*. Finally, the TAGs yield could reach 254 mg TAG/g DCW (Ferreira et al., 2018a).

Reviewing the impacts of the metabolic engineering strategy as a whole, it can be concluded that for CFAs production, facilitating the cycling of fatty acids from membrane phospholipids to storage triglycerides was successful. Compared with the strain only expressing *E coli cfa*, the CFAs concentration in TAGs by DCW was improved by around 3-fold in the final strain. Although CFAs yield was improved, employing lipid metabolising enzymes such as fatty acid transferases with greater specificity for CFAs may further improve CFAs accumulation. In brief, the strains developed in this study strongly contribute to fundamental insights into CFAs microbial biosynthesis, they can also serve as a good reference for the production of other exotic fatty acids that are similarly converted on phospholipid membranes in yeast such as ricinoleic acid.

3.5 References

Beopoulos, A., Mrozova, Z., Thevenieau, F., Le Dall, M.-T., Hapala, I., Papanikolaou, S., Chardot, T., Nicaud, J.-M. 2008. Control of lipid accumulation in the yeast Yarrowia lipolytica. *Applied and environmental microbiology*, **74**(24), 7779-7789.

Bligh, E.G., Dyer, W.J. 1959. A rapid method of total lipid extraction and purification. *Canadian journal of biochemistry and physiology*, **37**(8), 911-917.

Bossie, M.A., Martin, C.E. 1989. Nutritional regulation of yeast delta-9 fatty acid desaturase activity. *Journal of bacteriology*, **171**(12), 6409-6413.

Czabany, T., Athenstaedt, K., Daum, G. 2007. Synthesis, storage and degradation of neutral lipids in yeast. *Biochimica et Biophysica Acta (BBA)-Molecular and Cell Biology of Lipids*, **1771**(3), 299-309.

Daum, G., Wagner, A., Czabany, T., Athenstaedt, K. 2007. Dynamics of neutral lipid storage and mobilization in yeast. *Biochimie*, **89**(2), 243-248.

Dmochowska, A., Dignard, D., Maleszka, R., Thomas, D. 1990. Structure and transcriptional control of the Saccharomyces cerevisiae POX1 gene encoding acylcoenzyme A oxidase. *Gene*, **88**(2), 247-252.

Færgeman, N.J., Black, P.N., Zhao, X.D., Knudsen, J., DiRusso, C.C. 2001. The acyl-CoA synthetases encoded within FAA1 and FAA4 in Saccharomyces cerevisiae function as components of the fatty acid transport system linking import, activation and intracellular utilization. *Journal of Biological Chemistry*, 276(40): 37051-37059..

Ferreira, R., Teixeira, P.G., Gossing, M., David, F., Siewers, V., Nielsen, J. 2018a. Metabolic engineering of Saccharomyces cerevisiae for overproduction of triacylglycerols. *Metabolic engineering communications*, **6**, 22-27.

Ferreira, R., Teixeira, P.G., Siewers, V., Nielsen, J. 2018b. Redirection of lipid flux toward phospholipids in yeast increases fatty acid turnover and secretion. *Proceedings of the National Academy of Sciences*, **115**(6), 1262-1267.

Gontier, E., Thomasset, B., Wallington, E., Wilmer, J. 2008. Plant Cyclopropane Fatty Acid Synthase Genes and Uses Thereof, Google Patents.

Grogan, D.W., Cronan, J.E. 1997. Cyclopropane ring formation in membrane lipids of bacteria. *Microbiol. Mol. Biol. Rev.*, **61**(4), 429-441.

Grogan, D.W., Cronan Jr, J.E. 1997. Cyclopropane ring formation in membrane lipids of bacteria. *Microbiology and Molecular Biology Reviews*, **61**(4), 429-441.

Hiltunen, J.K., Mursula, A.M., Rottensteiner, H., Wierenga, R.K., Kastaniotis, A.J., Gurvitz, A. 2003. The biochemistry of peroxisomal β-oxidation in the yeast Saccharomyces cerevisiae. *FEMS microbiology reviews*, **27**(1), 35-64.

Huang, Y.-S., Chaudhary, S., Thurmond, J.M., Bobik, E.G., Yuan, L., Chan, G.M., Kirchner, S.J., Mukerji, P., Knutzon, D.S. 1999. Cloning of Δ12-and Δ6-desaturases from Mortierella alpina and recombinant production of γ-linolenic acid in Saccharomyces cerevisiae. *Lipids*, **34**(7), 649-659.

Jiang, W., Peng, H., Ledesma Amaro, R., Haritos, V.S. 2021. Metabolic Engineering of Yeast for Enhanced Natural and Exotic Fatty Acid Production. in: *Emerging Technologies for Biorefineries, Biofuels, and Value-Added Commodities*, Springer, pp. 207-228.

Kainou, K., Kamisaka, Y., Kimura, K., Uemura, H. 2006. Isolation of Δ12 and ω3-fatty acid desaturase genes from the yeast Kluyveromyces lactis and their heterologous expression to produce linoleic and α-linolenic acids in Saccharomyces cerevisiae. *Yeast*, **23**(8), 605-612.

Kang, Y., Zarzycki-Siek, J., Walton, C.B., Norris, M.H., Hoang, T.T. 2010. Multiple FadD acyl-CoA synthetases contribute to differential fatty acid degradation and virulence in Pseudomonas aeruginosa. *PLoS One*, **5**(10), e13557.

Klug, L., Daum, G. 2014. Yeast lipid metabolism at a glance. *FEMS yeast research*, **14**(3), 369-388.

Papanikolaou, S., Aggelis, G. 2011. Lipids of oleaginous yeasts. Part I: Biochemistry of single cell oil production. *European Journal of Lipid Science and Technology*, **113**(8), 1031-1051.

Pech-Canul, Á., Nogales, J., Miranda-Molina, A., Álvarez, L., Geiger, O., Soto, M.J., López-Lara, I.M. 2011. FadD is required for utilization of endogenous fatty acids released from membrane lipids. *Journal of bacteriology*,. **193**(22), 6295-6304.

Peng, H., He, L., Haritos, V.S. 2018a. Enhanced Production of High-Value Cyclopropane Fatty Acid in Yeast Engineered for Increased Lipid Synthesis and Accumulation. *Biotechnology journal*, **14**(4), 1800487 .

Peng, H., He, L., Haritos, V.S. 2018b. Metabolic engineering of lipid pathways in Saccharomyces cerevisiae and staged bioprocess for enhanced lipid production and cellular physiology. *Journal of Industrial Microbiology and Biotechnology*, **45**(8), 707-717.

Peng, H., Moghaddam, L., Brinin, A., Williams, B., Mundree, S., Haritos, V.S. 2018c. Functional assessment of plant and microalgal lipid pathway genes in yeast to enhance microbial industrial oil production. *Biotechnology and applied biochemistry*, **65**(2), 138-144.

Runguphan, W., Keasling, J.D. 2014. Metabolic engineering of Saccharomyces cerevisiae for production of fatty acid-derived biofuels and chemicals. *Metabolic engineering*, **21**, 103-113.

Schmid, K.M. 1999. Cyclopropane fatty acid expression in plants, Google Patents.

Shockey, J., Kuhn, D., Chen, T., Cao, H., Freeman, B., Mason, C. 2018. Cyclopropane fatty acid biosynthesis in plants: phylogenetic and biochemical analysis of Litchi Kennedy pathway and acyl editing cycle genes. *Plant cell reports*, **37**(11), 1571-1583.

Siloto, R.M., Truksa, M., He, X., McKeon, T., Weselake, R.J. 2009. Simple methods to detect triacylglycerol biosynthesis in a yeast-based recombinant system. *Lipids*, **44**(10), 963.

Soto, M.J., Fernández-Pascual, M., Sanjuan, J., Olivares, J. 2002. A fadD mutant of Sinorhizobium meliloti shows multicellular swarming migration and is impaired in nodulation efficiency on alfalfa roots. *Molecular microbiology*, **43**(2), 371-382.

Suzuki, M., Shinohara, Y., Fujimoto, T. 2012. Histochemical detection of lipid droplets in cultured cells. in: *Cell Imaging Techniques*, Springer, pp. 483-491.

Taylor, F.R., Cronan Jr, J.E. 1979. Cyclopropane fatty acid synthase of Escherichia coli. Stabilization, purification, and interaction with phospholipid vesicles. *Biochemistry*, **18**(15), 3292-3300.

Valle-Rodríguez, J.O., Shi, S., Siewers, V., Nielsen, J. 2014. Metabolic engineering of Saccharomyces cerevisiae for production of fatty acid ethyl esters, an advanced biofuel, by eliminating non-essential fatty acid utilization pathways. *Applied energy*, **115**, 226-232.

Wang, A.Y., Grogan, D.W., Cronan Jr, J.E. 1992. Cyclopropane fatty acid synthase of Escherichia coli: deduced amino acid sequence, purification, and studies of the enzyme active site. *Biochemistry*, **31**(45), 11020-11028.

Weimar, J.D., DiRusso, C.C., Delio, R., Black, P.N. 2002. Functional role of fatty Acyl coenzyme a synthetase in the transmembrane movement and activation of exogenous long-chain fatty acids: amino acid residues within the ATP/AMP signature motif of FadD of Escherichia coli are required for enzyme activity and fatty acid transport. *Journal of Biological Chemistry*, **277**(33): 29369-29376.

Xue, P., Siloto, R.M., Wickramarathna, A.D., Mietkiewska, E., Weselake, R.J. 2013. Identification of a pair of phospholipid: diacylglycerol acyltransferases from developing flax (Linum usitatissimum L.) seed catalyzing the selective production of trilinolenin. *Journal of Biological Chemistry*. M113. 475699.

Yu, X.-H., Prakash, R.R., Sweet, M., Shanklin, J. 2014. Coexpressing Escherichia coli cyclopropane synthase with Sterculia foetida lysophosphatidic acid acyltransferase enhances cyclopropane fatty acid accumulation. *Plant physiology*, **164**(1), 455-465.

Yu, X.H., Cahoon, R.E., Horn, P.J., Shi, H., Prakash, R.R., Cai, Y., Hearney, M., Chapman, K.D., Cahoon, E.B., Schwender, J. 2018. Identification of bottlenecks in the accumulation of cyclic fatty acids in camelina seed oil. *Plant biotechnology journal*, **16**(4), 926-938.

3.6 Supplementary information

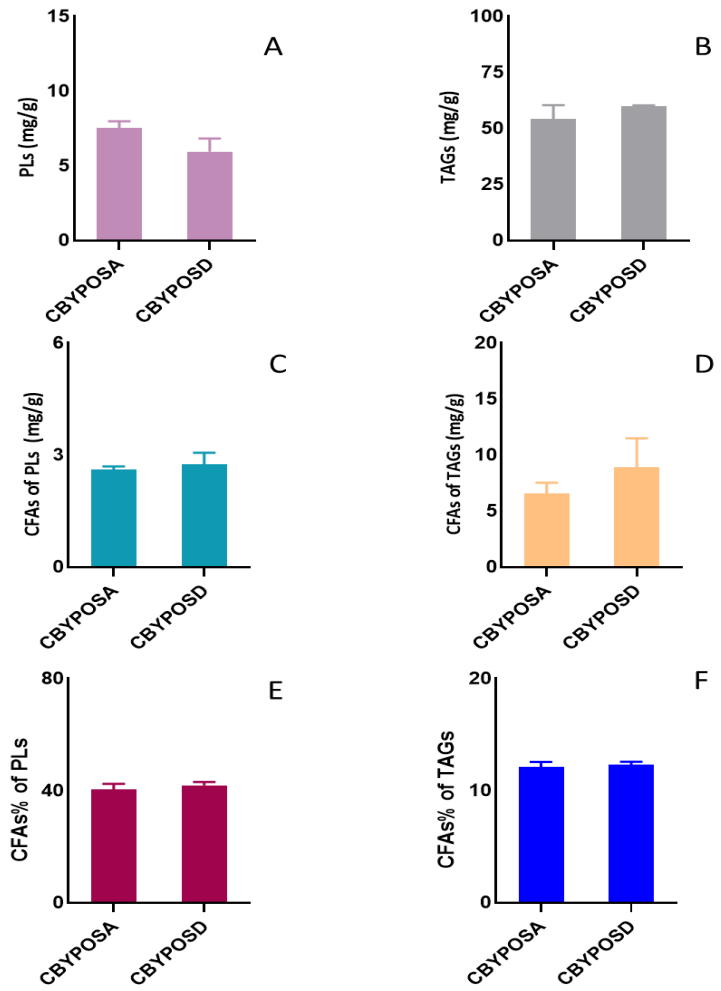

Fig S3. 1 Fatty acids analysis of the strains CBYPOSA and CBYPOSD, (**A**) total PLs content (mg/g), (**B**) total TAGs content (mg/g), (**C**) CFAs of PLs (mg/g), (**D**) CFAs of TAGs (mg/g), (**E**) percentage of CFAs to total fatty acids of PLs fraction, (**F**) percentage of CFAs to total fatty acids of TAGs fraction. Values are means of triplicate experiments ± SD.

CHAPTER 4

TRANSFERRAL OF THE CFAs METABOLIC ENGINEERING STRATEGY DEVELOPED FOR *SACCHAROMYCES CEREVISIAE* TO *YARROWIA LIPOLYTICA*

This page is intentionally blank

Chapter 4 Transferral of the CFAs metabolic engineering strategy developed for *Saccharomyces cerevisiae* to *Yarrowia lipolytica*

Abstract

Y. lipolytica as an oleaginous yeast is a potential host organism for exotic fatty acids production. In this chapter, the CFAs metabolic engineering strategy developed for *S. cerevisiae* (Chapter 3), which cycled fatty acids from membranes to triacylglycerols, was transferred into *Y. lipolytica*. The most impactful genes verified in Chapter 3 were introduced into *Y. lipolytica* genome having a background of lipid enhancement. While overall lipid content, total CFAs content and the proportion of fatty acids that were oleic acid were increased in engineered *Y. lipolytica*, the low expression of *E. coli* cyclopropane fatty acid synthetase restricted the quantity of CFAs that could be produced. Thus, improved *cfa* expression will be the required first step before the effectiveness of the fatty acid cycling strategy can be fully tested in *Y. lipolytica*.

4.1 Introduction

Oleaginous microorganisms can produce bio-oils with high yield, which naturally accumulate lipids occupying from 20% to 80% of the dry cell weight (DCW) (Sitepu et al., 2014). Modifying these oleaginous microorganisms to produce lipids of higher utility than standard fatty acids often faces the challenge of a lack of genetic tools and metabolic pathway knowledge to improve productivity. Among oleaginous microorganisms, the yeast *Yarrowia lipolytica* (*Y. lipolytica*) has attracted a lot of attention due to its interesting biotechnological characteristics. Firstly, the status of *Y. lipolytica* is generally regarded as safe meaning it is compatible with food products and safe to expose to humans (Groenewald et al., 2014). Also, it is able to use a range of industrial or low-value feedstocks as carbon sources including chemicals, hydrocarbons, and waste carbon due to its strong tolerance and adaptability (Fickers et al., 2005; Markham et al., 2017; Papanikolaou & Aggelis, 2009). In addition, a rapidly developing synthetic biology toolset as well as metabolic plasticity has enabled *Y. lipolytica* to produce a variety of novel products including exotic lipids. Therefore, in recent years, *Y. lipolytica* has become a popular platform organism across both academia and industry.

As an oleaginous yeast, *Y. lipolytica* is an ideal host to study and produce lipid and lipid-derived products such as fatty acid esters and alcohols (Markham & Alper, 2018b). So far, *Y. lipolytica* has been successfully used to produce some unusual fatty acids with a considerable yield. For example, ricinoleic acid (RA) can be accumulated up to 43% of the total lipids in *Y. lipolytica* through genetic modification, and the yield reached 60 mg/g DCW (Béopoulos et al., 2014). In addition, eicosapentaenoic acid (EPA) occupying approximately 50% of the total fatty acids was obtained in engineered *Y. lipolytica* strains (Hong et al., 2014). Besides, *Y. lipolytica* was also engineered to produce conjugated linoleic acid (CLA) (Zhang et al., 2013; Zhang et al., 2012). The best-engineered *Y. lipolytica* strain can produce 4 g/L of CLA

from soybean oil-based media, which accounted for 44% of total fatty acids (30% of DCW) (Zhang et al., 2013).

In addition, metabolic engineering *Y. lipolytica* for CFAs production has made some progress. In 2018, Markham et al. expressed multiple copies of *E. coli cfa* gene in *Y. lipolytica,* blocked β-oxidation by deleting *pex*10 and *mfe1* and overexpressed the native diacylglycerol acyl transferase *dga1* to improve CFAs yield in *Y. lipolytica.* A further strain was constructed by mutating the regulatory protein encoded by MGA2 paired with *dga1* overexpression and *cfa* expression, which was able to produce 200 mg/L of C19:0 CFAs in small-scale fermentation. Moreover, more than 3 g/L of C19:0 CFAs was achieved in bioreactor fermentation, which accounted for up to 32.7% of total lipids (Markham & Alper, 2018a). In 2019, Czerwiec et al. tested a range of *cfa* genes from bacteria and plants in *Y. lipolytica*. It was revealed that the *E. coli cfa* gene was preferred because it can produce both C17 and C19 cyclopropane products. They also optimised the expression of the *E. coli cfa* gene with different promoter strengths, finally achieved the CFAs yield at 45% of the total lipid content with fed-batch fermentation (Czerwiec et al., 2019).

Although these strategies can improve CFAs production, they cannot completely overcome the bottleneck of CFAs production in yeast. As chapter 3 revealed, CFAs are generated on membrane lipids of recombinant *S. cerevisiae,* and likely in the same location in *Y. lipolytica*, causing CFAs accumulation in the membrane. Therefore, in this chapter, the metabolic engineering strategy of cycling of fatty acids from membrane phospholipids to storage triglycerides developed for CFAs production in *S. cerevisiae* was adopted to engineer *Y. lipolytica,* with the intention to increase CFAs productivity (Fig 4.1). In addition, the study allowed a comparison of the implementation of the same engineering strategy in two different biotechnology yeasts.

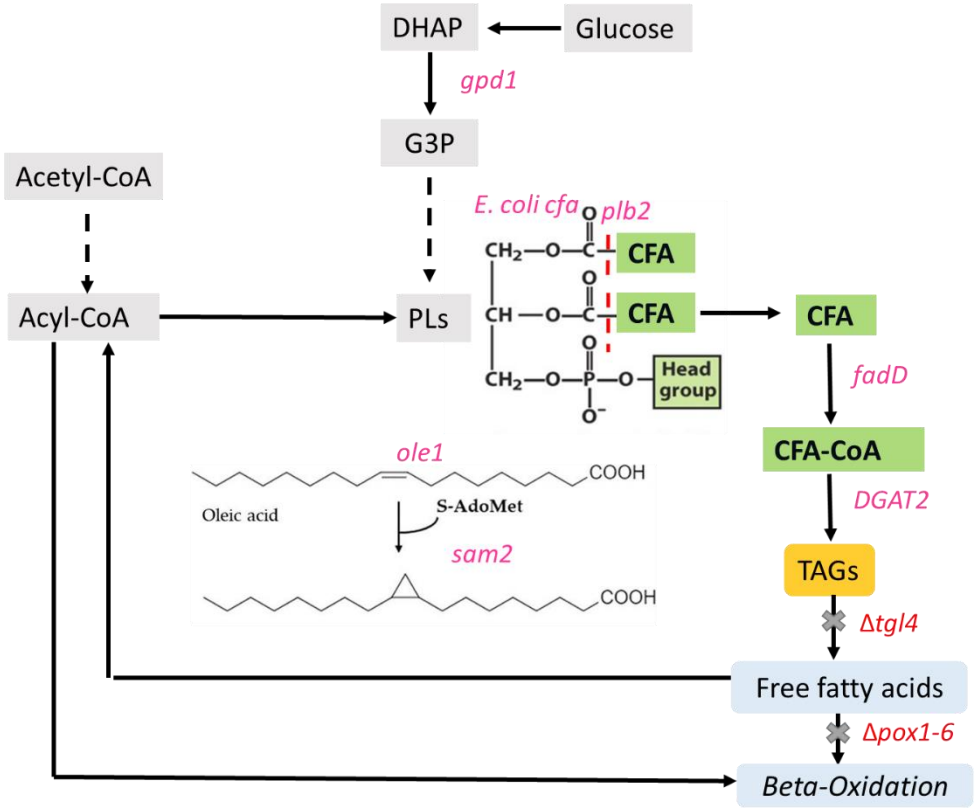

Fig 4.1 Workflow of engineered lipid pathway for CFAs biosynthesis in *Y. lipolytica*. The genes heterogeneously expressed or overexpressed in *S. cerevisiae* are shown in pink text, genes deleted are red. The genes *ole1* and *sam2* were applied to increase the substrates of *cfa* synthase the unsaturated fatty acids and S-adenosyl-L-methionine, respectively. The overexpression of *gpd1* enhances the metabolic flux to phospholipid generation. The expression of *plb2* was used to cleave the fatty acid chains containing CFAs to form free fatty acids, The expression of *fadD* was used to convert CFAs in free fatty acids form to acyl-CoA form. In addition, the overexpression of *dgat2* and deletions of *tgl4* and *pox1-6* contributed to CFA-CoA storage in TAGs and prevent the degradation of TAGs. *ole1:* Δ9 Fatty acid desaturase, *sam2*: S-adenosylmethionine synthase, *DAGT2*: diacylglycerol acyltransferase, *fadD*: fatty acyl-CoA synthetase from *Sinorhizobium meliloti, gpd1*: glycerol-3-phosphate dehydrogenase, *Δtgl4:* the deletion of triglyceride lipase 4, *Δpox1-6*: the deletion of fatty-acyl coenzyme A oxidase 1-6.

4.2 Materials and Methods

4.2.1 Yeast strains, plasmids, and culture condition

The following genes were used in this study: *cfa* (cyclopropane-fatty-acyl-phospholipid synthase) from *Escherichia coli*, *fadD* (fatty acyl-CoA synthetase) from *Sinorhizobium meliloti*, *ole1* (Δ9 Fatty acid desaturase), *plb2* (lysophospholipase 2), and *sam2* (S-adenosylmethionine synthase 2) from *S. cerevisiae*, *gpd1* (Glycerol-3-phosphate dehydrogenase) and *dgt2* (diacylglycerol acyltransferase) from *Y. lipolytica*. The Kozak sequence AAACA was added to the 5' end of all genes, which was used to increase the expression (Runguphan & Keasling, 2014). All genes were assembled into integrated vectors under the promoter TEF through the YaTK Golden Gate system developed by Ledesma Amaro et al (He et al., 2020). The gene *tgl4*, triacylglycerol lipase 4, and *pox1-6* encoding acyl-coenzyme A oxidase were deleted by homologous recombination (Ledesma-Amaro et al., 2015). All plasmids used in this study were listed in Table 4. 1.

Table 4.1 The plasmids used in this project

Plasmid name	**Description**
CZUS	pZUS1.1-*ura*-P_{TEF}-*Eccfa*
PZUS	pZUS1.2-*ura*- P_{TEF}-*plb2*
FZUS	pZUS1.3-*ura*- P_{TEF}-*fadD*
CPZUA	pZUA2.2-*ura*-P_{TEF}-*Eccfa*-P_{TEF}-*plb2*
CPFZUA	pZUA2.3-*ura*-P_{TEF}-*Eccfa*-P_{TEF}-*plb2*-P_{TEF}-*fadD*
OZLA	pZLS1.1-*leu*-P_{TEF}-*ole1*
SZLA	pZLS1.2-*leu*-PTEFF-*ole1*

OSZLA	pZLA-*leu*-P_{TEF}-*ole1*-P_{TEF}-*sams*

The plasmids were transferred into *Y. lipolytica* strains by the lithium-acetate method. *Y. lipolytica* Pold strain derived from the wild type strain W29 (ATCC20460) was used as parental strain to construct CFAs-producing strains. All strains examined in this study were prototrophic and details are listed in Table 4.2.

Table 4.2 Engineered *Y. lipolytica* strains for CFAs production

Strains	**Genotype and genes for incorporation**
WT2900	Parental strain Po1d-*Ura-Leu*
Y3820	Pold-*dgat2-gpd-Δpox1-6-Δtgl4-ura-leu* (Ledesma-Amaro et al., 2015)
CPold	Po1d-*Eccfa-ura-leu*
CY3820	Po1d-*Eccfa-dgat2-gpd-Δpox1-6-Δtgl4-ura-leu*
CY3820OS	Po1d-*Eccfa-ole1-sam2-dgat2-gpd-Δpox1-6-Δtgl4-ura-leu*
CY3820POS	Po1d- *Eccfa-ole1-sam2-plb-dgat2-gpd-Δpox1-6-Δtgl4-ura-leu*
CY3820POSF	Po1d- *Eccfa-ole1-sam2-plb-fadd-dgat2-gpd-Δpox1-6-Δtgl4-ura-leu*

NEB® Turbo Competent *E. coli* cells were used for all cloning and plasmid propagation. The *E. coli* transformants were selected on LB agar plates and cultured in the broth of LB medium with the antibiotic ampicillin (100 μg/ml) or spectinomycin (100 μg/ml) at 37°C. The *Y. lipolytica* transformants were selected on YNB -Ura +Leu, YNB +Ura -Leu, or YNB -Ura -Leu agar plates containing 3.4 g/L yeast nitrogen base, 10 g/L agar, 50 mM phosphate buffer, 20 g/L glucose, and 5 g/L Ura or 10 g/L Leu when necessary. *Y. lipolytica* transformants were checked by yeast colony PCR and were cultured in the corresponding YNB liquid medium.

4.2.2 CFAs production in flask cultures

Seed cultures for all the engineered strains were conducted in 3 ml YNB -Ura -Leu liquid medium at 30°C with 250 rpm agitation overnight. After that, cells were transferred into 50 ml of YNB -Ura -Leu liquid medium in 250 ml flasks at 30°C with 250 rpm agitation. The initial OD_{600} of each culture was set at 0.5. After 72 h cultivation, cells were centrifuged and washed with sterile distilled water, then stored in -80℃. Next, the wet biomass was dried by freeze-drying. After that, the dry biomass was weighed, then used for lipid analysis and lipid yield calculation.

4.2.3 Lipid analysis

Yeast cells collected after 72 h were lyophilised at -80°C then fatty acid analysis was carried out according to an adapted Bligh Dyer procedure (Bligh & Dyer, 1959). Around 20 - 30 mg dry yeast cells were weighed for lipid analysis and 20 mg tridecanoic (C13:0) acid was added as an internal standard. Acidified methanol solution (methanol/hydrochloric acid/chloroform (10:1:1), 2 ml) was added for transesterification of lipids. Samples were heated at 80°C for 1 h then cooled to room temperature. Subsequently, 1 ml 0.9% saline and 2 ml hexane were added to each sample and fatty acid methyl esters were extracted in the hexane fraction for analysis by GC-FID as described in Chapter 3.

4.3 Results

4.3.1 Fatty acid analysis of engineered *Y. lipolytica* strains

Analysis of total fatty acids revealed the overexpression of *dgat2* and deletion of *tgl4* and *pox1-6* increased the accumulation of lipids in *Y. lipolytica*. Compared with the strain only expressing *E. coli cfa*, the total fatty acids content (mg/g) was increased by 4-5-fold under the effect of *dgat2* overexpression and *tgl4* and *pox1-6* deletions (Table 4.3). Also, it was found

that there was a similar trend in the titer of total fatty acids (mg/L), which was consistent with the result of the *Y. lipolytica* strain having the same background and cultured to a similar fermentation timepoint in a previous report (Czerwiec et al., 2019). The effect of the pathway engineering strategy on the fatty acid composition of the *Y. lipolytica* strains is shown in Fig 4.2 and Table 4.4. The gene *ole1* encoding Δ9 fatty acid desaturase introduces a double bond between the carbon 9 and 10 of the saturated fatty acyl substrates palmitic acid (C16:0) and stearic acid (C18:0) (Fujimori et al., 1997). As Table 4.4 and Fig 4.2 show, after the expression of *ole1*, both the content of unsaturated fatty acids (C16:1, C18:1, and C18:2) and their titer in flask fermentations were obviously increased. However, although both C19 CFAs and C17 CFAs were detected when *E. coli cfa* was expressed in *Y. lipolytica*, as per earlier reports, CFAs production was relatively low compared with the strains with the same background and cultivation time in prior reports (Czerwiec et al., 2019; Markham & Alper, 2018a). Besides, compared with the engineered *S. cerevisiae* strains in chapter 3, CFAs production was also low. Therefore, the strategy applied in *Y. lipolytica* didn't obtain as good result as that in *S. cerevisiae*.

Table 4.3 Mean (± SD) total fatty acids (TFAs) in engineered *Y. lipolytica* strains at 72 h of flask culture

strains	TFAs (mg/g)	TFAs (mg/L)
Cpold	22.7 ± 1.3	129 ± 7
CY3820	81.0 ± 7.8	428 ± 30
CY3820OS	105.1 ± 14.8	565 ± 113
CY3820POS	94.3 ± 5	515 ± 73
CY3820POSF	105.5 ± 9.4	582 ± 31

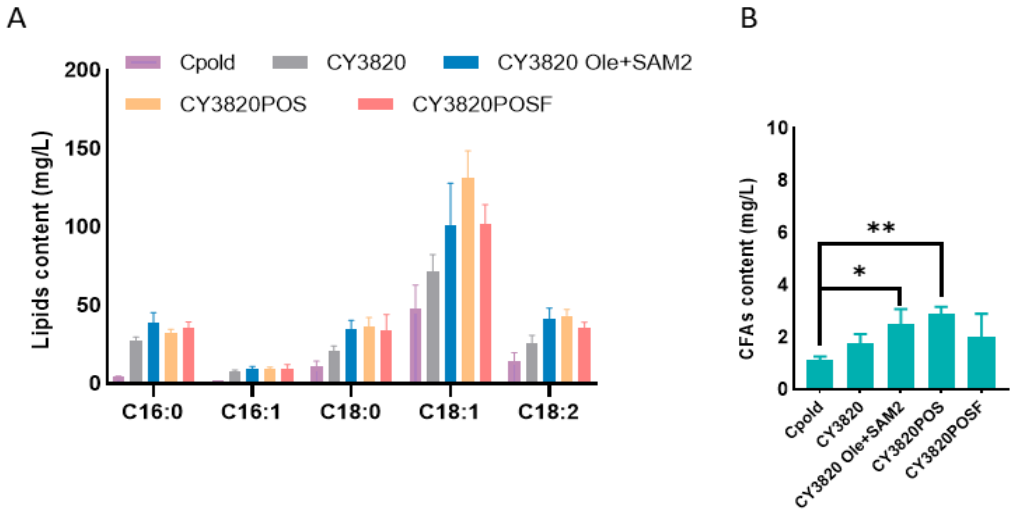

Fig 4.2 Fatty acid distributions in lipids of all *Y. lipolytica* strains used in this study, (**A**) standard fatty acids production by engineered *Y. lipolytica* strains, (**B**) CFAs production by engineered *Y. lipolytica* strains. Values are means of triplicate experiments ± SD. * Represented that the effect of the factor was significant at $p < 0.05$ (t-test). ** Represented that the effect of the factor was significant at $p < 0.01$(t-test).

Table 4.4 Fatty acid composition of all wild type and engineered *Y. lipolytica* strains used in this study

	Fatty acid composition (mg/g, DCW)						
Strains	C16:0	C16:1	C18:0	C18:1	C18:2	CFAs	CFAs % of TAGs
Cpold	4.63±0.2	1.54±0.06	2.44±0.16	10.39±0.59	3.13±0.33	0.32±0.04	1.41% ± 0.14
CY3820	27.43±0.28	7.59±1.02***	7.83±0.77	26.98±2.24***	9.6±1.36	0.66±0.09	0.82% ± 0.07
CY3820 Ole+SAM2	38.90±6.27	9.09±1.84**	10.97±2.24	31.42±4.66**	12.92±1.02	0.78±0.05	0.75% ± 0.15
CY3820POS	32.14±2.43	9.19±1.30**	8.86±0.24	31.83±0.21**	10.58±1.31	0.71±0.1	0.75% ± 0.07
CY3820POSF	35.26±3.9	9.46±2.67**	11.36±1.65	35.05±3.32**	12.4±1.43	0.67±0.23	0.65% ± 0.24

Notes: * Represented that the effect of the factor was significant at $p < 0.05$ (t-test). Values are means of triplicate experiments ± SD. ** Represented that the effect of the factor was significant at $p < 0.01$(T-test) *** Represented that the effect of the factor was significant at $p < 0.001$(t-test).

4.4 Discussion

Compared with the improvement in CFAs yield due to implementing the metabolic engineering strategy of cycling fatty acids from membranes to TAGs in *S. cerevisiae* (Chapter 3), the effect of introducing the same into *Y. lipolytica* was modest. There was a significant increase in overall lipid generated via increased flux of fatty acids toward TAGs and blocking of degradation pathways, however, CFAs proportion of total fatty acids did not increase with the implementation of specific CFAs metabolic engineering.

CFAs yields were dramatically improved in *Y. lipolytica* by increasing the copy number of the *cfa* gene in previous research (Markham & Alper, 2018a), whereas only a single copy of the *cfa* gene was introduced in this study and likely contributed to the lower CFAs yield obtained. Furthermore, Czerwiec et al. optimised the expression of *E. coli cfa* with increased promoter strengths. Strong promoters such as 4UAS-pTEF, 8UAS-pTEF, and Hp8d significantly improved CFAs yield. By contrast, our study employed relatively weak strength promoters, pTEF, and probably also contributed to low yields of CFAs through lower *Eccfa* expression in engineered *Y. lipolytica* (Czerwiec et al., 2019).

Furthermore, several of the genes used in this engineering work, *Eccfa*, *ole1*, *sam2*, *plb2*, and *fadD*, were not codon-optimised for *Y. lipolytica*, which may have influenced the gene expression to some degree. Countering this point is the increase in total fatty acids and monounsaturated Δ9 fatty acids in the CY3820 Ole+SAM2 strain, indicating that *ole1* was functional in this strain.

In summary, compared with both of Markham & Alper and Czerwiec et al.'s work, CFAs yield in our engineered strains are lower. Therefore, the next steps in the work would require RT-PCR and Western blot to confirm the level of gene and protein expression. Then, *Y. lipolytica* could be further engineered with stronger promoters on *Eccfa* and multiple copies

inserted. Due to the low expression of *cfa* in the engineered *Y. lipolytica* strains and low production of CFAs in phospholipids, the effectiveness of the metabolic strategy demonstrated in *S. cerevisiae* could not be fully tested here. After verifying and improving the expression of the key gene *Eccfa*, the impact of the strategy to cycle CFAs from phospholipids to TAGs would be important to implement. The suggested experiments were not conducted due to time constraints of completing the Ph. D and restrictions on laboratory access during the COVID-19 pandemic.

4.5 Reference

Béopoulos, A., Verbeke, J., Bordes, F., Guicherd, M., Bressy, M., Marty, A., Nicaud, J.-M. 2014. Metabolic engineering for ricinoleic acid production in the oleaginous yeast Yarrowia lipolytica. *Applied microbiology and biotechnology*, **98**(1), 251-262.

Bligh, E.G., Dyer, W.J. 1959. A rapid method of total lipid extraction and purification. *Canadian journal of biochemistry and physiology*, **37**(8), 911-917.

Czerwiec, Q., Idrissitaghki, A., Imatoukene, N., Nonus, M., Thomasset, B., Nicaud, J.M., Rossignol, T. 2019. Optimization of cyclopropane fatty acids production in Yarrowia lipolytica. *Yeast*, **36**(3), 143-151.

Fickers, P., Benetti, P.-H., Waché, Y., Marty, A., Mauersberger, S., Smit, M., Nicaud, J.-M. 2005. Hydrophobic substrate utilisation by the yeast Yarrowia lipolytica, and its potential applications. *FEMS yeast research*, **5**(6-7), 527-543.

Fujimori, K., Anamnart, S., Nakagawa, Y., Sugioka, S., Ohta, D., Oshima, Y., Yamada, Y., Harashima, S. 1997. Isolation and characterization of mutations affecting expression of the Δ9-fatty acid desaturase gene, OLE1, in Saccharomyces cerevisiae. *FEBS letters*, **413**(2), 226-230.

Groenewald, M., Boekhout, T., Neuvéglise, C., Gaillardin, C., van Dijck, P.W., Wyss, M. 2014. Yarrowia lipolytica: safety assessment of an oleaginous yeast with a great industrial potential. *Critical reviews in microbiology*, **40**(3), 187-206.

He, Q., Szczepanska, P., Yuzbashev, T., Lazar, Z., Ledesma-Amaro, R. 2020. De novo production of resveratrol from glycerol by engineering different metabolic pathways in Yarrowia lipolytica. *Metab Eng Commun*, **11**, e00146.

Hong, S.-P., Sharpe, P.L., Xue, Z., Yadav, N.S., Zhang, H., Zhu, Q.Q. 2014. Recombinant microbial host cells for high eicosapentaenoic acid production, Google Patents.

Ledesma-Amaro, R., Dulermo, T., Nicaud, J.M. 2015. Engineering Yarrowia lipolytica to produce biodiesel from raw starch. Biotechnology for biofuels, 8(1), 1-12.

Markham, K., Cordova, L., Hill, A., Alper, H. 2017. Yarrowia lipolytica as a cell factory for oleochemical biotechnology. *Consequences of Microbial Interactions with Hydrocarbons, Oils, and Lipids: Production of Fuels and Chemicals*, 1-18.

Markham, K.A., Alper, H.S. 2018a. Engineering Yarrowia lipolytica for the production of cyclopropanated fatty acids. *Journal of industrial microbiology & biotechnology*, **45**(10), 881-888.

Markham, K.A., Alper, H.S. 2018b. Synthetic biology expands the industrial potential of Yarrowia lipolytica. *Trends in biotechnology*, **36**(10), 1085-1095.

Papanikolaou, S., Aggelis, G. 2009. Biotechnological valorization of biodiesel derived glycerol waste through production of single cell oil and citric acid by Yarrowia lipolytica. *Lipid technology*, **21**(4), 83-87.

Runguphan, W., Keasling, J.D. 2014. Metabolic engineering of Saccharomyces cerevisiae for production of fatty acid-derived biofuels and chemicals. *Metabolic engineering*, **21**, 103-113.

Sitepu, I.R., Garay, L.A., Sestric, R., Levin, D., Block, D.E., German, J.B., Boundy-Mills, K.L. 2014. Oleaginous yeasts for biodiesel: current and future trends in biology and production. *Biotechnology advances*, **32**(7), 1336-1360.

Zhang, B., Chen, H., Li, M., Gu, Z., Song, Y., Ratledge, C., Chen, Y.Q., Zhang, H., Chen, W. 2013. Genetic engineering of Yarrowia lipolytica for enhanced production of trans-10, cis-12 conjugated linoleic acid. *Microbial cell factories*, **12**(1), 1-8.

Zhang, B., Rong, C., Chen, H., Song, Y., Zhang, H., Chen, W. 2012. De novo synthesis of trans-10, cis-12 conjugated linoleic acid in oleaginous yeast Yarrowia lipolytica. *Microbial cell factories*, **11**(1), 1-8.

CHAPTER 5

ENGINEERING METHANOL ASSIMILATION IN *YARROWIA LIPOLYTICA* FOR HIGH-VALUE BIOPRODUCTION

This page is intentionally blank

Chapter 5 Engineering methanol assimilation in *Yarrowia lipolytica* for high-value bioproduction

Abstract

In recent years, *Y. lipolytica* has quickly developed as a popular non-conventional microorganism for bioproduction. Also, by applying advanced synthetic biology tools, *Y. lipolytica* is a potential host microorganism for methanol bioconversion to high-value products. In this chapter, a heterologous methanol assimilation pathway was first simulated, the selected genes constructed into plasmids and inserted into *Y. lipolytica* genome. Further engineering, including enhancement of the non-oxidative pentose phosphate pathway and adaptive laboratory evolution, were implemented to improve the efficiency of methanol utilisation. Assessment of growth and ^{13}C-methanol isotope tracer studies were used to evaluate methanol utilisation efficiency and assimilatory routes. In addition, a resveratrol synthesis pathway was introduced into *Y. lipolytica* which was cultured on methanol as a co-substrate. Finally, ^{13}C incorporation into resveratrol demonstrated that engineered *Y. lipolytica* strains were able to assimilate methanol into industrially relevant chemicals.

5.1 Introduction

The fast development of industrial biomanufacturing results in high pressure on the traditional carbon sources which are predominantly sugar feedstocks, and face competition with their availability in the food supply and impacts of heavy reliance on agriculture (Clomburg et al., 2017; Naik et al., 2010). Methanol as a non-food carbon feedstock for biomanufacturing has been recently drawing interest due to its natural abundance, flexible production processes, and availability as an industrial by-product (Schrader et al., 2009; Zhang et al., 2017). It is commonly produced by conversion of syngas which is derived from natural gas or renewable methane resources or hydrogenation of CO_2 (Bertau et al., 2014; Du et al., 2016). Also, compared with glucose, methanol is more reduced with the degree of reduction per carbon at 6, which can be beneficial for production with a high yield (Whitaker et al., 2015). However, the conversion of methanol by non-methylotrophic microbes is a major challenge. While natural methylotrophs can metabolise and grow on methanol as a carbon source and/or energy source, they are usually difficult to engineer, or their natural capacity to produce valuable compounds is very limited (Schrader et al., 2009; Woolston et al., 2018). However, engineering industrially robust and well-characterised platform microorganisms that already possess mature genetic manipulation tools, to become synthetic methylotrophs is a promising alternative.

In recent years, synthetic methylotrophic *E. coli* has made great progress (Chen et al., 2020; Keller et al., 2020; Meyer et al., 2018; Woolston et al., 2018). In 2015, it was first demonstrated that the methanol assimilation pathway established by Mdh, Hps, and Phi in *E. coli* was functional, which laid the foundation for the research of synthetic methylotrophic *E. coli* (Müller et al., 2015b*)*. Subsequently, Price et al., (2016), rerouted glucose catabolism through the pentose phosphate pathway rather than via glycolysis and enhanced Ru5P generation in cells grown on methanol and glucose to improve the efficiency of methanol

utilisation, (Bennett et al., 2018), (Woolston et al., 2018). In 2019 a breakthrough in synthetic methylotrophic *E. coli* was published by Chen et al., (2020). Whereby they employed adaptive laboratory evolution (ALE) to solve the issue of formaldehyde toxicity, resulting in the synthetic methylotrophic *E. coli* strain growing solely on methanol with the doubling time of 8.5 h and an OD600nm achieved of 2.

Compared with prokaryotes, engineering eukaryotes to become synthetic methylotrophs is more complicated due to relatively advanced physiological features. So far, reports of synthetic methylotrophic eukaryotes are few. To date, there have been attempts to engineer *S. cerevisiae* for synthetic methylotrophic yeast (Espinosa et al., 2020a; Espinosa et al., 2020b; Vartiainen et al., 2019). In 2020, Espinosa et al. engineered and tested three methanol assimilation pathways in *S. cerevisiae*, which identified the bacterial ribulose monophosphate pathway as the most effective methanol assimilation pathway in *S. cerevisiae (*Espinosa et al., 2020a*)*. In 2021, Zhan. et al applied a thermodynamic-based module-circuits strategy combined with ALE to engineer S. cerevisiae, which resulted in *S. cerevisiae* growing on methanol with an OD_{600} achieved of 0.2 (Zhan et al.).

In recent years, the oleaginous yeast *Yarrowia lipolytica* (*Y. lipolytica*) has emerged as an important biotechnological industrial yeast due to its attractive biotechnological characteristics. Firstly, *Y. lipolytica* is widely used to produce lipids and lipid-derived compounds based on its oleaginous characteristic (Ledesma-Amaro & Nicaud, 2016). Additionally, with the development of synthetic biology and molecular biology tools, *Y. lipolytica* can be readily genetically manipulated, which enables *Y. lipolytica* to have wider applications in biotechnology, such as protein production, organic acids and nutraceuticals (Ledesma-Amaro & Nicaud, 2016; Markham & Alper, 2018). Therefore, engineering *Y. lipolytica* as a synthetic methylotroph has the potential for the production of valuable products grown on non-sugar feedstocks. In 2019, Vartiainen et al. expressed *hps* and *phi* of

B. methanolicus in *Y. lipolytica* to construct the RuMP pathway for methanol assimilation. Nevertheless, methanol was not utilised even with glycerol or yeast extract as co-substrates (Vartiainen et al., 2019). Therefore, until now, there have been no reports of successful synthetic methylotrophic *Y. lipolytica*.

Here the generation of the first *Y. lipolytica* strains that are able to utilise methanol for energy, growth and product formation is reported. The approach to successful synthetic methylotrophs involved genome-scale metabolic modelling to direct enzyme selection and pathways for methanol assimilation. Regeneration of C1-acceptor was employed to overcome formaldehyde toxicity and channel the substrate, which further improved methanol assimilation in *Y. lipolytica* which was subsequently proven by ^{13}C-methanol tracer studies. Furthermore, the conversion of methanol to resveratrol was achieved, thus demonstrating the production of high-value compounds by the synthetic methanol-assimilating *Y. lipolytica* strains.

5.2 Methods and Materials

5.2.1 Plasmid construction

Y. lipolytica plasmids were constructed through the YaTK system developed by Ledesma Amaro et al. (He et al., 2020) and are listed in Table 5.1. All genes involved in the methanol assimilation pathway, PPP pathway, and resveratrol synthesis pathway were codon-optimised for *Y. lipolytica* expression and synthesised commercially by GeneArt or Twist. There are two versions for the genes involved in the methanol assimilation pathway and PPP pathway– one set incorporated the peroxisomal signal peptide (CTAAGCTG) which was introduced at the 3’ end of each gene. The second set lacked any organelle targeting sequence for ultimately a cytosolic location. Genes with peroxisomal signal peptides were used as the templates to amplify the genes lacking peroxisomal signal peptides. The genes were cloned

into YaTK vector under the control of TEF promoter to generate single-gene cassettes and multigene cassettes by Golden Gate Assembly. ZETA sequences bookended in the expression cassette, which allow random integration in *Y. lipolytica* strains containing the ZETA-docking platform. After NotI digestion, all expression cassettes were integrated at the random locus of the *Y. lipolytica* genome by the lithium acetate transformation method or electroporation. Transformants were selected on YNBUra, YNBLeu, or YNB according to their phenotype then the presence of target genes was checked by yeast colony PCR. The LoxP-Cre system was applied to recycle the selection markers.

The restriction enzymes were obtained from New England Biolabs (NEB). PCR amplifications were carried out in a thermal cycler (Thermofisher) with Q5 High-Fidelity 2X Master Mix (NEB). PCR fragments were purified with QIAgen Purification Kit (Qiagen, Hilden, Germany). Phire plant direct PCR master mix (Thermo Fisher Scientific) was used for yeast colony PCR. All the reactions were performed according to the manufacturer instructions

Table 5.1 List of the plasmids used in this study. All plasmids were generated in this study. (p): genes with signal peptides targeted to the peroxisome; (c) genes without signal peptides.

Plasmid	**Detail**	**Plasmid**	**Detail**
pYaM01	*PTEF-AOX1 (p)*	pYaM13	*PTEF-MDH (c)*
pYaM02	*PTEF-DAS1 (p)*	pYaM14	*PTEF-PHI (c)*
pYaM03	*PTEF-CAT1 (p)*	pYaM15	*PTEF-HPS (c)*
pYaM04	*PTEF-AOX1 (p)-PTEF-DAS1 (P)-PTEF-CAT1 (p)*	pYaM16	*PTEF-MDH (c)-PTEF-PHI (c)-PTEF-HPS (c)*
pYaM05	*PTEF-AOX1 (c)*	pYaM17	*PTEF- FBA1 (p)*
pYaM06	*PTEF-DAS1 (c)*	pYaM18	*PTEF-SHB17 (p)*
pYaM07	*PTEF-CAT1 (c)*	pYaM19	*PTEF-DAK2 (p)*
pYaM08	*PTEF-AOX1 (c)-PTEF-DAS1 (c)-PTEF-CAT1 (c)*	pYaM20	*PTEF-FBA1 (p)-PTEF-DAK2 (P)-PTEF-SHB17 (p)*
pYaM09	*PTEF-MDH (p)*	pYaM21	*PTEF- FBA1 (c)*
pYaM10	*PTEF-PHI (p)*	pYaM22	*PTEF-SHB17 (c)*
pYaM11	*PTEF-HPS (p)*	pYaM23	*PTEF-DAK2 (c)*
pYaM12	*PTEF-MDH (p)-PTEF-PHI (P)-PTEF-HPS (p)*	pYaM24	*PTEF-FBA1 (c)-PTEF-DAK2 (c)-PTEF-SHB17 (c)*

Plasmid	Detail
pYaM25	*PTEF-RPE1-2 (P)*
pYaM26	*PTEF-FBP1 (P)*
pYaM27	*PTEF-RKI1-2(P)*
pYaM28	*PTEF-RPE1-2 (P)-PTEF-FBP1 (P)-PTEF-RKI1-2(P)*
pYaM29	*PTEF-RPE1-2 (c)*
pYaM30	*PTEF-FBP1 (c)*
pYaM31	*PTEF-RKI1-2(c)*
pYaM32	*PTEF-RPE1-2 (c)-PTEF-FBP1 (c)-PTEF-RKI1-2(c)*
pYaM33	*PTEF-PFK(p)*
pYaM34	*PTEF-TKT(p)*
pYaM35	*PTEF-PFK(p)-PTEF-TKT(p)*
pYaM36	*PTEF-PFK(c)*
pYaM37	*PTEF-TKT(c)*
pYaM38	*PTEF-PFK(c)-PTEF-TKT(c)*
PYaM39	*PTEF-FjTAL-PTEF-VvVst-PTEF-4CL*

5.2.2 Strains and media composition

E. coli Turbo cells were used for plasmid propagation and storage, and cultured in LB broth media (1% tryptone, 0.5% yeast extract, 1% NaCl) with kanamycin (50 μg/mL), ampicillin (100 μg/ml) or spectinomycin (100 μg/ml) at 37°C.

Wild type *Y. lipolytica* strain W29 (ATCC20460) and its derived strains Po1d (Ura- Leu-) were used in this study (Le Dall et al., 1994). The prototrophic strains constructed in this study are listed in Table 5.2 and a rationale for the expected phenotype. For the growth test, *Y. lipolytica* strains were pre-cultured in 14 ml plastic tubes with 2ml YNB -Ura -Leu medium containing 6.8 g/L yeast nitrogen base (YNB) medium without amino acids, 50 mM phosphate buffer (pH 6.8), and 10 g/L glucose. Cells were pelleted and washed twice with sterilised water to remove glucose. Subsequently, growth experiments were performed on YNB medium with 2% methanol or sodium formate supplemented with 0.5% yeast extract in the 14 ml plastic tube with 2 ml medium. Duplication was carried out for the growth test. All chemical reagents were purchased from Sigma-Aldrich.

Table 5.2 *Y. lipolytica* strains used in this study. All strains were generated in this study

Short Name	Strain/plasmid	Rationale for expected phenotype	Name	Strain/plasmid	Rationale for expected phenotype
Parental strain	WT2900 Ura+, Leu+		Po1dCb	Po1d, pYaM16	The strain expressing bacterial essential methanol assimilation pathway, and genes expressed in the cytoplasm
Po1d	Ura-, Leu-		Po1dPy2	Po1d, pYaM04, pYaM20	The strain expressing yeast essential methanol assimilation pathway, overexpression of *FBA1*, *DAK2*, and *SHB17*, and genes targeted to the peroxisome.
Po1dPy	Po1d, pYaM04	The strain expressing yeast essential methanol assimilation pathway, and genes targeted to the peroxisome.	Po1dPy3	Po1d, pYaM04, pYaM20, pYaM28	The strain expressing yeast essential methanol assimilation pathway, overexpression of *FBA1*, *DAK2*, *SHB17*, *RPE1-2*, *FBP1* and *RKI1-2*, and genes targeted to the peroxisome.
Po1dCy	Po1d, pYaM08	The strain expressing yeast essential methanol assimilation pathway, and genes expressed in the cytoplasm	Po1dPy-XuMP	Po1d, pYaM04, pYaM20, pYaM28, pYaM35	The strain expressing yeast essential methanol assimilation pathway, enhancing XuMP cycle and genes targeted to the peroxisome.
Po1dCb	Po1d, pYaM16	The strain expressing bacterial essential methanol assimilation pathway, and genes expressed in the cytoplasm	Po1dPb2	Po1d, pYaM12, pYaM20	The strain expressing bacterial essential methanol assimilation pathway, overexpression of *FBA1and SHB17*, and genes targeted to the peroxisome.

Short Name	Strain/plasmid	Rationale for expected	Name	Strain/plasmid	Rationale for expected

		phenotype			**phenotype**
Po1dPb3	Po1d, pYaM12, pYaM20, pYaM28	The strain expressing bacterial essential methanol assimilation pathway, overexpression of *FBA1*, *SHB17*, *RPE1-2*, *FBP1*, and *RKI1-2*, and genes targeted to the peroxisome.	Po1dCy2	Po1d, pYaM08, pYaM24	The strain expressing yeast essential methanol assimilation pathway, overexpression of *FBA1*, *DAK2*, and *SHB17*, and genes expressed in the cytoplasm.
Po1dPb-RuMP	Po1d, pYaM12, pYaM20, pYaM28, pYaM35	The strain expressing bacterial essential methanol assimilation pathway, enhancing RuMP cycle and genes targeted to the peroxisome.	Po1dCy3	Po1d, pYaM08, pYaM24, pYaM32	The strain expressing yeast essential methanol assimilation pathway, overexpression of *FBA1*, *DAK2*, *SHB17*, *RPE1-2*, *FBP1* and *RKI1-2*, and genes expressed in the cytoplasm.
Po1dCy-XuMP	Po1d, pYaM08, pYaM24, pYaM32, pYaM38	The strain expressing yeast essential methanol assimilation pathway, enhancing XuMP cycle and genes expressed in the cytoplasm.	Po1dCb3	Po1d, pYaM16, pYaM24, pYaM32	The strain expressing bacterial essential methanol assimilation pathway, overexpression of *FBA1*, *SHB17*, *RPE1-2*, *FBP1*, and *RKI1-2*, and genes expressed in the cytoplasm.
Po1dCb2	Po1d, pYaM16, pYaM24	The strain expressing bacterial essential methanol assimilation pathway, overexpression of FBA1and SHB17, and genes expressed in the cytoplasm.	Po1dCb-RuMP	Po1d, pYaM16, pYaM24, pYaM32, pYaM38	The strain expressing bacterial essential methanol assimilation pathway, enhancing RuMP cycle and genes expressed in the cytoplasm.

Short Name	Strain/plasmid	Rationale for expected phenotype	Name	Strain/plasmid	Rationale for expected phenotype
Po1d-Res	Po1d, PYaM39	Constructing the metabolic pathway to produce resveratrol	Pold-Pb-RuMP-Res	Po1d, pYaM12, pYaM20, pYaM28, pYaM35, PYaM39	The strain expressing bacterial essential methanol assimilation pathway, enhancing RuMP cycle, genes targeted to the peroxisome and constructing the metabolic pathway to produce resveratrol.
Pold-Cb-RuMP-Res	Po1d, pYaM16, pYaM24, pYaM32, pYaM38, PYaM39	The strain expressing bacterial essential methanol assimilation pathway, enhancing RuMP cycle, genes expressed in the cytoplasm, and constructing the metabolic pathway to produce resveratrol	P42	42nd passage of evolved Po1d strain (-Ura, -Leu)	
P42Py	P42, pYaM04	Yeast essential methanol assimilation pathway expressed, and genes targeted to the peroxisome.	P42Pb	P42, pYaM12	Bacterial essential methanol assimilation pathway expressed, and genes targeted to the peroxisome.
P42Cy	P42, pYaM08	Yeast essential methanol assimilation pathway expressed, and genes expressed in the cytoplasm	P42Py2	P42, pYaM04, pYaM20	Yeast essential methanol assimilation pathway expressed, overexpression of *FBA1*, *DAK2*, and *SHB17*, and genes targeted to the peroxisome.

Short Name	Strain/plasmid	Rationale for expected phenotype	Name	Strain/plasmid	Rationale for expected phenotype
P42Cb	P42, pYaM16	Bacterial essential methanol assimilation pathway expressed, and genes expressed in the cytoplasm	P42Py3	P42, pYaM04, pYaM20, pYaM28	yeast essential methanol assimilation pathway expressed, overexpression of *FBA1*, *DAK2*, *SHB17*, *RPE1-2*, *FBP1*, and *RKI1-2*, and genes targeted to the peroxisome.
P42Pb2	P42, pYaM12, pYaM20	Bacterial essential methanol assimilation pathway expressed, overexpression of *FBA1and SHB17*, and genes targeted to the peroxisome.	P42Cb2	P42, pYaM16, pYaM24	Bacterial essential methanol assimilation pathway expressed, overexpression of FBA1and SHB17, and genes expressed in the cytoplasm.
P42Pb3	P42, pYaM12, pYaM20, pYaM28	Bacterial essential methanol assimilation pathway expressed, overexpression of *FBA1*, *SHB17*, *RPE1-2*, *FBP1*, and *RKI1-2*, and genes targeted to the peroxisome.	P42Cb3	P42, pYaM16, pYaM24, pYaM32	Bacterial essential methanol assimilation pathway expressed, overexpression of *FBA1*, *SHB17*, *RPE1-2*, *FBP1*, and *RKI1-2*, and genes expressed in the cytoplasm.
P42Cy2	P42, pYaM08, pYaM24	Yeast essential methanol assimilation pathway expressed, overexpression of *FBA1*, *DAK2*, and *SHB17*, and genes expressed in the cytoplasm.	P42Cy3	P42, pYaM08, pYaM24, pYaM32	Yeast essential methanol assimilation pathway expressed, overexpression of *FBA1*, *DAK2*, *SHB17*, *RPE1-2*, *FBP1*, and *RKI1-2*, and genes expressed in the cytoplasm.

5.2.3 Adaptive Laboratory Evolution (ALE)

The first ALE approach was applied to improve tolerance of *Y. lipolytica* strain to methanol. *Y. lipolytica* Po1d as the parental strain was exposed to YPD medium with 2% glucose and the maximum limit methanol. After 24 – 72 h (once cultures reached stationary phase), the culture was used as a seed for the inoculation into fresh medium set at 0.1 initial OD_{600}. The new fresh culture was incubated under the same condition (250 rpm, 28°C). Based on the culture growth, gradually increasing the concentration of methanol over the range of 2%-5% (v/v) until tens of passages were achieved. (The contribution of Ms. Jingjing Liu towards generating the methanol tolerant culture is acknowledged.)

The second ALE approach employed the engineered strains PoldPy-XuMP, PoldPb-RuMP, PoldCy-XuMP, and PoldCb-RuMP (Table 5.2) was aimed at improving the methanol utilisation efficiency of these engineered strains. Cells were grown in YNB medium with 2% methanol but with gradually reduced yeast extract at 0.5 initial OD_{600}. The procedure was repeated until a stable specific growth rate was reached in the YNB medium with 2% methanol and 0.25% yeast extract. 42 and 40 subculturing were done for the first and second-round ALE, respectively.

5.2.4 ^{13}C metabolic tracer analysis

For ^{13}C-labelled intracellular metabolite analysis, the wild type strain W29 and the engineered strains PoldPb-RuMP and PoldCb-RuMP were cultured in 40 ml in 250 ml flasks at 28°C and 250 rpm until mid-exponential growth phase (40 h). The medium contained YNB without amino acids, 0.5% yeast extract, and 2% ^{13}C-methanol (Sigma-Aldrich, MO, USA). For the quenching of intracellular metabolites, 40 mL precooled (-20°C) methanol was quickly injected into the cell culture in an ethanol-dry ice bath and mixed by vortex (1 s). After centrifugation at -10°C and 4000*xg* for 5 min, the supernatant was removed. Then the

cell pellet was resuspended in 40 ml precooled (-20°C) methanol as a wash step and centrifuged again under the same condition. The resulting cell pellet was dissolved in 5 ml 75% preheated ethanol (80°C) to ensure cell lysis and extraction of intracellular metabolites. After 5 min incubation at 80°C in a water bath, the mixture was vortexed again for 30 s and then quickly cooled in an ethanol-dry ice bath. Subsequently, the mix was centrifuged under the same conditions described above, then 1 ml of the supernatant was removed for LC-MS analysis.

5.2.5 Resveratrol production in engineered *Y. lipolytica*

Engineered strains were precultured in 2 ml medium containing 6.8 g/L YNB medium without amino acids, 50 mM phosphate buffer (pH 6.8), and 10 g/L glucose in 14 ml plastic tubes at 28°C with 250 rpm agitation. Following this, the cells were pelleted and washed twice with sterile distilled water after centrifugation, and then transferred into a 50 ml production medium in 250 ml flasks at 0.5 initial OD_{600}. The production medium contained YNB medium supplemented with 0.5% yeast extract and 2% methanol at 28°C with 250 rpm. For the ^{13}C labelling in resveratrol investigation, ^{13}C-methanol was used in place of methanol. After 48 h incubation, the supernatant was collected after centrifugation of the culture at 4000xg, then mixed with an equal volume of absolute ethanol and centrifuged at 2272xg for 30 min. 1 ml of supernatant was removed for analysis of resveratrol concentration by HPLC. Injections were made into an Ulti-Mate3000 HPLC (Thermo Scientific) equipped with a Hypersile GOLD column (150 x 4.6 mm, particle size 5 μm) and the mobile phase of 70% acetonitrile and 0.1% formic acid was used as the eluent at 0.1 ml/min^{-1} flow rate. Resveratrol was detected by absorbance at 304 nm with a retention time of 6.4 min. Resveratrol concentrations were calculated by comparison with standard curves. Resveratrol standards were purchased from Sigma-Aldrich. The ^{13}C-labelling in resveratrol was determined by LC-MS by specialist mass spectroscopist, Dr. David Bell.

5.3 Results

5.3.1 Rational design *in silico* for methanol assimilation in *Y. lipolytica*

Genome-scale metabolic modelling (GSMM) was used to simulate potential engineering strategies for methanol assimilation in *Y. lipolytica* and preferred engineering strategies. The simulation was performed by Mr. Lucas Coppens.

The model iYali4 was used as the base model to represent *Y. lipolytica*'s metabolic network (Kerkhoven et al., 2016). In the first instance, the ability of wild type *Y. lipolytica* to use methanol as the only carbon substrates were evaluated. No growth on methanol was concluded. Subsequently, enzymes and pathways enabling *Y. lipolytica* to assimilate methanol were analysed *in silico*. Natural methylotrophs have developed multiple pathways to assimilate methanol as the sole carbon source and energy (Chistoserdova, 2011). Here, the methanol assimilation pathways from *Bacillus methanolicus* (*B. methanolicus*) and *Pichia pastoris* (*P. pastoris*) were selected to study, as they are representatives of natural methylotrophic prokaryotes or eukaryotes (Zhang et al., 2017). GSMM of iYali4 was applied into which reactions catalysed by the enzymes from *B. methanolicus* including methanol dehydrogenase (Mdh), hexulose phosphate synthase (Hps), and phosphohexuloisomerase (Phi) or from *P. pastoris* including alcohol oxidase (Aox1) and dihydroxyacetone synthase (Das1). *In silico* insertion of the reactions catalysed by Das1 or Hps and Phi as found in the formaldehyde assimilation pathways in *P. pastoris* or *B. methanolicus* allowed the GSMM to use formaldehyde as a growth substrate with improved efficiency. Furthermore, the introduction of the *P. pastoris* gene *AOX1* or *B. methanolicus* gene *mdh* additionally allowed the GSMM to also use methanol as a growth substrate but at a very low growth rate.

The GSMM predicted the recycling of C1 acceptor xylulose 5-phosphate (Xu5P) or ribulose-5-phosphate (Ru5P) could be accelerated by enhancing the yeast xylulose monophosphate

(XuMP) or bacterial ribulose monophosphate (RuMP) pathways. The yeast xylulose monophosphate (XuMP) pathway is associated with *Y. lipolytica* genes *dak2* (dihydroxyacetone kinase 1), *shb17* (sedoheptulose 1,7-bisphosphatase), *fba* (fructose-bisphosphate aldolase), *rpe* (ribulose-phosphate 3-epimerase), *fbp* (fructose-1,6-bisphosphatase), *rki1* (ribose-5-phosphate isomerase) and *das1* (Fig 5.1). As the function of Das for regeneration of Xu5P from G3P and S7P by the carboxylation reaction is predicted (Rußmayer et al., 2015), TKL as transketolase was integrated as well to ensure the carboxylation reaction was unobstructed. In comparison, the bacterial ribulose monophosphate (RuMP) pathway involved inserting the *Y. lipolytica* genes, *shb17*, *fba*, *rpe*, *rki1*, *das1*, *fbp*, *tkl*, and *pfk* (6-phosphofructokinase) (Fig 5.1).

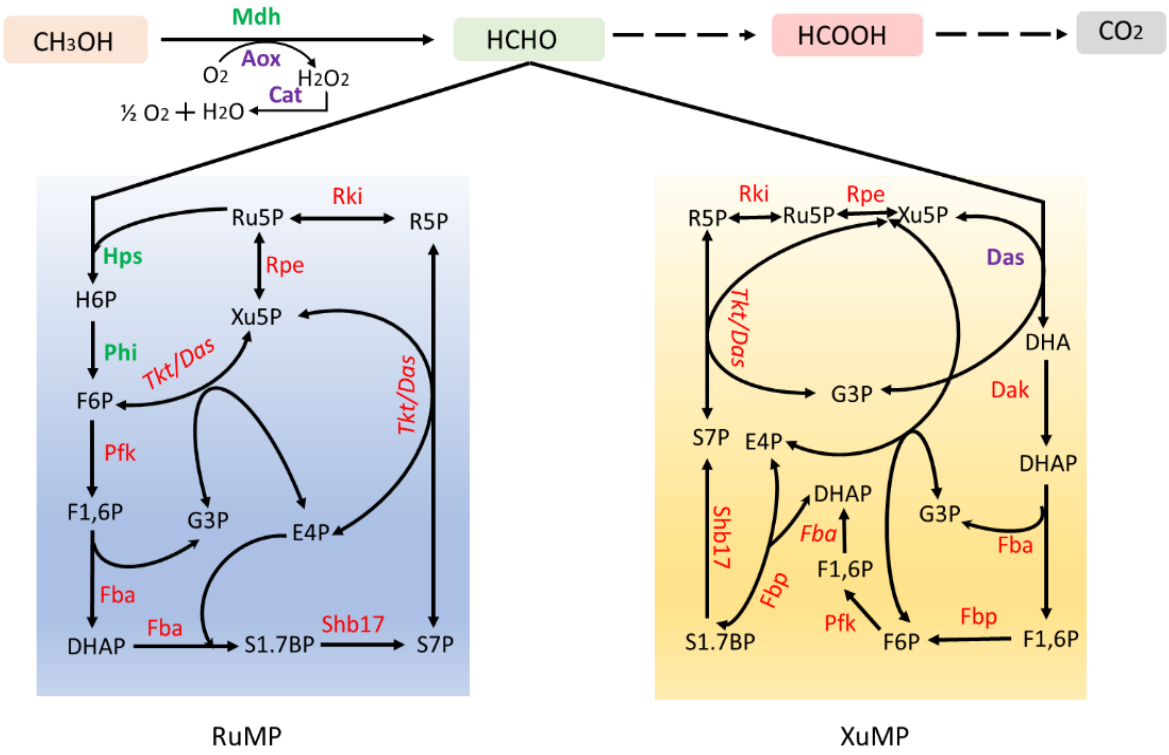

Fig 5.1 Methanol assimilation pathway engineered in *Y. lipolytica*. Bacterial NAD+ -dependent methanol assimilation pathway and yeast O_2-dependent methanol assimilation pathway were engineered into *Y. lipolytica*, respectively. The acceptor of formaldehyde Ru5P and Xu5P was improved by enhancing the RuMP or XuMP cycle to drive methanol

assimilation. Besides all genes expressed in the cytoplasm, the peroxisomal compartment strategy was also applied, which targeted all genes to the peroxisome. The essential genes for methanol assimilation from *B. methanolicus* and *P. pastoris* are green and purple, respectively. The genes for enhancing the PPP pathway are in red. Hexulose 6-phosphate (H6P), fructose 6-phosphate (F_6P), fructose 1,6-bisphosphate ($F_{1,6}BP$), ribulose 5-phosphate (Ru5P), xylulose 5-phosphate (Xu5P), glyceraldehyde 3-phosphate (G3P), dihydroxyacetone phosphate (DHAP), erythrose-4-phosphate (E4P), sedoheptulose-1,7-bisphosphate (S1,7BP), sedoheptulose-7-phosphate (S7P), ribose 5-phosphate (R5P), dihydroxyacetone (DHA).

Furthermore, the xylulose-monophosphate cycle of methanol assimilation was reported to be entirely localised to peroxisomes (Fukuoka et al., 2019; Rußmayer et al., 2015). Also, peroxisomes provide an important site for detoxification of H_2O_2 and proper partitioning of formaldehyde in methylotrophic yeast (van der Klei et al., 2006). Based on the significance of peroxisomes in methanol metabolism in methylotrophic yeast, the peroxisomal compartment was simulated in the model, which revealed these genes could achieve the growth of the organism with peroxisomal activity. However, a slight reduction was observed in the GSMM when expressing the pathway in peroxisomes as compared to the cytoplasm. This was an artefact of the limited set of metabolites that can be exchanged between cytoplasm and peroxisome, resulting in limited access to intermediates such as G3P, Ru5P, and Xu5P which would reduce the efficiency of carbon utilisation. However, it was reasoned that the peroxisomal approach would still be worth experimenting with, as it could mimic the natural methylotrophic yeast *P. pastoris*, with all the steps of methanol assimilation occurring in the peroxisome (Fukuoka et al., 2019; Rußmayer et al., 2015). Also, from these simulations, it is clear that the pathway based on *B. methanolicus* methanol assimilation is more efficient than the *P. pastoris* pathway in terms of carbon utilisation (Table 5.3). It is

speculated that *B. methanolicus* pathway couples methanol dehydrogenation by *mdh* to NADH production, which is not present in the *P. pastoris* pathway.

Table 5.3 Simulation outcomes of *Y. lipolytica* growth on glucose or methanol with expressed candidate genes for methanol assimilation sourced from different organisms

Carbon source	**WT**	**Pichia genes cytoplasmic**	**Pichia genes peroxisomal**	**Bacillus genes cytoplasmic**	**Bacillus genes peroxisomal**
Glucose	0.056	0.056	0.056	0.056	0.056
Methanol	0	0.049	0.045	0.084	0.078

5.3.2 Experimental investigation of *Y. lipolytica* strains to utilise methanol

Given the computational insight into potential methanol utilisation in *Y. lipolytica*, improving formaldehyde consumption by increasing the C1 receptors in different methanol assimilation pathways could drive the entire methanol assimilation. RuMP and XuMP pathways were enhanced to increase the ribulose-5-phosphate (Ru5P) and xylulose 5-phosphate (Xu5P) as the co-substrates of formaldehyde in the bacterial NAD^+-dependent and yeast O_2-dependent methanol assimilation pathways, respectively. Meanwhile, the peroxisomal compartment strategy was applied by targeting the genes for methanol assimilation to peroxisomes, which mimicked native methylotrophic yeast.

In addition, the methanol utilisation pathways were also engineered into the first approach evolved strain (42nd passage) that possessed high tolerance to methanol. As Fig 5.2B shows, compared with the parental strain, the tolerance of the evolved strain to methanol increased to 5% (v/v). Also, before ALE, when the cells grew on YPD with 5% (v/v) methanol, large cell aggregates were obviously formed. However, as the cells evolved and tolerance increased, the phenomenon of cell aggregation was gradually reduced (Fig 5.2A). Especially, when it

reached the 42nd passage, the performance of the evolved strain growing on the YPD medium with 5% methanol become similar to that of the parental strain growing on the same without methanol. Therefore, the evolved strain was expected to better utilise methanol.

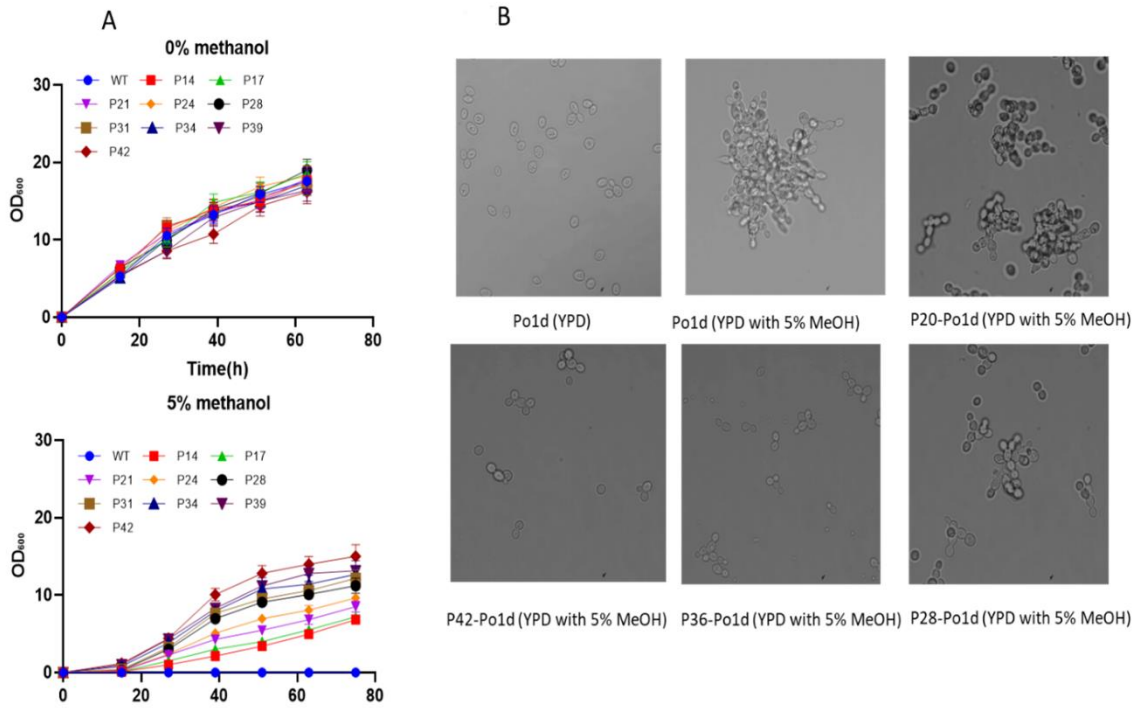

Fig 5.2 (**A**) Growth of the parental strain (WT) and evolved strains on YPD with 5% methanol. (**B**) Optical microscope imaging of the phenomenon of cell aggregations of the parental strain and evolved strains growing in the medium with/without methanol. Values are means of triplicate experiments ± SD

To investigate the capacity of *Y. lipolytica* strains for methanol utilisation, strains were cultured in liquid YNB medium without glucose supplemented with 0.5% yeast extract and 2% methanol. As Fig 5.3A shows, the strains grew steadily with yeast extract as a helper substrate of methanol. Compared with the engineered *Y. lipolytica* strains grown in yeast extract only, a growth increase of the engineered *Y. lipolytica* strains expressing NAD^+-dependent or O_2-dependent pathways was achieved in the presence of methanol, which increased around 2-3-fold in final OD_{600} (Fig 5.3A). However, although evolved strains could

bear higher methanol concentrations, they didn't show faster growth when methanol was supplemented. For example, as Fig 5.3B suggested, the OD_{600} difference of engineered evolved strains cultured with/without methanol at different time points was similar or even lower than that of engineered non-evolved strains. In addition, the peroxisomal compartmentalisation strategy for methanol assimilation enzymes didn't make a significant improvement in the growth on methanol

Despite that some strategies applied in this project did not achieve the desired improved assimilation of methanol, after engineering the yeast O_2-dependent pathway and bacterial NAD+-dependent pathway, *Y. lipolytica* strains grew better when methanol was supplemented, especially when the co-substrate of formaldehyde assimilation was increased by enhancement of RuMP and XuMP pathways (Fig 5.3B). For example, the maximal OD_{600} difference of Po1dCb and Po1dPb strains between with/ without methanol as the auxiliary carbon source reached 0.057 ± 0.03 and 0.075 ± 0.007, respectively, while that of Po1dCb-RuMP and Po1dPb-RuMP strains reached 0.142 ± 0.006 and 0.141 ± 0.01, respectively. There was the same trend after enhancing the XuMP pathway. The maximal OD difference of Po1dCy and Po1dPy are 0.055 ± 0.05 and 0.066 ± 0.03, respectively, but enhancement of the XuMP pathway improved the OD difference up to 0.074 ± 0.04 and 0.1 ± 0.03, respectively. Therefore, the RuMP and XuMP cycle enhancement were useful to improve the methanol utilisation efficiency.

A

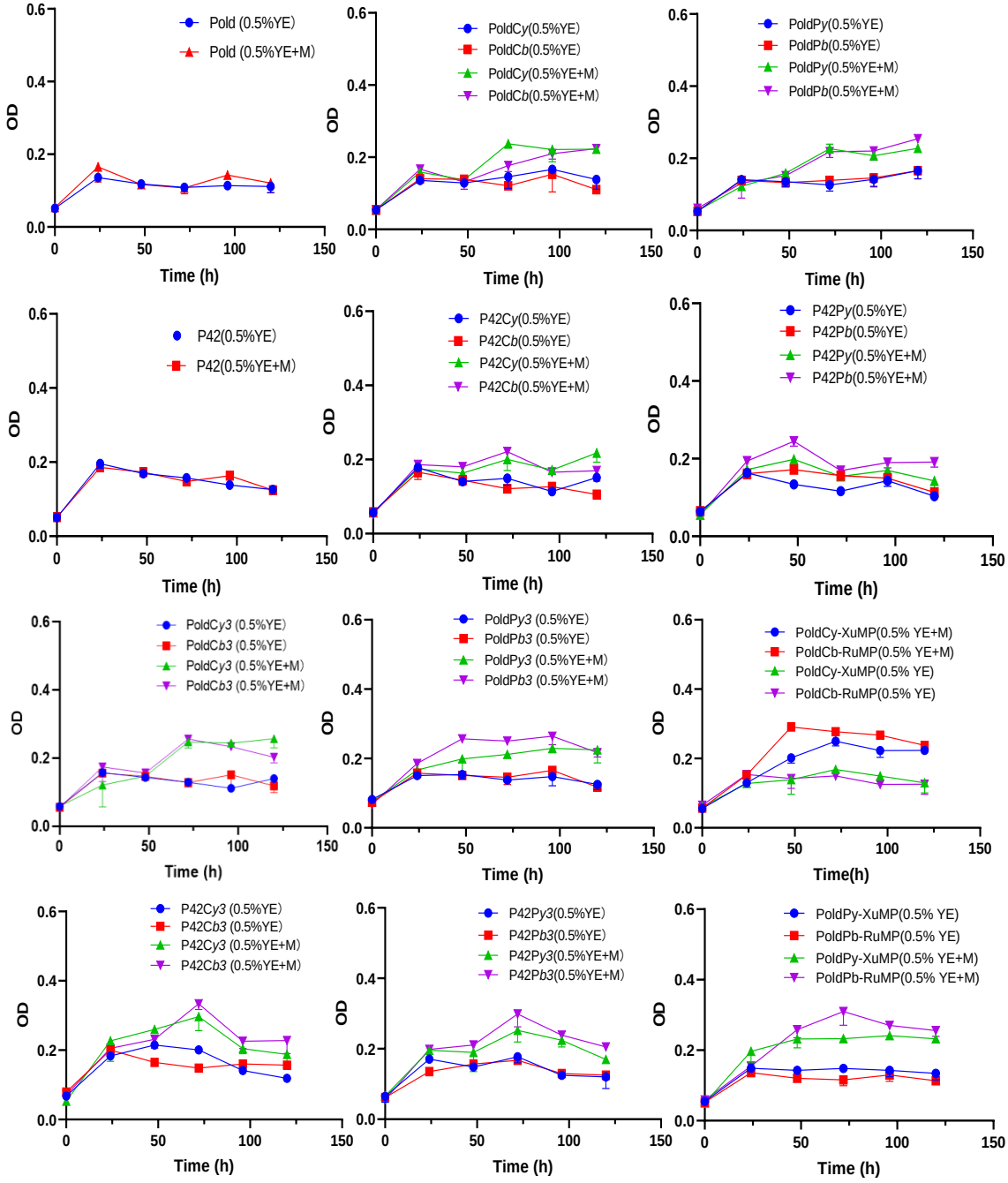
Pold (0.5%YE)
Pold (0.5%YE+M)
PoldCy(0.5%YE)
PoldCb(0.5%YE)
PoldCy(0.5%YE+M)
PoldCb(0.5%YE+M)
PoldPy(0.5%YE)
PoldPb(0.5%YE)
PoldPy(0.5%YE+M)
PoldPb(0.5%YE+M)
P42(0.5%YE)
P42(0.5%YE+M)
P42Cy(0.5%YE)
P42Cb(0.5%YE)
P42Cy(0.5%YE+M)
P42Cb(0.5%YE+M)
P42Py(0.5%YE)
P42Pb(0.5%YE)
P42Py(0.5%YE+M)
P42Pb(0.5%YE+M)
PoldCy3 (0.5%YE)
PoldCb3 (0.5%YE)
PoldCy3 (0.5%YE+M)
PoldCb3 (0.5%YE+M)
PoldPy3 (0.5%YE)
PoldPb3 (0.5%YE)
PoldPy3 (0.5%YE+M)
PoldPb3 (0.5%YE+M)
PoldCy-XuMP(0.5% YE+M)
PoldCb-RuMP(0.5% YE+M)
PoldCy-XuMP(0.5% YE)
PoldCb-RuMP(0.5% YE)
P42Cy3 (0.5%YE)
P42Cb3 (0.5%YE)
P42Cy3 (0.5%YE+M)
P42Cb3 (0.5%YE+M)
P42Py3(0.5%YE)
P42Pb3(0.5%YE)
P42Py3(0.5%YE+M)
P42Pb3(0.5%YE+M)
PoldPy-XuMP(0.5% YE)
PoldPb-RuMP(0.5% YE)
PoldPy-XuMP(0.5% YE+M)
PoldPb-RuMP(0.5% YE+M)
OD
Time (h)
Time(h)

B

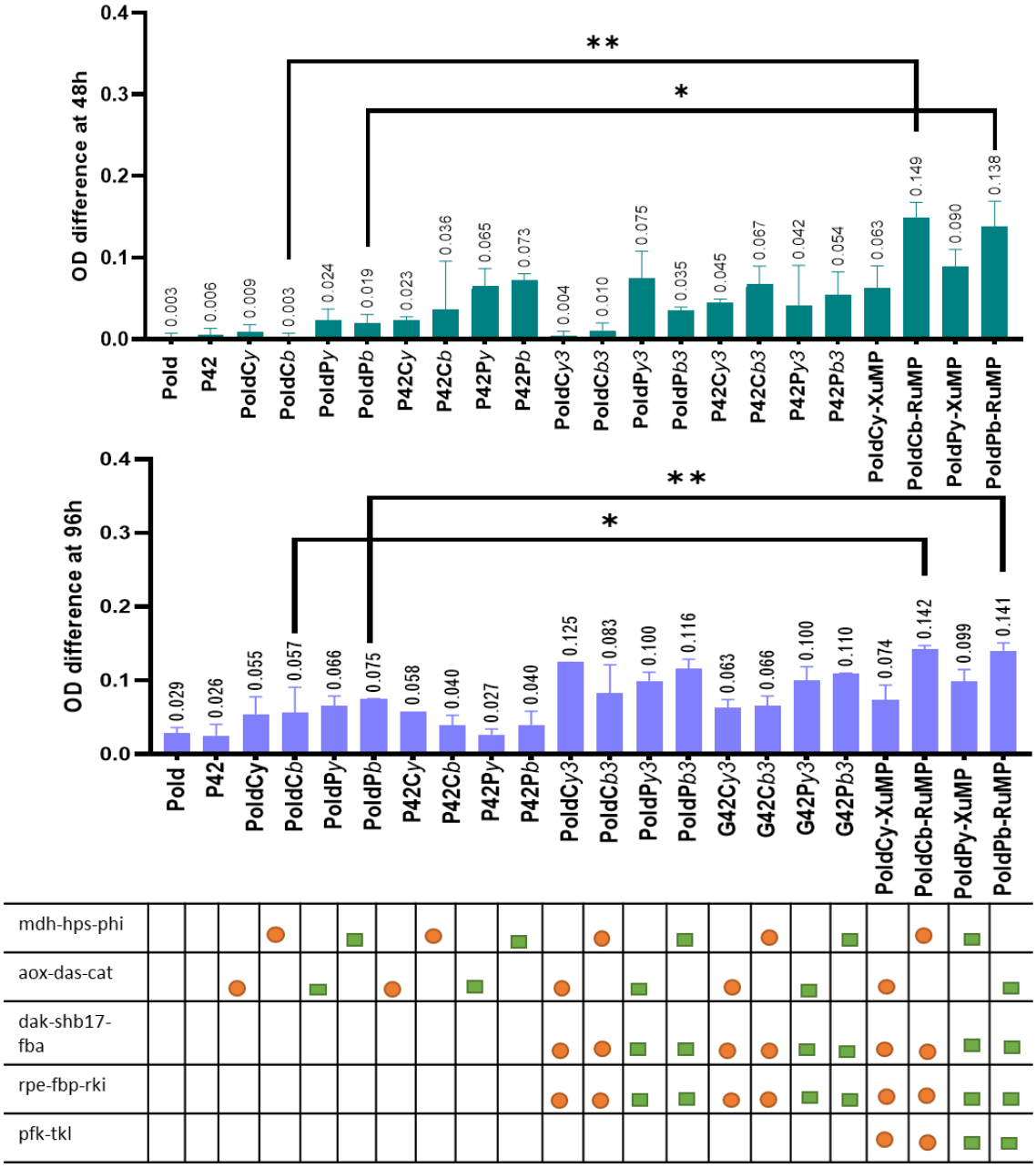

Fig 5. 3 Engineering of the methanol utilization pathway in *Y. lipolytica*. (**A**) Growth profiles of all engineered strains grown in liquid YNB medium without glucose with 0.5 % yeast extract (YE) or with 0.5% yeast extract and 2% Methanol. (**B**) The difference between engineered strains grown in the presence and absence of methanol plus 0.5% YE at different time points. Values are means of triplicate experiments ± SD. ● represented that the genes were expressed in cytoplasm. ■ represented that the genes were targeted to peroxisome.

Notes: * Represented that the effect of the factor was significant at $p < 0.05$ (Students t-test). ** Represented that the effect of the factor was significant at $p < 0.01$ (t-test).

5.3.3 ^{13}C-metabolic tracer analysis

To confirm that the methanol utilisation indeed proceeds via the synthetic methanol assimilation pathway in *Y. lipolytica*, we performed steady-state labelling experiments with ^{13}C labelled methanol. Because the performance of Po1dCb-XuMP and Po1d Pb-XuMP strains had the highest growth in the presence of methanol, these two engineered strains were selected for the ^{13}C-labelling experiment. Analysis of ^{13}C-incorporation was mainly focused on metabolites of the central carbon metabolic pathway such as the TCA cycle and pentose phosphate pathway. ^{13}C-labelled TCA cycle including in fumarate (Fum) and succinate (Suc), ^{13}C-labelled hexulose 6-phosphate (H6P), and ^{13}C-labelled adenylates AMP were detected in the *Y. lipolytica* wild type strain (Fig 5.4), which revealed that *Y. lipolytica* has a previously unknown native capacity for methanol assimilation.

Furthermore, as expected, compared with the wild type strain, the higher proportions of ^{13}C-labelled intracellular metabolites were observed in the engineered strain Po1dCb-RuMP and PoldPb-RuMP, suggesting methanol utilisation efficiency in engineered strains was improved. For example, the engineered strain Po1dCb-RuMP and PoldPb-RuMP incorporated up to 17.49%±0.15 and 20.27%±4.06 methanol carbon into H6P (Fig 5.4), respectively, which is the first metabolite from methanol assimilation. In addition, the carbon labelling percentage of TCA cycle intermediates increased, for instance, ^{13}C-labelled carbon at 8.28%±2.13 and 6.02%± 0.00 in Cit was detected in these two engineered strains but none was detected in Cit in the wild type strain. Also, ^{13}C-labelled carbon of Fum increased to 9.27%±1.60 and 9.29%±2.91 in the engineered strain Po1dCb-RuMP and PoldPb-RuMP while only 6.75%±1.12 in wild type. The same trend also occurred with Suc intermediates (Fig 5.4).

Interestingly, glutathione (GSH) labelled by ^{13}C-methanol-derived carbons were also raised to 16.87% ± 0.33 and 22.72% ± 0.46 in PoldCb-RuMP and Po1dPb-RuMP strain, respectively. These results indicated the formaldehyde dissimilation through the GSH-dependent oxidation pathway was active in the engineered strains Po1dCb-RuMP and PoldPb-RuMP, which can reduce the accumulation of intracellular formaldehyde. It also can be inferred that the synthesis of GSH as the co-factor of the GSH-dependent oxidation pathway was upregulated by methanol metabolism to promote detoxification, therefore, higher labelled GSH was detected by ^{13}C tracer in engineered strains. In addition, methanol flux via the dissimilation pathway may also lead to higher NADH production from the last step of the conversion of HCOOH to CO_2. (Fig 5.4).

Notably, high ^{13}C labelling of some phospholipids was detected in both wild type and engineered *Y. lipolytica* strains. Also observed was the high concentration of ^{13}C label in serine in both wild type and engineered strains, which can both enter the TCA cycle to support cell growth but also is an indispensable precursor of phospholipids, especially phosphatidylserine. As Fig 5.4 shows, the level of ^{13}C in phosphatidylserine is also very high, which reached the range between 40% ~ 50%.

To assess whether the growth observed for engineered *Y. lipolytica* strains on methanol with yeast extract could be entirely attributed to the dissimilation pathway as opposed to the assimilation pathway, or both, an experiment comparing growth on methanol or formate with yeast extract was performed. As shown in Fig 5.5, engineered *Y. lipolytica* strains had improved growth on methanol over formate. However, significant growth was observed for the engineered strains grown on formate plus yeast extract where the OD600nm increased by 32% and 48% in the engineered strains Po1dPb-RuMP and Po1dCb-RuMP respectively, which infers that the dissimilation pathway plays an important role in promoting *Y. lipolytica* strains growth on methanol.

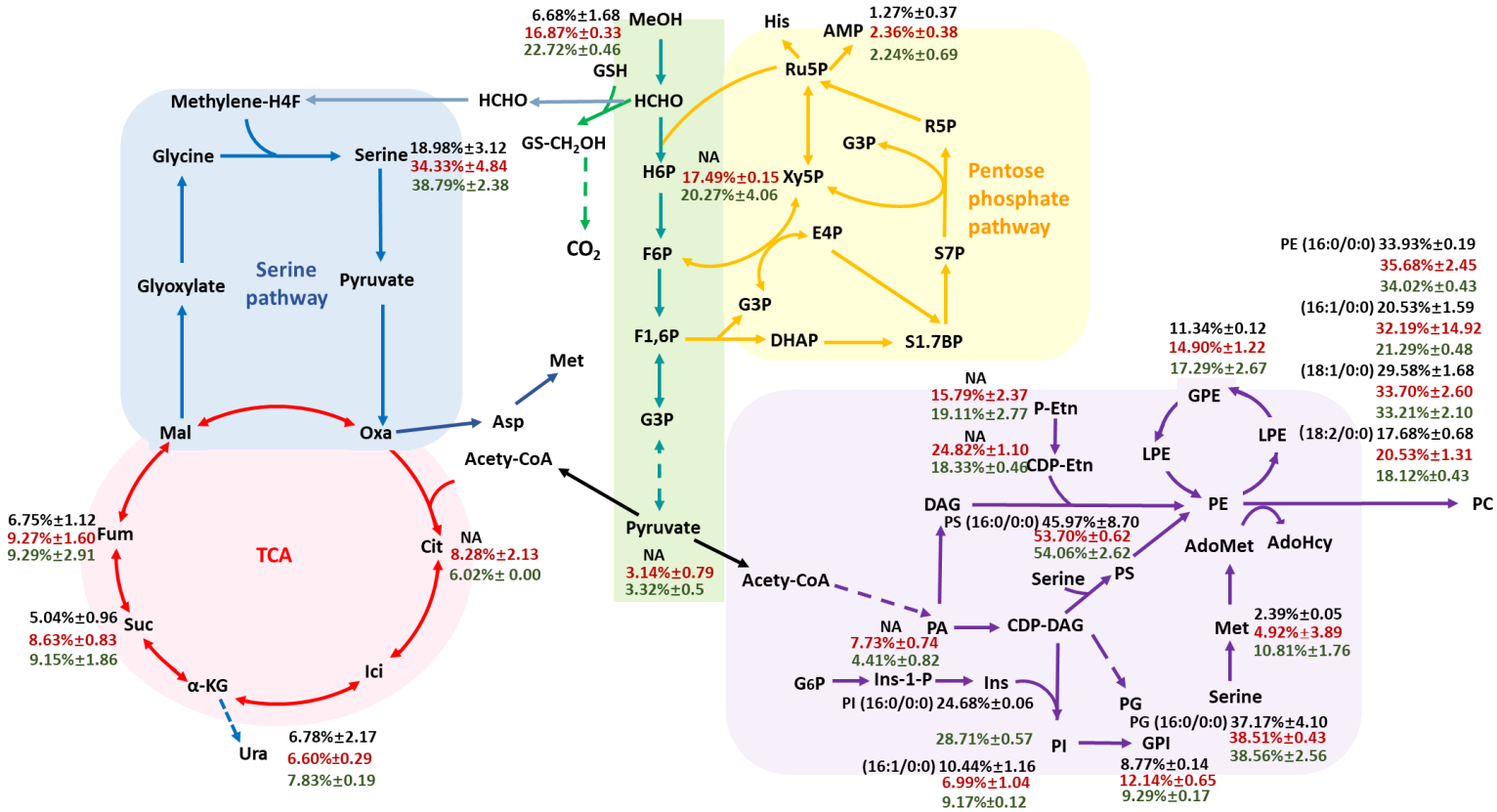

Fig 5.4 ^{13}C-labelling in intracellular metabolites from wild type *Y. lipolytica* strains (black), PoldCb-RuMP (red), and PoldPb-RuMP (green) cultivated in liquid YNB without glucose supplemented 0.5% yeast extract and 2% 13C-methanol. Values are means of triplicate experiments ± SD.

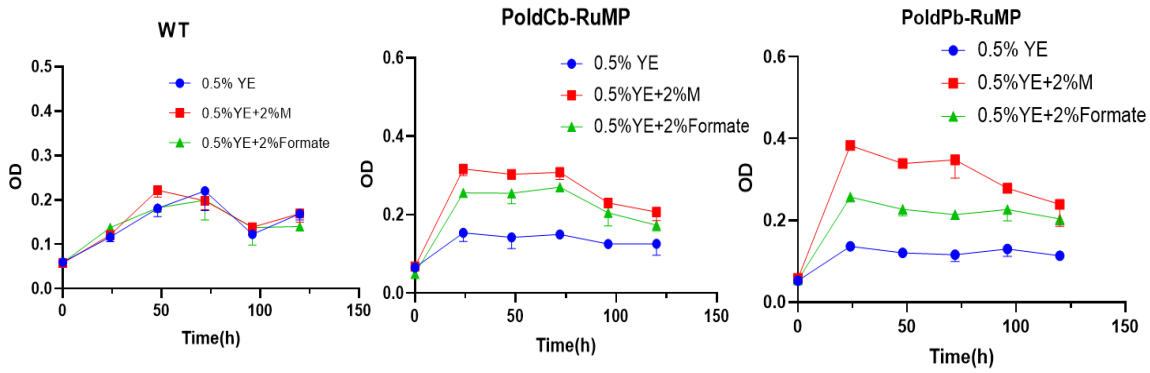

Fig 5.5 Comparison of *Y. lipolytica* strains growing on the liquid YNB medium without glucose with 0.5 % yeast extract (YE) or with 0.5 % yeast extract and 2 % methanol or with 0.5% yeast extract and 2% formate. Values are means of triplicate experiments ± SD

5.3.4 Conversion of methanol to resveratrol

In order to evaluate the capability of the engineered *Y. lipolytica* strains to convert methanol to products and further demonstrate assimilation, Po1dPb-RuMP and Po1dCb-RuMP strains were engineered to produce resveratrol. The resveratrol production pathway was contracted by integration of tyrosine ammonia-lyase (*FjTAL*) from *Flavobacterium johnsoniae* (Li et al., 2015), 4-coumaroyl-CoA ligase (*4CL1*) from *Arabidopsis thaliana* (Shin et al., 2012), and resveratrol synthase (*VvVST*) from *Vitis vinifera* (Li et al., 2015) (Fig 5.6A). After 48 h of culture in 0.5% yeast extract with 2% methanol, the Po1d strain engineered with the resveratrol synthesis pathway only, produces resveratrol at 3.69 mg/L in the media, whereas a titer of 4.09 mg/L was obtained for Po1dCb-RuMP strain, an increase in yield of 10.8% (Fig 5.6B). A similar result was obtained from the Po1dPb-RuMP strain, which yielded 4.30±0.09 mg/L, representing a 16.5% increase in titer over Po1d/resveratrol. ^{13}C-methanol was used to trace the fate of carbon from the substrate into resveratrol for the synthetic methylotrophic *Y. lipolytica* strains. LCMS analysis of the culture supernatants revealed a ^{13}C label at 35.1% of the resveratrol pool from the Po1dCb-RuMP strain when the culture was grown in ^{13}C-

methanol. By comparison, ^{13}C of 27.5% (Fig 5.6C) was measured in the Po1dPb-RuMP strain.

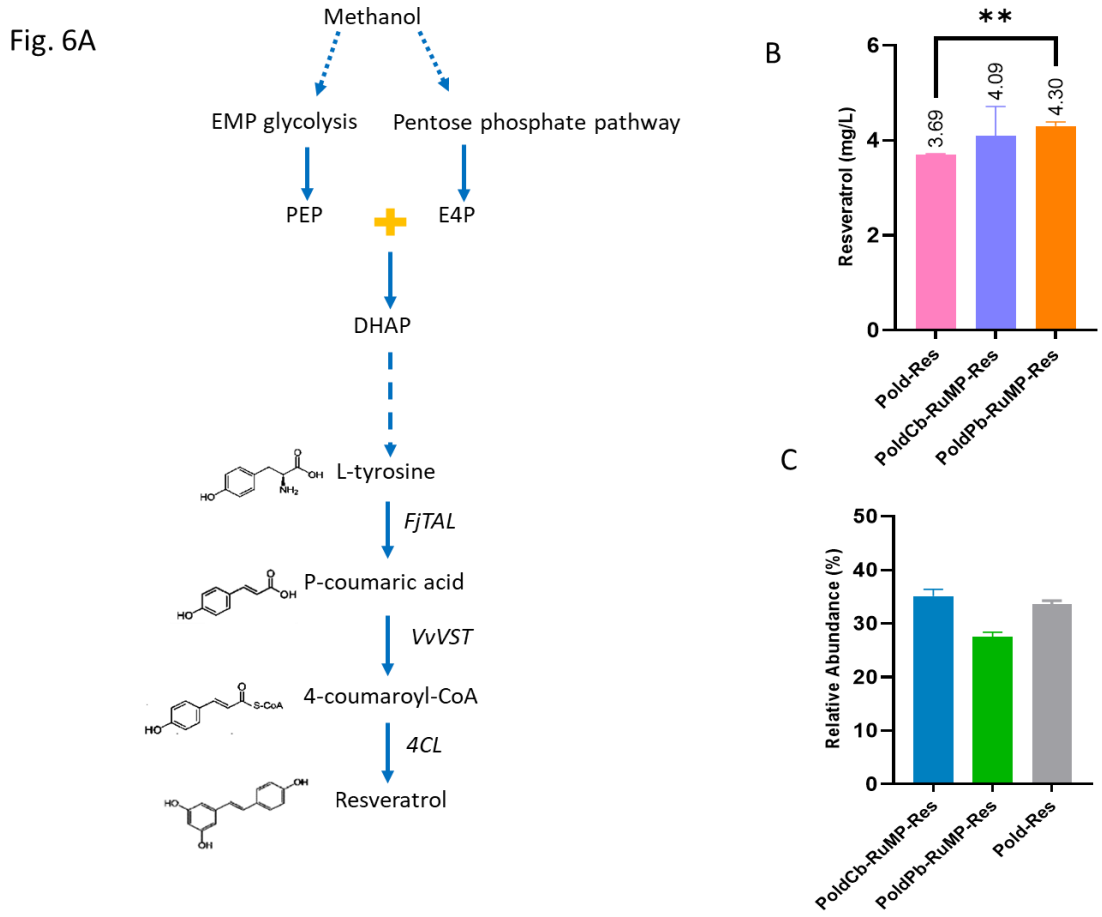

Fig 5.6 Conversion of methanol into resveratrol, a high-value polyphenol product (**A**) The pathway to convert methanol to resveratrol. (**B**) Resveratrol yield from *Y. lipolytica* strains cultivated in liquid YNB medium without glucose supplemented 0.5% yeast extract and 2% methanol. (**C**) ^{13}C-labelling data for resveratrol production. Values are means of triplicate experiments ± SD. Notes: * Represented that the effect of the factor was significant at $p < 0.05$ (Students t-test). ** Represented that the effect of the factor was significant at $p < 0.01$ (t-test).

5.4 Discussion

At the initiation of this research, it was expected that methanol assimilation pathway would be a completely exogenous metabolic pathway for *Y. lipolytica*. Therefore, constructing the effective methanol assimilation pathway in *Y. lipolytica* to support growth and production is challenging. In order to tackle this issue, here, we applied the strategy of rational design of the methanol assimilation pathway *in silico* combined with metabolic engineering and ^{13}C tracer analysis, and finally, methanol utilisation as a carbon source for the growth and bioproduction of *Y. lipolytica* was demonstrated. Here, the GSMM model was applied to predict *Y. lipolytica* growth on methanol with the expression of bacterial NAD+-dependent pathway or yeast O_2-dependent pathway.

In order to promote the integration of synthetic methanol metabolic pathway and endogenous metabolic pathways of *Y. lipolytica*, the strategy of accelerating the acceptor of formaldehyde by enhancing RuMP and XuMP pathway was predicted in simulations, which revealed this strategy could drive methanol assimilation. Subsequently, 7 genes associated with RuMP and 8 genes associated with XuMP were integrated into the chromosome of parent *Y. lipolytica* strains only expressing bacterial NAD+-dependent pathway or yeast O_2-dependent pathway. Recombinant expression of these genes related to RuMP or XuMP led to a dramatic improvement in methanol assimilation. Also, compared with the *Y. lipolytica* strains only expressing the essential genes of methanol assimilation, a faster growth rate on methanol was observed with the enhancement of the RuMP and XuMP pathway. Although the strategy of peroxisome-based targeting of methanol-utilisation proteins was attempted, this did not lead to obvious growth improvement, potentially due to limitations in exchange of required metabolic intermediates between the peroxisome and cytoplasm. Compared with yeast O_2-dependent pathway, *Y. lipolytica* containing bacterial NAD+-dependent pathway grew better on methanol, which was consistent with Wang et al. (Wang, Olofsson-Dolk et al. 2021). In addition, in order to assist in methanol metabolism in engineered *Y. lipolytica* strains, ALE

was performed. Although ALE did not make a significant improvement in methanol utilisation efficiency, the methanol tolerance of *Y. lipolytica* was dramatically improved. We are interested in the genomic characterisation of mutations that evolved for methanol tolerance, which will be investigated in the future.

Recently, a native methanol assimilation pathway was reported in *S. cerevisiae* and the efficiency of methanol utilisation via the native methanol assimilation pathway was significantly improved by ALE (Espinosa et al., 2020a; Espinosa et al., 2019). Intriguingly, ^{13}C labelled carbon was detected in some key metabolites such as serine, Fum, and Suc from wild type *Y. lipolytica* strains grown in ^{13}C-methanol. This study is also the first report to demonstrate that wild type *Y. lipolytica* strains possess a weak capacity for methanol assimilation. Additionally, the ^{13}C tracer experiments provided an in-depth analysis of methanol assimilation fluxes. In the engineered strains PoldCb-RuMP and PoldPb-RuMP strains, more intermediates such as H6P and Cit in the central carbon metabolic pathway containing high-level ^{13}C labelled carbon were detected. These metabolites were not found ^{13}C labelled in the wild type strain.

GSH is an indispensable cofactor for formaldehyde dissimilation (Yurimoto et al., 2005; Zhang et al., 2017). It was also found that carbon labelling in GSH was considerable in the engineered strains and above the wild type strain, which suggests the utilisation of methanol results in a higher turnover of GSH biosynthesis, potentially due to the stress response. Higher turnover of GSH may also result in a higher flux of methanol via the dissimilation pathway due to the higher availability of the co-substrate. Formaldehyde dissimilation reduces the toxicity of this metabolite and protects the cells from its various effects including electrophilic additions to proteins and genetic materials, but it also regenerates reducing equivalents, which is relevant to cell growth (Gutheil et al., 1997; Müller et al., 2015a; Vorholt, 2002). Although a higher growth rate was obtained from engineered strains in

methanol compared with formate, the experiment revealed that the formaldehyde dissimilation pathway likely plays a key role when *Y. lipolytica* is cultured on methanol.

Notably, significant quantities of ^{13}C were accumulated in phospholipids such as phosphatidylserine (PS) and phosphatidylethanolamine (PE), potentially revealing the response of cells to methanol because the cell membrane is an important barrier against toxic compounds. It has demonstrated that the composition and structure of cellular membrane decide formaldehyde tolerance (Azachi et al., 1996). It is inferred that a considerable quantity of ^{13}C label in phospholipids by carbon metabolic flux is self-defence to the toxic compounds such as methanol and formaldehyde. The increased turnover of membrane lipids where *Y. lipolytica* is cultured in methanol could be useful for the production of high-value lipids such as cyclopropane fatty acids (Chpt 3, 4) where the exotic fatty acid is generated on the phospholipid membrane before it is cycled to lipid stores. A further benefit may be achieved from the presence of cyclopropanated fatty acids in yeast membranes; their presence in microbial phospholipid membranes has been shown to be protective against the toxic level of alcohols (Pini et al., 2009).

Besides, serine is a precursor of phospholipid and an important intermediate metabolite for cell growth which also contained high ^{13}C labelled carbon derived from methanol. It is discovered that methylene-H_4F can be formed in the process of formaldehyde dissimilation through the H4F pathway in native methylotrophs, and the first step of the H4F pathway is that formaldehyde spontaneously condenses with H4F (Wang et al., 2020; Zhang et al., 2017). The same reaction is also able to occur in *Y. lipolytica*, which can promote serine biosynthesis. Furthermore, the recent work by Zhan et al. (2021), which appeared during the conduct of this research, reported the glyoxylate-based serine pathway could resist methanol by reducing the cytoplasmic accumulation of formaldehyde/formic acid (Zhan et al.). Therefore, it can be concluded that serine plays a crucial role in methanol utilisation.

Finally, we demonstrated that methanol utilisation in *Y. lipolytica* can sustain the production of new products such as resveratrol. Resveratrol is a natural polyphenolic compound with high value, which has a positive effect on human health, i.e., antitumor, anti-inflammatory, antidiabetic, antithrombotic, and anti-aging (He et al., 2020; Jeandet et al., 2012; Li et al., 2015), therefore, it is of strong interest to the pharmaceutical, food and cosmetic industries. The pathway for resveratrol synthesis was expressed in the yeast and produced from methanol. Although a helper substrate is still required for the growth of *Y. lipolytica* on methanol, it has been shown that methanol can be converted to high-value chemical compounds by these methanol assimilating strains. These results suggest that methanol is a promising and potential carbon source for microbial fermentation, which is an important step towards the biotechnological application of methanol conversion to the product. Also, that *Y. lipolytica* is a robust yeast that can be engineered for synthetic methylotrophy and versatile product biosynthesis.

5.5 Reference

Azachi, M., Henis, Y., Shapira, R., Oren, A. 1996. The role of the outer membrane in formaldehyde tolerance in Escherichia coli VU3695 and Halomonas sp. MAC. *Microbiology*, **142**(5), 1249-1254.

Bennett, R.K., Gonzalez, J.E., Whitaker, W.B., Antoniewicz, M.R., Papoutsakis, E.T. 2018. Expression of heterologous non-oxidative pentose phosphate pathway from Bacillus methanolicus and phosphoglucose isomerase deletion improves methanol assimilation and metabolite production by a synthetic Escherichia coli methylotroph. *Metabolic engineering*, **45**, 75-85.

Bertau, M., Offermanns, H., Plass, L., Schmidt, F., Wernicke, H.-J. 2014. *Methanol: the basic chemical and energy feedstock of the future*. Springer.

Chen, F.Y.-H., Jung, H.-W., Tsuei, C.-Y., Liao, J.C. 2020. Converting Escherichia coli to a Synthetic Methylotroph Growing Solely on Methanol. *Cell*, **182**(4): 933-946. e914..

Chistoserdova, L. 2011. Modularity of methylotrophy, revisited. *Environmental microbiology*, **13**(10), 2603-2622.

Clomburg, J.M., Crumbley, A.M., Gonzalez, R. 2017. Industrial biomanufacturing: the future of chemical production. *Science*, **355**(6320), aag0804.

Du, X.L., Jiang, Z., Su, D.S., Wang, J.Q. 2016. Research progress on the indirect hydrogenation of carbon dioxide to methanol. *ChemSusChem*, **9**(4), 322-332.

Espinosa, M.I., Gonzalez-Garcia, R.A., Valgepea, K., Plan, M., Scott, C., Pretorius, I.S., Marcellin, E., Paulsen, I.T., Williams, T.C. 2020a. Engineering and Evolution of Methanol Assimilation in Saccharomyces cerevisiae. *bioRxiv*, 717942.

Espinosa, M.I., Gonzalez-Garcia, R.A., Valgepea, K., Plan, M.R., Scott, C., Pretorius, I.S., Marcellin, E., Paulsen, I.T., Williams, T.C. 2020b. Adaptive laboratory evolution of native methanol assimilation in Saccharomyces cerevisiae. *Nature communications*, **11**(1), 1-12.

Espinosa, M.I., Valgepea, K., Gonzalez-Garcia, R.A., Scott, C., Pretorius, I.S., Marcellin, E., Paulsen, I.T., Williams, T. 2019. Native and synthetic methanol assimilation in Saccharomyces cerevisiae. *bioRxiv*, 717942.

Fukuoka, H., Kawase, T., Oku, M., Yurimoto, H., Sakai, Y., Hayakawa, T., Nakagawa, T. 2019. Peroxisomal Fba2p and Tal2p complementally function in the rearrangement pathway for xylulose 5-phosphate in the methylotrophic yeast Pichia pastoris. *Journal of bioscience and bioengineering*, **128**(1), 33-38.

Gutheil, W.G., Kasimoglu, E., Nicholson, P.C. 1997. Induction of glutathione-dependent formaldehyde dehydrogenase activity in Escherichia coli and Hemophilus influenza. *Biochemical and biophysical research communications*, **238**(3), 693-696.

He, Q., Szczepanska, P., Yuzbashev, T., Lazar, Z., Ledesma-Amaro, R. 2020. De novo production of resveratrol from glycerol by engineering different metabolic pathways in Yarrowia lipolytica. *Metab Eng Commun*, **11**, e00146.

Jeandet, P., Delaunois, B., Aziz, A., Donnez, D., Vasserot, Y., Cordelier, S., Courot, E. 2012. Metabolic engineering of yeast and plants for the production of the biologically active hydroxystilbene, resveratrol. *Journal of Biomedicine and Biotechnology*, **2012**.

Keller, P., Noor, E., Meyer, F., Reiter, M.A., Anastassov, S., Kiefer, P., Vorholt, J.A. 2020. Methanol-dependent Escherichia coli strains with a complete ribulose monophosphate cycle. *Nature communications*, **11**(1), 1-10.

Kerkhoven, E.J., Pomraning, K.R., Baker, S.E., Nielsen, J. 2016. Regulation of amino-acid metabolism controls flux to lipid accumulation in Yarrowia lipolytica. *NPJ systems biology and applications*, **2**(1), 1-7.

Le Dall, M.-T., Nicaud, J.-M., Gaillardin, C. 1994. Multiple-copy integration in the yeast Yarrowia lipolytica. *Current genetics*, **26**(1), 38-44.

Ledesma-Amaro, R., Nicaud, J.-M. 2016. Yarrowia lipolytica as a biotechnological chassis to produce usual and unusual fatty acids. *Progress in lipid research*, **61**, 40-50.

Li, M., Kildegaard, K.R., Chen, Y., Rodriguez, A., Borodina, I., Nielsen, J. 2015. De novo production of resveratrol from glucose or ethanol by engineered Saccharomyces cerevisiae. *Metabolic Engineering*, **32**, 1-11.

Markham, K.A., Alper, H.S. 2018. Synthetic biology expands the industrial potential of Yarrowia lipolytica. *Trends in biotechnology*, **36**(10), 1085-1095.

Meyer, F., Keller, P., Hartl, J., Gröninger, O.G., Kiefer, P., Vorholt, J.A. 2018. Methanol-essential growth of Escherichia coli. *Nature communications*, **9**(1), 1-10.

Müller, J.E., Heggeset, T.M., Wendisch, V.F., Vorholt, J.A., Brautaset, T. 2015a. Methylotrophy in the thermophilic Bacillus methanolicus, basic insights and

application for commodity production from methanol. *Applied microbiology and biotechnology*, **99**(2), 535-551.

Müller, J.E., Meyer, F., Litsanov, B., Kiefer, P., Potthoff, E., Heux, S., Quax, W.J., Wendisch, V.F., Brautaset, T., Portais, J.-C. 2015b. Engineering Escherichia coli for methanol conversion. *Metabolic engineering*, **28**, 190-201.

Naik, S.N., Goud, V.V., Rout, P.K., Dalai, A.K. 2010. Production of first and second generation biofuels: A comprehensive review. *Renewable and Sustainable Energy Reviews*, **14**(2), 578-597.

Pini, C.V., Bernal, P., Godoy, P., Ramos, J.L., Segura, A. 2009. Cyclopropane fatty acids are involved in organic solvent tolerance but not in acid stress resistance in Pseudomonas putida DOT-T1E. *Microbial biotechnology*, **2**(2), 253-261.

Price, J.V., Chen, L., Whitaker, W.B., Papoutsakis, E., Chen, W. 2016. Scaffoldless engineered enzyme assembly for enhanced methanol utilization. *Proceedings of the National Academy of Sciences*, **113**(45), 12691-12696.

Rußmayer, H., Buchetics, M., Gruber, C., Valli, M., Grillitsch, K., Modarres, G., Guerrasio, R., Klavins, K., Neubauer, S., Drexler, H. 2015. Systems-level organization of yeast methylotrophic lifestyle. *BMC biology*, **13**(1), 1-25.

Schrader, J., Schilling, M., Holtmann, D., Sell, D., Villela Filho, M., Marx, A., Vorholt, J.A. 2009. Methanol-based industrial biotechnology: current status and future perspectives of methylotrophic bacteria. *Trends in biotechnology*, **27**(2), 107-115.

Shin, S.-Y., Jung, S.-M., Kim, M.-D., Han, N.S., Seo, J.-H. 2012. Production of resveratrol from tyrosine in metabolically engineered Saccharomyces cerevisiae. *Enzyme and Microbial Technology*, **51**(4), 211-216.

van der Klei, I.J., Yurimoto, H., Sakai, Y., Veenhuis, M. 2006. The significance of peroxisomes in methanol metabolism in methylotrophic yeast. *Biochimica et Biophysica Acta (BBA)-Molecular Cell Research*, **1763**(12), 1453-1462.

Vartiainen, E., Blomberg, P., Ilmén, M., Andberg, M., Toivari, M., Penttilä, M. 2019. Evaluation of synthetic formaldehyde and methanol assimilation pathways in Yarrowia lipolytica. *Fungal biology and biotechnology*, **6**(1), 27.

Vorholt, J.A. 2002. Cofactor-dependent pathways of formaldehyde oxidation in methylotrophic bacteria. *Archives of microbiology*, **178**(4), 239-249.

Wang, G., M. Olofsson-Dolk, F. G. Hansson, S. Donati, X. Li, H. Chang, J. Cheng, J. Dahlin and I. Borodina (2021). "Engineering Yeast Yarrowia lipolytica for Methanol Assimilation." ACS Synthetic Biology, **10**(12), 3537−3550

Wang, Y., Fan, L., Tuyishime, P., Zheng, P., Sun, J. 2020. Synthetic Methylotrophy: A Practical Solution for Methanol-Based Biomanufacturing. *Trends in Biotechnology*, **38**(6): 650-666 .

Whitaker, W.B., Sandoval, N.R., Bennett, R.K., Fast, A.G., Papoutsakis, E.T. 2015. Synthetic methylotrophy: engineering the production of biofuels and chemicals based on the biology of aerobic methanol utilization. *Current opinion in biotechnology*, **33**, 165-175.

Woolston, B.M., King, J.R., Reiter, M., Van Hove, B., Stephanopoulos, G. 2018. Improving formaldehyde consumption drives methanol assimilation in engineered E. coli. *Nature communications*, **9**(1), 1-12.

Yurimoto, H., Kato, N., Sakai, Y. 2005. Assimilation, dissimilation, and detoxification of formaldehyde, a central metabolic intermediate of methylotrophic metabolism. *The Chemical Record*, **5**(6), 367-375.

Zhan, C., Li, X., Baidoo, E.E., Yang, Y., Sun, Y., Wang, S., Wang, Y., Wang, G., Nielsen, J., Keasling, J.D. The Glyoxylate-Serine Pathway Enables Conversion of Saccharomyces cerevisiae to a Synthetic Methylotroph. *SSRN Electronic J.* 2021

Zhang, W., Zhang, T., Wu, S., Wu, M., Xin, F., Dong, W., Ma, J., Zhang, M., Jiang, M. 2017. Guidance for engineering of synthetic methylotrophy based on methanol metabolism in methylotrophy. *RSC advances*, **7**(7), 4083-4091.

This page is intentionally blank

CHAPTER 6

CONCLUSIONS AND OUTLOOK

This page is intentionally blank

Chapter 6 Conclusions and outlook

6.1 Conclusion

In modern society, rapid industrialisation has led to unsustainable development and its effects on the planet are clear in terms of rising anthropogenic CO_2 emissions to the atmosphere and global warming, and widespread land clearing for agriculture and to accommodate growing populations. Seeking sustainable, green and new alternative ways to generate energy and products could effectively address this crisis. For example, biologically produced lipids can be both alternative energy and product (oleochemical) sources possessing high energy density and attracting increasing attention. In particular, some unusual fatty acids can have a wide application due to their unique properties. This thesis studied the biosynthesis of cyclopropane fatty acids in yeast and their potential as the host microorganisms for CFAs microbial cell factories. Meanwhile, methanol is an abundant, low-cost C1 compound available as an industrial by-product or generated from waste sources. Here, yeast was engineered to utilise methanol for growth, energy and the production of some high-value products, which can be used as an important example for future production.

6.1.1 Redirection of cyclopropane fatty acids flux toward triacylglycerol to increase cyclopropane fatty acids turnover in *S. cerevisiae*.

While cyclopropane fatty acids are distributed widely in some plants, bacterial and fungi, the natural production yield is very low and unlikely to be improved. So far, the yeasts *S. cerevisiae* and *Y. lipolytica* have been successfully employed as microbial hosts for a variety of chemicals and biofuels with considerable yields. Therefore, they have good potential for CFAs production. However, CFAs are exotic fatty acids for yeast and the synthesis routes and amenability to metabolic engineering in these hosts were unknown. In this chapter, the ability of native enzymes in *S. cerevisiae* to utilise revealed that these enzymes, which can

exhibit exquisite specificity, could handle this exotic fatty acid and esterify CFAs into TAGs. The subcellular localisation of heterologously-expressed enzyme demonstrated the cyclopropane synthetase acted on the plasma and internal membranes of yeast. CFAs positional analysis in phospholipids showed CFAs appeared in both fatty acids in the membrane. In order to contribute more CFAs to storage in triacylglycerols, a strategy to redirect cyclopropane fatty acids flux toward triacylglycerols was applied, which included three steps: to overcome the substrate limitations for cyclopropane-fatty-acyl-phospholipid synthase, increase the phospholipid fatty acid turnover rate and prevention of triacylglycerols degradation. It was demonstrated that overcoming the substrate limitation for cyclopropane synthetase significantly increased the overall CFAs content, although CFAs remained at a high concentration on the membrane. Subsequently, CFAs were turned over from phospholipids to triacylglycerols with the help of phospholipase B, diacylglycerol acyltransferases from *Arabidopsis thaliana* (*AtDGAT1*) and a long-chain fatty acyl-CoA synthase from *Sinorhizobium meliloti* (*fadD*). The last step was aimed to prevent triacylglycerol degradation by deleting key enzymes triacylglycerol lipase 3 (*tgl3*) and acyl-coenzyme A oxidase (*pox1*). Compared with the strain which only expressed cyclopropane-fatty-acyl-phospholipid synthase, CFAs of TAG_S increased to 12.17 mg/g and 21.31% of triacylglycerols by the strategy redirection of cyclopropane fatty acids flux toward triacylglycerols.

6.1.2 Engineering *Y. lipolytica* for CFAs production

Making full use of the characteristics of high oil production by oleaginous yeast, the strategy verified in *S. cerevisiae* was transferred into *Y. lipolytica*. All the genes used to increase CFAs yield in *S. cerevisiae* were assembled into the integration vectors for *Y. lipolytica* expression. Although all genes introduced were confirmed to be present in engineered *Y. lipolytica*, CFAs yield in the strains was low and the quantity was slightly improved by the

presence of additional metabolic engineering genes. While there may be multiple reasons contributing to the low CFAs yield, the clear issue was low CFAs production from low cyclopropane synthetase expression. Had the CFAs production been substantially higher, the strategy of cycling of fatty acids from membranes to lipid stores, as demonstrated in *S. cerevisiae*, would have been properly tested. Time and laboratory access restrictions limited the ability to fully test these ideas.

6.1.3 Engineering methanol utilisation in *Y. lipolytica* for high value bioproduction

Methanol is an abundant carbon feedstock with high reduced energy and an ideal alternative to traditional sugar carbon sources for microbial growth. In this chapter, methanol as an auxiliary carbon source to support the growth of *Y. lipolytica* was demonstrated by constructing the essential methanol assimilation and enhancing the pentose phosphate pathway, which successfully linked with the endogenous central carbon metabolism of *Y. lipolytica*. ^{13}C-methanol tracer analysis of *Y. lipolytica* showed that important intermediate metabolites such as serine and H6P were labelled from ^{13}C methanol metabolism, which further demonstrated that methanol is utilised by our engineered *Y. lipolytica* strains. Also, when the methanol was added into the culture medium as an auxiliary carbon source, higher cell growth of engineered yeast was obtained. In addition, the resveratrol synthesis pathway was constructed in *Y. lipolytica* engineered for methanol utilisation to demonstrate that high-value products could result from methanol as a feedstock. Higher yields and ^{13}C-methanol incorporation into resveratrol were demonstrated in the methanol engineered strain. Based on the above results, it can be concluded that the *Y. lipolytica* conversion platform is promising for methanol conversion to products.

6.2 Outlook

The outcomes of this thesis exemplified the construction of a yeast cell factory for unusual fatty acids, also, provide an important reference for the use of a novel carbon source for microbial utilisation, which can be extended to other microorganisms and other high-value products. Based on these achievements, further research is recommended for the future including:

6.2.1 Further increasing flux of CFAs from the membrane to storage

In chapter 3, phospholipase B2 was overexpressed to help release CFAs from PLs. Although the CFAs content in PLs was dramatically decreased with the lipase expression, CFAs remained on the PLs membrane, which was the main bottleneck for further improving CFAs production in yeast. Besides phospholipase B2, phospholipase B1 and B3 can also cleave the fatty acids chains at both of *sn*-1 and *sn*-2 positions from the glycerol backbone in phospholipids. Therefore, in order to release more CFAs from PLs, investigation of other lipases such as phospholipase B1 and B3 could be tested for this effect. However, it is risky to overexpress more phospholipase because it would break the metabolic balance of membranes and potentially cause cell death. Further approaches include selecting phospholipase or diacylglycerol transferase candidates with a preference for CFAs from the organisms natively producing CFAs, could allow a greater specific CFAs turnover from PLs to triacylglycerols.

6.2.2 Improving CFAs yield in engineered *Y. lipolytica*

The first step is to increase cyclopropane synthetase expression in *Y. lipolytica* via the use of stronger promoters and the introduction of increased copies of the gene. Once established, the original goal of investigating the impact of increased flux from membranes to storage could be tested and optimised as described in the previous section. There are multiple bioprocess

parameters that could also be implemented to improve yields at the bioreactor scale such as 2-stage or fed-batch cultures, extended time culturing, tailored substrates for cyclopropane formation such as oleic acid feeding.

6.2.3 Long-term adaptive laboratory evolution combined with reverse engineering for methanol utilisation

Although it has been shown that engineered *Y. lipolytica* have improved growth with methanol as an auxiliary carbon source, methanol utilisation efficiency needs improvement for this to be a viable bioprocess. Importation of synthetic methanol utilisation pathways into heterologous strains causes metabolite imbalance and the challenge remains as to how best to integrate heterogeneous methanol utilisation pathways into endogenous metabolic pathways for effective methanol metabolism and growth. It has been demonstrated that adaptive laboratory evolution (ALE) combined with reverse engineering is a powerful strategy to improve the performance of engineered organisms and to inform us of the impacts of the radical metabolic changes brought about by synthetic methanol engineering. However, ALE usually requires a long term to be effective and appropriate cultural conditions. Because of the time limits of the Ph.D., the second-approach ALE was restricted to three months. In order to improve the methanol utilisation efficiency of engineered *Y. lipolytica* strains to achieve the ultimate goal of methanol as the sole carbon source to support the growth, longer periods of ALE are required. Advantageous mutations generated during ALE enable metabolically engineered strains to adapt to imposed methanol metabolic pathways and improve the cells' tolerance to methanol, resulting in better utilisation of methanol. Reverse engineering can further enhance these advantageous mutations.

Appendix. Supplementary material

DNA sequence of *ECcfa*

ATGTCATCTTCTTGTATTGAAGAAGTTTCTGTTCCAGATGATAATTGGTACAGAAT
TGCAAATGAATTATTGTCAAGAGCAGGTATTGCTATTAATGGTTCTGCACCAGCT
GATATTAGAGTTAAAAATCCAGATTTCTTTAAAAGAGTTTTGCAAGAAGGTTCAT
TAGGTTTGGGTGAATCATACATGGATGGTTGGTGGGAATGTGATAGATTGGATAT
GTTTTTCTCTAAAGTTTTGAGAGCTGGTTTGGAAAATCAATTACCACATCATTTTA
AAGATACTTTGAGAATTGCAGGTGCTAGATTGTTTAATTTGCAATCTAAAAAGAG
AGCTTGGATTGTTGGTAAAGAACATTACGATTTGGGTAATGATTTGTTTTCAAGA
ATGTTAGATCCATTCATGCAATACTCATGTGCTTACTGGAAAGATGCTGATAATT
TGGAATCAGCTCAACAAGCAAAATTAAAAATGATTTGTGAAAAATTGCAATTAA
AACCAGGTATGAGAGTTTTGGATATTGGTTGTGGTTGGGGTGGTTTAGCTCATTA
CATGGCTTCTAATTATGATGTTTCTGTTGTTGGTGTTACTATTTCTGCTGAACAAC
AAAAGATGGCTCAAGAAAGATGTGAAGGTTTGGATGTTACAATTTTATTGCAAG
ATTACAGAGATTTGAATGATCAATTTGATAGAATTGTTTCTGTTGGTATGTTTGAA
CATGTTGGTCCAAAGAATTACGATACATACTTTGCTGTTGTTGATAGAAATTTGA
AACCAGAAGGTATTTTCTTATTGCATACTATTGGTTCTAAAAAGACTGATTTGAA
TGTTGATCCATGGATTAATAAGTACATTTTTCCAAATGGTTGTTTGCCATCAGTTA
GACAAATTGCTCAATCTTCAGAACCACATTTTGTTATGGAAGATTGGCATAATTT
TGGTGCTGATTATGATACAACTTTGATGGCTTGGTACGAAAGATTTTTGGCAGCT
TGGCCAGAAATTGCTGATAATTATTCAGAAAGATTCAAAAGAATGTTTACTTATT
ACTTGAATGCATGTGCTGGTGCTTTTAGAGCTAGAGATATTCAATTATGGCAAGT
TGTCTTTAGTAGAGGTGTAGAAAATGGTTTGAGAGTAGCAAGATGA

DNA sequence of *sam2*

ATGTCTAAGTCAAAGACATTTTTGTTTACTTCTGAATCAGTTGGTGAAGGTCATCC
AGATAAAATTTGTGATCAAGTTTCAGATGCAATTTTGGATGCTTGTTTAGAACAA
GATCCATTTTCTAAGGTTGCATGTGAAACTGCTGCAAAAACTGGTATGATCATGG
TTTTCGGTGAAATCACTACAAAGGCTAGATTAGATTACCAACAAATCGTTAGAGA
TACTATTAAGAAAATTGGTTACGATGATTCTGCTAAGGGTTTCGATTACAAGACA
TGTAACGTTTTGGTTGCAATCGAACAACAATCACCAGATATTGCTCAAGGTTTGC
ATTACGAAAAATCTTTGGAAGATTTGGGTGCAGGTGACCAAGGTATTATGTTTGG
TTACGCTACTGATGAAACACCAGAAGGTTTGCCATTGACTATCTTGTTGGCTCAT
AAATTGAATATGGCTATGGCAGATGCTAGAAGAGATGGTTCATTGCCTTGGTTAA
GACCAGATACTAAGACACAAGTTACTGTTGAATACGAAGATGATAATGGTAGAT
GGGTTCCAAAGAGAATCGATACAGTTGTTATTTCAGCACAACATGCTGATGAAAT
TTCTACTGCTGATTTGAGAACACAATTACAAAAGGATATTGTTGAAAAAGTTATT
CCAAAAGATATGTTGGATGAAAATACTAAATATTTTATTCAACCATCTGGTAGAT
TTGTTATTGGTGGTCCACAAGGTGACGCTGGTTTGACAGGTAGAAAGATCATCGT
TGATGCATACGGTGGTGCTTCTTCAGTTGGTGGTGGTGCTTTTTCTGGTAAAGATT
ACTCAAAGGTTGATAGATCAGCTGCTTATGCTGCAAGATGGGTTGCTAAATCATT
GGTTGCTGCTGGTTTGTGTAAGAGAGTTCAAGTTCAATTTTCTTATGCTATCGGTA
TTGCTGAACCATTGTCTTTACATGTTGATACATACGGTACTGCTACAAAGTCTGAT

GATGAAATCATCGAAATTATTAAGAAAAATTTCGATTTGAGACCAGGTGTTTTAG
TTAAAGAATTGGATTTGGCAAGACCAATATATTTGCCAACTGCTTCATACGGTCA
TTTCACAAACCAAGAATACTCTTGGGAAAAGCCAAAGAAATTGGAATTTTAATA
A

DNA sequence of *plb2*

ATGCAATTGAGAAACATCTTGCAAGCATCTTCATTAATTTCAGGTTTGTCTTTAGC
TGCTGATTCTTCTTCTACTACTGGTGACGGTTATGCTCCATCTATTATTCCATGTC
CATCAGATGATACTTCTTTAGTTAGAAATGCTTCAGGTTTGTCTACTGCTGAAAC
AGATTGGTTGAAGAAAAGAGATGCTTACACTAAGGAAGCATTACATTCATTTTTG
TCAAGAGCTACATCAAACTTCTCTGATACTTCATTGTTATCTACATTGTTTTCATC
TAATTCATCTAATGTTCCAAAAATTGGTATTGCTTGTTCTGGTGGTGGTTATAGAG
CTATGTTAGGTGGTGCAGGCATGATTGCTGCAATGGATAATAGAACTGATGGTGC
TAATGAACATGGTTTGGGTGGTTTGTTACAATCATCTACATACTTATCAGGTTTGT
CTGGTGGTAATTGGTTAACTGGTACATTGGCTTGGAACAACTGGACTTCTGTTCA
AGAAATCGTTGATCACATGTCTGAATCAGATTCTATTTGGAACATCACAAAGTCT
ATCGTTAATCCAGGTGGTTCAAATTTGACTTACACAATCGAAAGATGGGAATCTA
TCGTTCAAGAAGTTCAGGCTAAGTCAGATGCAGGTTTTAATATTTCATTATCTGA
TTTGTGGGCAAGAGCTTTATCATACAATTTCTTTCCATCTTTGCCAGATGCTGGTT
CAGCATTAACTTGGTCATCTTTGAGAGATGTTGATGTTTTTAAAAACGGTGAAAT
GCCATTGCCAATTACAGTTGCAGATGGTAGATACCCAGGTACTACTGTTATTAAT
TTGAACGCTACTTTGTTCGAGTTTACTCCATTCGAAATGGGTTCATGGGACCCAT
CTTTGAACGCTTTTACTGATGTTAAGTATTTGGGTACTAACGTTACAAACGGTAA
ACCAGTTAATAAGGATCAATGTGTTTCTGGTTACGATAATGCTGGTTTTGTTATTG
CTACATCAGCTTCTTTGTTTAATGAATTTTCTTTGGAAGCATCAACTTCTACATAC
TACAAGATGATCAACTCTTTTGCTAATAAGTATGTTAATAATTTGTCACAAGATG
ATGATGATATTGCAATCTATGCTGCAAATCCTTTTAAAGATACTGAATTTGTTGAT
AGAAATTACACATCATCTATCGTTGATGCTGATGATTTGTTTTTAGTTGATGGTGG
TGAAGATGGTCAAAATTTGCCATTAGTTCCATTGATTAAGAAAGAAAGAGATTTG
GATGTTGTTTTCGCTTTGGATATTTCTGATAACACTGATGAATCATGGCCATCTGG
TGTTTGTATGACTAACACTTATGAAAGACAATACTCTAAGCAGGGTAAAGGCATG
GCATTTCCATACGTTCCAGATGTTAACACATTTTTGAATTTGGGTTTGACTAATAA
GCCAACTTTCTTTGGTTGTGATGCTAAAAATTTGACTGATTTGGAATACATTCCAC
CATTAGTTGTTTACATCCCAAATACAAAACATTCTTTTAATGGTAACCAATCAAC
TTTGAAGATGAATTACAATGTTACAGAAAGATTGGGTATGATTAGAAATGGTTTT
GAAGCTGCAACTATGGGTAACTTCACAGATGATTCTAATTTCTTGGGTTGTATCG
GTTGTGCTATCATCAGAAGAAAGCAAGAATCTTTAAATGCAACTTTGCCACCAGA
ATGTACAAAGTGTTTCGCTGATTACTGTTGGAACGGTACTTTATCAACATCTGCT
AATCCAGAATTGTCTGGTAATTCTACTTACCAATCTGGTGCAATTGCTTCAGCAA
TTTCTGAAGCTACTGATGGTATTCCAATTACAGCATTGTTAGGTTCATCTACATCT
GGTAACACTACATCAAATTCTACTACATCAACTTCATCTAACGTTACATCAAATT
CTAATTCATCTTCAAACACTACATTAAATTCTAATTCTTCATCTTCATCTATTTCAT
CTTCAACTGCAAGATCATCTTCTTCTACTGCTAATAAGGCAAATGCTGCTGCTATT
TCTTATGCTAACACTAACACATTGATGTCATTGTTAGGTGCTATTACTGCATTATT
TGGTTTGATTTGATAA

DNA sequence of *ole1*

ATGCCTACATCAGGTACAACAATAGAATTAATAGACGACCAATTTCCAAAGGAC
GACAGTGCCTCATCAGGTATAGTAGACGAAGTCGATTTGACTGAAGCTAATATTT
TGGCTACTGGTTTGAATAAGAAAGCACCAAGAATTGTTAATGGTTTTGGTTCTTT
GATGGGTTCTAAAGAAATGGTTTCTGTTGAATTTGATAAAAAGGGTAATGAAAA
GAAATCTAATTTGGATAGATTATTGGAAAAAGATAATCAAGAAAAAGAAGAAGC
TAAAACTAAAATTCATATTTCTGAACAACCATGGACTTTGAATAATTGGCATCAA
CATTTGAATTGGTTGAATATGGTTTTGGTTTGTGGTATGCCAATGATTGGTTGGTA
CTTTGCTTTGTCTGGTAAAGTTCCATTACATTTGAATGTTTTCTTGTTTTCAGTTTT
CTATTACGCTGTTGGTGGTGTTTCTATTACTGCTGGTTACCATAGATTGTGGTCTC
ATAGATCATACTCTGCTCATTGGCCATTGAGATTATTTTATGCTATTTTTGGTTGT
GCTTCTGTTGAAGGTTCTGCTAAATGGTGGGGTCATTCTCATAGAATTCATCATA
GATACACTGATACATTGAGAGATCCATATGATGCTAGAAGAGGTTTGTGGTACTC
TCATATGGGTTGGATGTTATTGAAACCAAATCCAAAATACAAAGCTAGAGCAGA
TATTACAGATATGACTGATGATTGGACAATTAGATTTCAACATAGACATTACATT
TTGTTAATGTTGTTAACTGCATTTGTTATTCCAACATTGATTTGTGGTTACTTTTTC
AATGATTACATGGGTGGTTTAATATACGCTGGTTTTATTAGAGTTTTTGTTATTCA
ACAAGCTACTTTTTGTATTAATTCTTTGGCACATTATATTGGTACTCAACCATTTG
ATGATAGAAGAACTCCAAGAGATAATTGGATTACTGCAATTGTTACTTTTGGTGA
AGGTTACCATAATTTTCATCATGAATTTCCAACTGATTACAGAAATGCTATTAAA
TGGTATCAATACGATCCAACTAAAGTTATTATCTATTTGACTTCTTTGGTTGGTTT
GGCTTACGATTTGAAAAAGTTTTCTCAAAATGCAATTGAAGAAGCTTTAATTCAA
CAAGAACAAAAGAAAATTAATAAGAAAAAGGCTAAAATTAATTGGGGTCCAGTT
TTGACAGATTTGCCAATGTGGGATAAACAAACATTTTTGGCTAAATCTAAAGAAA
ATAAGGGTTTAGTTATTATTTCAGGTATTGTTCATGATGTTTCTGGTTACATTTCT
GAACATCCAGGTGGTGAAACTTTGATTAAAACAGCATTGGGTAAAGATGCTACT
AAAGCATTTTCTGGTGGTGTTTACAGACATTCAAATGCTGCACAAAATGTTTTGG
CTGATATGAGAGTTGCTGTTATTAAAGAATCTAAAAATTCAGCAATCAGAATGGC
ATCCAAGAGAGGTGAAATCTACGAAACTGGTAAATTCTTCTAA

DNA sequence of *fadD*

ATGGCCGAAGCCTCAACTCAACAAGCTGGTTCCTCTACCGCAAAAATCTGGTTAG
GTTCTTATCCTCCTGGTGTCCCTGCCGAAATAGGTCCATTGACTTATAGATCAATT
GGTGAATTTTTCGATCATGCTGTTGCACAATACTCATGGAGACCAGCTTTTACAT
GTATGGGTAAAGCTTTAACTTTTTCTGATTTGAATACTCATTCTGCTAAAATTGGT
GCTTGGTTGCAATCATTAGGTTTGGCTAAAGGTGACAGAGTTGCTGTTATGATGC
CAAATATTTTACAAAATCCAGTTATTGTTTACGGTATTTTGAGAGCAGGTTTTACT
GTTGTTAATGTTAATCCATTGTATACTCCAAGAGAATTGGAACATCAATTGGTTG
ATGCAGGTGCTAAAGCAATTTTTGTTTTGGAAAATTTTGCTCATACAGTTGAACA
AGTTTTGGCTAGAACAGAAGTTAAACATGTTGTTGTTGCTTCAATGGGTGACATG
TTGGGTGCTAAAGGTGCTATTGTTAATTTGGTTGTTAGAAGAGTTAAAAAGTTGG
TTCCAGCTTGGTCAATTCCAGGTCATTTGTCTTTTAAAACTGTTTTGGCAAAAGGT
GCTACTTTAGGTTTTAAAAGACCAAATGTTGCTCCAGGTGACGTTGCATTTTTGC
AATACACAGGTGGTACTACAGGTGTTTCTAAAGGTGCAACTTTGACTCATGCAAA
TTTGTTATCAAATATGGCACAAATGGAATTATGGTTGAATACTGCATTTTTAAGA
AAACCAAGACCAGAATCTTTGACTTTTATGTGTGCTTTGCCATTATACCATATTTT
TGCTTTGACAGTTAATTCTTTGATGGGTTTAGCTACTGGTGGTAATAATATTTTGA

TTCCAAATCCAAGAGATATTCCAGCTTTTGTTAAAGAATTAGGTAGATATAGAAC
TAATATTTTTCCAGGTTTGAATACTTTGTTTAATGCTTTGATGAATAATTCTGAAT
TCAGAAAATTGGATTTTTCTTCATTAATTTTGACTTTTGGTGGTGGTATGGCTGTT
CAAAGACCAGTTGCTGAAAGATGGTTGGAATTAACTGGTTGTCCAATTCATGAAG
GTTATGGTTTGTCAGAAACTTCTCCAGTTGCAACTGCTAATAGATTGGATACTGA
TGATTTTACAGGTACTATTGGTATTCCATTGCCATCAACAGAAGTTGAAATTAGA
GATGAAGATGGTAGAACTTTACCAGTTGGTGAAATTGGTGAAATTTGTATTAGAG
GTCCACAAGTTATGGCTGGTTACTGGCAAAGACCAGAAGAAACAGCTAGAGCAA
TTTCACCAGATGGTTTCTTTAGAACAGGTGACGTTGGTTTTATGAATGCAGAAGG
TTTGACAAAAATTGTTGATAGAAAGAAAGATATGATTTTGGTTTCAGGTTTTAAT
GTTTTTCCAAATGAAATTGAAGAAGTTGCAGCTACTCATCCAGGTATTTTGGAAT
GTGCTGCAATTGGTGTTGCTGATCCACATTCAGGTGAAGCTGTTAAATTGTTTGTT
GTTAGAAAAGATCCAAATTTGACAGAAGAAGAAGTTAAAAGACATTGTGCAGCA
TCATTGACTAATTATAAAAGACCAAGATATGTTGAATTCAGAACTGAATTGCCAA
AATCTAATGTAGGTAAAATCTTGAGAAAGGACTTGAGAGGTTGA

DNA sequence of *DuLACS*

ATGAAATCATTTGCTGCAAAAGTTGCAGAAGGTGTTAAAGGTATTGATGGTAAA
CCATCTGTTGGTCCAGTTTACAGAAATTTGTTGTCAGAAAAGGGTTTTCCACCAA
TTGATTCTGAAATTACTACAGCTTGGGATATTTTCTCTAAGTCAGTTGAAAAGTTC
CCAGATAATAATATGTTGGGTTGGAGAAGAATCGTTGATGAAAAGGTTGGTCCA
TACATGTGGAAGACTTACAAGGAAGTTTACGAAGAAGTTTTGCAAATTGGTTCAG
CATTAAGAGCTGCAGGTGCTGAACCAGGTTCTAGAGTTGGTATCTATGGTGTTAA
TTGTCCACAATGGATTATTGCTATGGAAGCATGTGCTGCACATACTTTGATCTGT
GTTCCATTGTACGATACATTAGGTTCTGGTGCAGTTGATTACATCGTTGAACATG
CTGAAATCGATTTCGTTTTCGTTCAAGATACAAAGATTAAAGGTTTGTTGGAACC
AGATTGTAAGTGTGCAAAGAGATTGAAGGCTATCGTTTCTTTTACTAACGTTTCT
GATGAATTGTCACATAAGGCATCTGAAATCGGTGTTAAGACATACTCTTGGATCG
ATTTCTTGCATATGGGTAGAGAAAAACCAGAAGATACTAATCCACCAAAGGCTT
TTAATATCTGTACAATCATGTACACTTCTGGTACATCAGGTGACCCAAAAGGTGT
TGTTTTGACTCATCAAGCTGTTGCAACATTCGTTGTTGGTATGGATTTGTACATGG
ATCAATTCGAAGATAAGATGACTCATGATGATGTTTACTTGTCATTTTTGCCATTG
GCACATATCTTGGATAGAATGAACGAAGAATATTTCTTTAGAAAGGGTGCTTCTG
TTGGTTACTACCATGGTAATTTGAACGTTTTGAGAGATGATATCCAAGAATTGAA
GCCAACATACTTAGCAGGTGTTCCAAGAGTTTTCGAAAGAATCCATGAAGGTATC
CAAAAGGCTTTGCAAGAATTGAACCCAAGAAGAAGATTCATTTTTAATGCATTGT
ACAAGCATAAGTTGGCTTGGTTGAATAGAGGTTACTCTCATTCAAAAGCTTCTCC
AATGGCAGATTTCATCGCTTTTAGAAAGATCCGTGATAAGTTAGGTGGTAGAATC
AGATTGTTAGTTTCAGGTGGTGCTCCATTGTCTCCAGAAATCGAAGAATTCTTGA
GAGTTACTTGTTGTTGTTTTGTTGTTCAAGGTTATGGTTTGACTGAAACATTAGGT
GGTACTGCATTGGGTTTTCCAGATGAAATGTGTATGTTAGGTACAGTTGGTATCC
CAGCTGTTTACAACGAAATCAGATTGGAAGAAGTTTCAGAAATGGGTTACGATC
CATTAGGTGAAAATCCAGCTGGTGAAATTTGTATCAGAGGTCAATGTATGTTCTC
TGGTTACTACAAGAACCCAGAATTGACTGAAGAAGTTATGAAAGATGGTTGGTTT
CATACAGGTGACATTGGTGAAATTTTGCCAAATGGTGTTTTGAAGATCATCGATA
GAAAGAAAAATTTGATTAAATTGTCACAGGGTGAATACGTTGCTTTGGAACATTT
GGAAAACATCTTCGGTCAAAACTCTGTTGTTCAAGATATCTGGGTTTACGGTGAC

TCTTTTAAATCAATGTTGGTTGCAGTTGTTGTTCCAAATCCAGAAACTGTTAATAG
ATGGGCTAAAGATTTGGGTTTTACAAAGCCATTCGTTGAATTGTGTTCATTTCCA
GAATTAAAGGAACATATCATCTCAGAATTGAAGTCTACTGCTGAAAAGAATAAG
TTGAGAAAGTTCGAATACATCAAGGCTGTTGCAGTTGAAACAAAGCCATTCGAT
GTTGAAAGAGATTTGGTTACTGCAACATTGAAAAATAGAAGAAACAATTTGTTG
AAGTACTACCAAGTTCAAATCGATGAAATGTACAGAAAGTTAGCTTCTAAGAAA
ATTTGA

DNA sequence of *AtLACS*

ATGAAATCATTTGCTGCAAAAGTTGAAGAAGGTGTTAAAGGTATTGATGGTAAA
CCATCTGTTGGTCCAGTTTACAGAAATTTGTTGTCAGAAAAGGGTTTTCCACCAA
TTGATTCTGAAATTACTACAGCTTGGGATATTTTCTCTAAGTCAGTTGAAAAGTTC
CCAGATAATAATATGTTGGGTTGGAGAAGAATCGTTGATGAAAAGGTTGGTCCA
TACATGTGGAAGACTTACAAGGAAGTTTACGAAGAAGTTTTGCAAATTGGTTCAG
CATTAAGAGCTGCAGGTGCTGAACCAGGTTCTAGAGTTGGTATCTATGGTGTTAA
TTGTCCACAATGGATTATTGCTATGGAAGCATGTGCTGCACATACTTTGATCTGT
GTTCCATTGTACGATACATTAGGTTCTGGTGCAGTTGATTACATCGTTGAACATG
CTGAAATCGATTTCGTTTTCGTTCAAGATACAAAGATTAAAGGTTTGTTAGAACC
AGATTGTAAGTGTGCAAAGAGATTGAAGGCTATCGTTTCTTTTACTAACGTTTCT
GATGAATTGTCACATAAGGCATCTGAAATCGGTGTTAAGACATACTCTTGGATCG
ATTTCTTGCATATGGGTAGAGAAAAACCAGAAGATACTAATCCACCAAAGGCTT
TTAATATCTGTACAATCATGTACACTTCTGGTACATCAGGTGACCCAAAAGGTGT
TGTTTTGACTCATCAAGCTGTTGCAACATTCGTTGTTGGTATGGATTTGTACATGG
ATCAATTCGAAGATAAGATGACTCATGATGATGTTTACTTGTCATTTTTGCCATTG
GCACATATCTTGGATAGAATGAACGAAGAATATTTCTTTAGAAAGGGTGCTTCTG
TTGGTTACTACCATGGTAATTTGAACGTTTTGAGAGATGATATCCAAGAATTGAA
GCCAACATACTTAGCAGGTGTTCCAAGAGTTTTCGAAAGAATTCATGAAGGTATT
CAAAAGGCTTTGCAAGAATTGAACCCAAGAAGAAGATTCATTTTTAATGCATTGT
ACAAGCATAAGTTGGCTTGGTTGAATAGAGGTTACTCTCATTCAAAAGCTTCTCC
AATGGCAGATTTCATCGCTTTTAGAAAGATCCGTGATAAGTTAGGTGGTAGAATT
AGATTGTTAGTTTCAGGTGGTGCTCCATTGTCTCCAGAAATCGAAGAATTCTTGA
GAGTTACTTGTTGTTGTTTTGTTGTTCAAGGTTATGGTTTGACTGAAACATTAGGT
GGTACTGCATTGGGTTTTCCAGATGAAATGTGTATGTTAGGTACAGTTGGTATTC
CAGCTGTTTACAACGAAATCAGATTGGAAGAAGTTTCAGAAATGGGTTACGATC
CATTAGGTGAAAATCCAGCTGGTGAAATTTGTATCAGAGGTCAATGTATGTTCTC
TGGTTACTACAAGAACCCAGAATTGACTGAAGAAGTTATGAAAGATGGTTGGTTT
CATACAGGTGACATTGGTGAAATTTTGCCAAATGGTGTTTTGAAGATCATCGATA
GAAAGAAAAATTTGATTAAATTGTCACAGGGTGAATACGTTGCTTTGGAACATTT
GGAAAACATCTTCGGTCAAAACTCTGTTGTTCAAGATATCTGGGTTTACGGTGAC
TCTTTTAAATCAATGTTGGTTGCAGTTGTTGTTCCAAATCCAGAAACTGTTAATAG
ATGGGCTAAAGATTTGGGTTTTACAAAGCCATTCGAAGAATTGTGTTCATTTCCA
GAATTAAAGGAACATATCATCTCAGAATTGAAGTCTACAGCAGAAAAGAATAAG
TTGAGAAAGTTCGAATACATCAAGGCTGTTACTGTTGAAACAAAGCCATTCGATG
TTGAAAGAGATTTGGTTACTGCAACATTGAAAAATAGAAGAAACAATTTGTTGA
AGTACTACCAAGTTCAAATCGATGAAATGTACAGAAAGTTAGCTTCTAAGAAAA
TTTGA

DNA sequence of *cfa-gfp*

ATGTCAAAAGGTGAAGAATTGTTTACTGGTGTAGTTCCTATATTGGTCGAATTGG
ATGGTGACGTCAACGGTCATAAGTTTAGTGTCTCAGGTGAAGGTGAAGGTGACG
CTACTTACGGTAAATTGACATTAAAATTCATTTGTACAACTGGTAAATTGCCAGT
TCCATGGCCAACATTGGTTACAACTTTTGGTTACGGTGTTCAATGTTTTGCTAGAT
ACCCAGATCATATGAAACAACATGATTTCTTTAAATCTGCAATGCCAGAAGGTTA
TGTTCAAGAAAGAACTATTTTCTTTAAAGATGATGGTAATTATAAAACTAGAGCT
GAAGTTAAATTTGAAGGTGACACATTGGTTAATAGAATTGAATTGAAAGGTATTG
ATTTTAAAGAAGATGGTAATATTTTAGGTCATAAATTGGAATATAATTACAATTC
TCATAATGTTTACATTATGGCTGATAAACAAAAGAATGGTATTAAAGTTAATTTT
AAAATTAGACATAATATTGAAGATGGTTCTGTTCAATTAGCAGATCATTACCAAC
AAAATACACCAATTGGTGACGGTCCAGTTTTATTGCCAGATAATCATTACTTGTC
TACTCAATCAGCTTTGTCTAAAGATCCAAATGAAAAGAGAGATCATATGGTTTTA
TTGGAATTTGTTACTGCTGCAGGTATTACACATGGTATGGATGAATTGTATAAAG
GTGGTGGTGGTTCAGGTGGTGGTGGTTCTTCATCTTCTTGTATTGAAGAAGTTTCT
GTTCCAGATGATAATTGGTACAGAATTGCAAATGAATTATTGTCAAGAGCAGGTA
TTGCTATTAATGGTTCTGCACCAGCTGATATTAGAGTTAAAAATCCAGATTTCTTT
AAAAGAGTTTTGCAAGAAGGTTCATTAGGTTTGGGTGAATCATACATGGATGGTT
GGTGGGAATGTGATAGATTGGATATGTTTTTCTCTAAAGTTTTGAGAGCTGGTTT
GGAAAATCAATTACCACATCATTTTAAAGATACTTTGAGAATTGCAGGTGCTAGA
TTGTTTAATTTGCAATCTAAAAAGAGAGCTTGGATTGTTGGTAAAGAACATTACG
ATTTGGGTAATGATTTGTTTTCAAGAATGTTAGATCCATTCATGCAATACTCATGT
GCTTACTGGAAAGATGCTGATAATTTGGAATCAGCTCAACAAGCAAAATTAAAA
ATGATTTGTGAAAAATTGCAATTAAAACCAGGTATGAGAGTTTTGGATATTGGTT
GTGGTTGGGGTGGTTTAGCTCATTACATGGCTTCTAATTATGATGTTTCTGTTGTT
GGTGTTACTATTTCTGCTGAACAACAAAAGATGGCTCAAGAAAGATGTGAAGGT
TTGGATGTTACAATTTTATTGCAAGATTACAGAGATTTGAATGATCAATTTGATA
GAATTGTTTCTGTTGGTATGTTTGAACATGTTGGTCCAAAGAATTACGATACATA
CTTTGCTGTTGTTGATAGAAATTTGAAACCAGAAGGTATTTTCTTATTGCATACTA
TTGGTTCTAAAAAGACTGATTTGAATGTTGATCCATGGATTAATAAGTACATTTTT
CCAAATGGTTGTTTGCCATCAGTTAGACAAATTGCTCAATCTTCAGAACCACATT
TTGTTATGGAAGATTGGCATAATTTTGGTGCTGATTATGATACAACTTTGATGGCT
TGGTACGAAAGATTTTTGGCAGCTTGGCCAGAAATTGCTGATAATTATTCAGAAA
GATTCAAAAGAATGTTTACTTATTACTTGAATGCATGTGCTGGTGCTTTTAGAGCT
AGAGATATTCAATTATGGCAAGTTGTCTTTAGTAGAGGTGTAGAAAATGGTTTGA
GAGTAGCAAGATGA

DNA sequence of *aox*

ATGGCTATCCCCGAAGAGTTTGATATCCTAGTTCTAGGTGGTGGATCCAGTGGATCCTGT
ATTGCCGGAAGATTGGCAAACTTGGACCACTCCTTGAAAGTTGGTCTTATCGAAGCAGGT
GAGAACAACCTCAACAACCCATGGGTCTACCTTCCAGGTATTTACCCAAGAAACATGAA
GTTGGACTCCAAGACTGCTTCCTTCTACACTTCTAACCCATCTCCTCACTTGAATGGTAGA
AGAGCCATTGTTCCATGTGCTAACGTCTTGGGTGGTGGTTCTTCTATCAACTTCATGATGT
ACACCAGAGGTTCTGCTTCTGATTACGATGACTTCCAAGCCGAGGGCTGGAAAACCAAG
GACTTGCTTCCATTGATGAAAAAGACTGAGACCTACCAAAGAGCTTGCAACAACCCTGA
CATTCACGGTTTCGAAGGTCCAATCAAGGTTTCTTTCGGTAACTACACCTACCCAGTTTGC
CAGGACTTCTTGAGGGCTTCTGAGTCCCAAGGTATTCCATACGTTGACGACTTGGAAGAC

TTGGTTACTGCTCACGGTGCTGAACACTGGTTGAAGTGGATCAACAGAGACACTGGTCGT
CGTTCCGACTCTGCTCATGCATTTGTCCACTCTACTATGAGAAACCACGACAACTTGTACT
TGATCTGTAACACGAAGGTCGACAAAATTATTGTCGAAGACGGAAGAGCTGCTGCTGTT
AGAACCGTTCCAAGCAAGCCTTTGAACCCAAAGAAGCCAAGTCACAAGATCTACCGTGC
TAGAAAGCAAATCGTTTTGTCTTGTGGTACCATCTCCTCTCCATTGGTTTTGCAAAGATCC
GGTTTTGGTGACCCAATCAAGTTGAGAGCCGCTGGTGTTAAGCCTTTGGTCAACTTGCCA
GGTGTCGGAAGAAACTTCCAAGACCACTACTGTTTCTTCAGTCCTTACAGAATCAAGCCT
CAGTACGAGTCTTTCGATGACTTCGTCCGTGGTGATGCTGAGATTCAAAAGAGAGTCTTT
GACCAATGGTACGCCAATGGTACTGGTCCTCTTGCCACTAACGGTATCGAAGCTGGTGTC
AAGATCAGACCAACACCAGAAGAACTCTCTCAAATGGACGAATCCTTCCAGGAGGGTTA
CAGAGAATACTTCGAAGACAAGCCAGACAAGCCAGTTATGCACTACTCCATCATTGCTG
GTTTCTTCGGTGACCACACCAAGATTCCTCCTGGAAAGTACATGACTATGTTCCACTTCTT
GGAATACCCATTCTCCAGAGGTTCCATTCACATTACCTCCCCAGACCCATACGCAGCTCC
AGACTTCGACCCAGGTTTCATGAACGATGAAAGAGACATGGCTCCTATGGTTTGGGCTTA
CAAGAAGTCTAGAGAAACCGCTAGAAGAATGGACCACTTTGCCGGTGAGGTCACTTCTC
ACCACCCTCTGTTCCCATACTCATCCGAGGCCAGAGCCTTGGAAATGGATTTGGAGACCT
CTAATGCCTACGGTGGACCTTTGAACTTGTCTGCTGGTCTTGCTCACGGTTCTTGGACTCA
ACCTTTGAAGAAGCCAACTGCAAAGAACGAAGGCCACGTTACTTCGAACCAGGTCGAGC
TTCATCCAGACATCGAGTACGATGAGGAGGATGACAAGGCCATTGAGAACTACATTCGT
GAGCACACTGAGACCACATGGCACTGTCTGGGAACCTGTTCCATCGGTCCAAGAGAAGG
TTCCAAGATCGTCAAATGGGGTGGTGTTTTGGACCACAGATCCAACGTTTACGGAGTCAA
GGGCTTGAAGGTTGGTGACTTGTCCGTGTGCCCAGACAATGTTGGTTGTAACACCTACAC
CACCGCTCTTTTGATCGGTGAAAAGACTGCCACTTTGGTTGGAGAAGATTTAGGATACTC
TGGTGAGGCCTTAGACATGACTGTTCCTCAGTTCAAGTTGGGCACTTACGAGAAGACCGG
TCTTGCTAGATTCTAA

DNA sequence of *das*

ATGGCTAGAATTCCAAAAGCAGTATCGACACAAGATGACATTCATGAATTGGTCATCAA
AACCTTCCGTTGTTACGTTCTCGACTTAGTCGAACAGTATGGTGGTGGTCACCCTGGTTCT
GCCATGGGTATGGTCGCCATTGGTATCGCTCTGTGGAAGTACCAGATGAAGTACGCTCCA
AATGATCCAGACTACTTCAACAGAGATCGTTTTGTCTTGTCAAACGGTCACGTCTGTCTG
TTCCAATACTTGTTCCAGCACTTAACTGGTTTGAAGGAGATGACTGTCAAGCAACTTCAA
TCTTACCACTCTTCCGATTATCACTCATTGACTCCTGGACACCCTGAAATTGAGAACCCTG
CTGTTGAGGTTACCACTGGTCCCCTGGGACAAGGTATCTCTAACGCTGTCGGTATGGCCA
TTGGTTCAAAGAACCTGGCCGCTACTTACAACAGACCTGGCTTCCCTGTCGTTGACAACA
CTATCTATGCTATTGTTGGTGATGCTTGTTTGCAAGAGGGACCTGCTTTGGAATCGATTTC
CTTAGCCGGTCACTTGGCCTTGGACAACCTTATTGTGATCTACGACAACAACCAGGTTTG
TTGTGATGGTTCCGTCGATGTTAACAACACCGAAGACATCTCCGCAAAGTTCAGAGCTCA
GAACTGGAATGTTATCGACATTGTAGACGGTTCTAGAGATGTCGCTACCATTGTCAAGGC
TATCGATTGGGCCAAGGCTGAGACTGAGAGACCAACTCTGATCAACGTTAGAACTGAAA
TTGGACAGGATTCTGCTTTCGGTAACCACCACGCTGCTCACGGTTCTGCTCTAGGTGAGG
AAGGTATCCGGGAGTTGAAGACTAAGTACGGTTTTAACCCTGCCCAAAAGTTCTGGTTCC
CTAAAGAAGTATACGACTTCTTTGCTGAGAAACCAGCTAAAGGTGACGAGTTAGTAAAG
AACTGGAAAAAGTTAGTTGATAGCTATGTCAAAGAGTACCCTCGTGAGGGACAAGAGTT
CCTTTCTCGTGTTAGAGGTGAGCTTCCAAAGAACTGGAGAACTTACATTCCTCAAGACAA
GCCTACCGAACCAACCGCCACCAGAACCTCTGCTAGAGAAATTGTTAGGGCCCTTGGAA
AGAACCTTCCTCAAGTTATTGCCGGTTCCGGTGACTTATCTGTCTCAATTCTTTTGAACTG
GGACGGAGTGAAGTACTTCTTCAACCCTAAGTTACAGACTTTCTGTGGATTAGGTGGTGA
CTACTCTGGTAGATATATTGAGTTTGGTATCAGAGAACACTCTATGTGTGCTATTGCCAA

CGGTTTGGCTGCATACAACAAGGGTACTTTCTTGCCTATTACCTCTACCTTCTACATGTTC
TACCTGTATGCAGCACCTGCCTTGCGTATGGCTGCTCTTCAAGAGTTGAAAGCGATTCAC
ATTGCTACACACGACTCTATTGGAGCTGGTGAAGATGGTCCAACCCACCAGCCTATTGCT
TTGTCTTCATTATTCAGAGCTATGCCCAACTTCTACTACATGAGACCAGCCGATGCTACC
GAAGTTGCAGCTCTGTTTGAAGTGGCTGTTGAGCTTGAACACTCCACATTGCTTTCTCTGT
CCAGACACGAGGTTGACCAATACCCAGGTAAGACTTCTGCCCAAGGAGCCAAAAGAGGT
GGTTACGTTGTTGAAGACTGCGAAGGAAAGCCAGATGTGCAACTGATCGGAACTGGTTC
CGAGTTGGAATTCGCTATTAAGACTGCTCGTTTGCTAAGACAACAGAAGGGATGGAAGG
TCAGAGTTCTGTCATTCCCATGTCAGAGATTGTTTGACGAGCAGTCTATTACTTACAGAC
GTTCCGTCCTTAGAAGAGGAGAAGTTCCAACTGTCGTTGTTGAGGCCTATGTCGCATACG
GATGGGAGAGATACGCCACTGCTGGTTACACCATGAACACCTTCGGTAAGTCTCTTCCTG
TTGAGGATGTCTACAAATACTTCGGATACACTCCTGAGAAGATTGGTGAGAGAGTGGTTC
AATATGTCAACTCTATCAAGGCTAGTCCTCAAATCCTTTACGAATTCCACGACTTGAAGG
GAAAACCAAAGCATGACAAGTTGTAA

DNA sequence of *cat*

ATGTCTGGAAAACGAGTCCCCACTTACACCACCACTAACGGTAACCCCGTCAAGGACCC
CCTCGCCTCCCAGCGAATCGGCAAGCACGGACCTCTCCTGCTCCAGGACTTTGCCCTGAT
CGACCTGCTCGCCCACTTCGACCGAGAGCGAATCCCCGAGCGAGTTGTCCACGCTAAGG
GATCCGGTGCTTACGGAGAGTTCGAGGTCACTGACGATATCACCGACCTCAACTGCGCCG
ATTTCTTGTCCAAGATCGGTAAGAAGACCAAGACCTTCACTCGATTCTCCACCGTTGGAG
GAGAGAAGGGATCCGCCGATGCTGCTCGAGACCCCCGAGGTTTCGCCACCAAGTTCTAC
ACCGACGAGGGAAACATTGACTGGGTCTACAACAACACCCCCGTCTTTTTCATCAGAGAC
CCCTCCAAGTTCCCCGTTTTCATCCACACTCAGAAGCGAAACCCCGAGACCAACCTCAAG
GACGCCACTATGATGTGGGACTACATTGCCAACAACCAGGAGTGTTGCCACCAGATCAT
GGTCCTCTTCTCCGACCGAGGTACTCCCGCTAACTACCGACAGATGAACGGTTACTCCGG
CCACACCTACAAGTGGATCAAGAAGGATGGCTCTTTCAACTACGTCCAGATCCACATGA
AGACCGACCAGGGCATCAAGAACCTCACCAATGACGAGGCTGTCGCTCTCTCCGGAACC
AACCCCGACCACGCCCAGGAAGACCTCTTCAACTCCATCAAGAGTGGCTCTTTCCCCTCT
TGGACTTGTTACGTCCAGGTCTGCACCCCCGAGCAGGCTGAGAAGCTCAAGTGGTCCGTC
TTTGACCTCACCAAGGTCTGGCCTCACGACCAGTTCCCTCTCAGACGATTCGGTAAGCTC
ACTCTTAACAAGAACGTCCAGAACTACTTCGCTGAGACCGAGCAGGCTGCCTTCTCTCCC
TCCAACACCGTCCCCGGCTGGGAGACCTCGGCCGATCCCGTCCTGCAGTCTCGACTCTTC
TCTTATCCCGATACTCAGCGACACCGACTCGGTACCAACTTCGCCCAGATCCCCGTCAAC
TGTCCCTACCATGCCCATACTCCTTACCACCGAGATGGTCAGATGGCTGTTAACGGCAAC
TCCGGCTCTCTGCCCAACTACCCCTCTTCTTTCGAGCCCCTGCAGTACCGACAGGACATC
AACCTGCATGAGAAGCACGAGAAGTGGGTTGGTGAGGCCGTCGCCTACCAGTGGGTTGT
CGGCACCGACGGTGTTGACTTCCAGCAGCCCGCTGAGCTCTGGAAGGTTCTTGGAAAGA
CCCCAGACCAGCAGGAACACCTTGTTTACAACATCGCTGTCTCTCTGTCCGGTGCTCGAC
CCGAGGTCCAGGACAAGACCTTTGGCATGTTCGACAAGGTCGATGCTCACTTCGGTAAGC
TCGTCCGAGACGCTACTCTTCAGCGATCTCCTCGATCCAAGCTTTAA

DNA sequence of *mdh*

ATGACAACAAACTTTTTCATTCCACCAGCCAGCGTAATTGGACGCGGTGCAGTAAAGGA
AGTAGGAACAAGACTTAAGCAAATTGGAGCTAAGAAAGCGCTTATCGTTACAGATGCAT
TCCTTCACAGCACAGGTTTATCTGAAGAAGTTGCTAAAAACATTCGTGAAGCTGGCGTTG
ATGTTGCGATTTTCCCAAAAGCTCAACCAGATCCAGCAGATACACAAGTTCATGAAGGTG

TAGATGTATTCAAACAAGAAAACTGTGATTCACTTGTTTCTATCGGTGGAGGTAGCTCTC
ACGATACAGCTAAAGCAATCGGTTTAGTTGCAGCAAACGGCGGAAGAATCAATGACTAT
CAAGGTGTAAACAGCGTAGAAAAACCAGTCGTTCCAGTAGTTGCAATCACTACAACAGC
TGGTACTGGTAGTGAAACAACATCTCTTGCGGTTATTACAGACTCTGCACGTAAAGTAAA
AATGCCTGTTATTGATGAGAAAATTACTCCAACTGTAGCAATTGTTGACCCAGAATTAAT
GGTGAAAAAACCAGCTGGATTAACAATCGCAACTGGTATGGATGCATTGTCCCATGCAA
TTGAAGCATATGTTGCAAAAGGTGCTACACCAGTTACTGATGCATTTGCTATTCAAGCAA
TGAAACTTATCAATGAATACTTACCAAAAGCGGTTGCGAACGGAGAAGACATCGAAGCA
CGTGAAAAAATGGCTTATGCACAATACATGGCAGGAGTGGCATTTAACAACGGTGGTTT
AGGACTAGTTCACTCTATTTCTCACCAAGTAGGTGGAGTTTACAAATTACAACACGGAAT
CTGTAACTCAGTTAATATGCCACACGTTTGCGCATTCAACCTAATTGCTAAAACTGAGCG
CTTCGCACACATTGCTGAGCTTTTAGGTGAGAATGTTGCTGGCTTAAGCACTGCAGCAGC
TGCTGAGAGAGCAATTGTAGCTCTTGAAAGAATCAACAAATCCTTCGGTATCCCATCTGG
CTATGCAGAAATGGGCGTGAAAGAAGAGGATATCGAATTATTAGCGAAAAACGCATACG
AAGACGTATGTACTCAAAGCAACCCACGCGTTCCTACTGTTCAAGACATTGCACAAATCA
TCAAAAACGCTATGTAA

DNA sequence of *hps*

ATGCAACTACAATTAGCTCTAGATTTGGTAAACATCGAAGAAGCAAAGCAAGTAGTAAG
TGAGGTACAGGAGTATGTCGATATCGTGGAAATCGGAACTCCGGTTATTAAAATTTGGG
GTCTTCAAGCTGTAAAAGCGGTTAAAGACGCATTCCCTCATTTACAAGTTTTAGCTGACA
TGAAAACTATGGATGCTGCAGCATATGAAGTTGCTAAAGCAGCTGAGCATGGCGCTGAT
ATCGTAACAATTCTTGCAGCAGCTGAAGATGTATCAATTAAAGGTGCTGTAGAAGAAGC
GAAAAAACTTGGCAAAAAAATCCTTGTTGACATGATCGCAATTAAAAACCTAGAAGAGC
GTGCAAAACAAGTGGATGAAATGGGCGTAGACTACATTTGCGTGCACGCTGGATACGAT
CTTCAAGCAGTAGGTAAAAACCCTCTAGAAGATCTTAAGAGAATTAAAGCTGTCGTGAA
AAATGCAAAAACTGCTATTGCAGGCGGAATCAAATTAGAAACATTACCTGAAGTTATCA
AAGCAGAACCGGATCTTGTCATTGTTGGCGGCGGTATTGCTAACCAAACTGATAAAAAA
GCAGCAGCTGAAAAAATTAATAAATTAGTTAAACAAGGGTTATGA

DNA sequence of *phi*

ATGCTGACAACTGAATTTTTAGCTGAAATTGTAAAAGAATTAAATAGTTCGGTTAACCAA
ATCGCCGATGAAGAAGCCGAAGCACTGGTTAACGGAATCCTTCAATCAAAGAAAGTTTT
TGTAGCCGGTGCAGGAAGATCCGGTTTTATGGCTAAATCCTTCGCAATGCGAATGATGCA
CATGGGTATTGATGCCTATGTCGTTGGCGAAACCGTAACACCTAACTATGAAAAAGAAG
ACATCTTAATCATTGGATCCGGCTCAGGAGAAACAAAAAGTCTCGTTTCCATGGCTCAAA
AAGCAAAAAGCATTGGCGGAACCATCGCGGCTGTAACGATCAACCCTGAATCAACAATT
GGGCAATTAGCGGATATCGTTATTAAAATGCCAGGTTCGCCTAAAGATAAATCAGAAGC
TAGAGAAACCATCCAACCAATGGGATCTCTTTTTGAACAAACCTTATTATTGTTCTATGA
TGCTGTCATTTTGAGATTCATGGAGAAAAAGGGCTTGGATACAAAAACAATGTACGGAA
GACATGCCAATCTCGAGTAG

DNA sequence of *rki1-2*

ATGTCCTCCGAACTGCCTCCTCTTGAGCAGGCCAAGCGAATCGCCGCCCACCAGGCCGTG
GAGCAACACTACCCCAAGGACGCCAAGGTCGTGGGCATTGGCTCAGGATCCACCGTGGT
CTACGTTGCCGAGAAGATTGCGTCGTTGCCCAAGGAGCTCACCAAGGACACCGTGTTCAT
TTCTACGGGTTTCCAGAGCAAGCAGCTGATCCAGAACGCCGGGTTGCGACTGGGATGCA

TCGACCAGTACTCCAACGGAGATCTGGACGTGGCGTTTGACGGCGCCGACGAGACCGAC
CCTCAGCTCAACTGCATCAAGGGCGGAGGAGCATGCCTCTTCCAGGAAAAGATTGTCGC
CGAGTGTGCCCGCAAGTTTGTCGTGGTGGCCGACTACCGAAAACAGTCCAAGGCTCTGG
GCACCGTGTGGATCCAGGGTATCCCCATTGAGGTGGTGCCCGACGCCTACAACAAGGTA
ATTGCTGATCTCAAGAAGATGGGCGCCCAGTCCGCGGTGCTGCGACCCGGCTCTCCCGGA
AAGGCGGGCCCCATCATCACCGACAATGGCAACTTCATTGTCGACGCCTACTTTGGCGAG
ATCCAACCCGACGCCGTCAAGGACCTGCACATCAAGATCAAGCTGCTGTTGGGCGTCGTT
GAGACCGGCCTCTTCACTAACGCGGACGTAGCGTACTTTGGAAACGCCGACGGAACCAT
CTCCACCATTACCAAGTAA

DNA sequence of *shb1*

*7*ATGGCCCCTCGAGTTATCTTTGTACGACACGGCGAGACCGAATGGTCAAAGTCCGGCCA
ACACACGTCGGTGACTGATCTGCCATTGACTGAGAACGGAGTCAAGCGAGTGCGAGCGA
CGGGACGGGCGCTGGTGGGCCGAAACCGGCTGGTGAACCCGGCGTACGTGGAGCACATT
TTTGTTTCGCCCCGATCTCGTGCCCAGCAGACGCTCAAGCTCTTTTTTGAGGACGAGCCC
GAGGCTCTCGCCAAGATCCCCCAGACCGTGACCGAAGACATTCGAGAGTGGGACTACGG
CAAGTACGAGGGCCGAAAGTCAGCCGAAATCCGGGCCGACCGAACCGCGCGAGGCATC
GACAAGGACGGCCACAAGTGGAACATTTGGTCCGACGGCTGCGAGGACGGAGAGTCGCC
CCAACAGGTGCAGAAGCGAGTGGACGAGCTCATCAAGGAGATCCGGGTGATCCACAAG
AAGGCGCTCGACGAGGGCAAGGAGCATTGCGACGTCATGGTGTTCGCACACGGCCACAT
CCTGCGAGTCTTTGCTCTGCGATGGGTCAACGGAGACATCACCATCAACCCGGCTCTGAT
TCTCGAGGCAGGAGGAGTCGGTGTGCTGTCTTACGAGCATAACAACATTGAGGAGCCAG
CCATTTACCTGGGAGGAGCCTTCTTTGTGCCCGACGAGGATGTGGAGAAGAACAGCGGA
GTCATTGCGCTGGCTGGGGGAGAGCAGAACTAG

DNA sequence of *dak*

ATGACCACTAAACAGTTCCAATTCGACTCGGATCCGCTCAATTCTGCCCTTGCCGCCACC
GCGGAGGCCTCAGGCCTCGCTTACCTCCCCAAGAGCAAGGTCATCTACTACCCTCTGACC
AACGACAAGGTGACGTTGATTTCAGGTGGAGGAGCTGGCCACGAGCCTGCTCAGACCGG
GTTTGTGGGTCCCGGACTGCTGGATGCGGCCGTGTCGGGCCAGATCTTTGCCTCACCTTC
CACCAAACAGATCATTGCCGGAGTCAATGCCGTCAAGTCGCAACGGGGCTCCATCATTAT
CGTCATGAACTACACTGGCGATGTGATCCACTTTGGAATGGCCGCCGAGCAGCTGCGGTC
CCGATATGACTACCACGCCGAACTGGTGTCCATTGGCGACGACATTTCCGTCAACAAGAA
GGCCGGACGACGAGGTCTGGCAGGAACCGTTCTTGTTCACAAGATCGCAGGCCATCTTG
CCCGAGATGGCTGGGACGTCGGAGTGCTTGCTGAAGCTCTGCGAACCACCGCCGCCAAC
CTGGCCACCGTGGCTGCGTCTCTGGAACACTGCACTGTACCTGGCAGAAAGTTCGAGACC
GAACTGGCGGCCGATGAGATGGAGATTGGCATGGGTATCCACAACGAGCCCGGTGTCAA
GACCATCAAGATTGGCAAGGTTGAGTCTCTGCTGGACGAATTGGTCGACAAGTTCGAGC
CCTCCAAGCAGGACTTTGTGCCCTTCAACAAGGGCGACGAGGTGGTGCTGCTGGTCAATT
CCCTCGGAGGAGTCTCTTCTCTGGAACTCCACGCCATTGCCAACATTGCCCAGACAAAGT
TCGAGAAGGTGCTGGGCGTCAAGACCGTGCGACTTATTGTTGGCAACTTCATGGCTGCCT
TCAACGGTCCTGGCTTCTCTTTGACTCTGCTCAACGTCACCACGACCGCCAAGAAGGGCA
ACTTTGACGTTCTGGGAGCCCTGGACGCTCCCGTGTCCACCGCCGCCTGGCCCTCTCTGC
AGCAGAAGGACAAGCCTGCCAACGGCGGTGTCCAGGAGGAGAAGGAGACCGACTCGGA
CAAGCCTGCTGAGCCTACTGGAATCAAGGCCGACGGAAAGCTGTTCAAGGCCATGATTG
AGAGTGCTGTTGACGATCTCAAGAAGGAGGAGCCCCAGATTACCAAATACGACACTATT
GCTGGCGATGGAGACTGTGGAGAGACTCTGTTGGCTGGAGGCGACGGTATTCTGGACGC

TATCAAGAACAAGAAGATTGACCTTGATGATGCCGCTGGAGTGGCTGATATTTCTCACAT
CGTCGAGAACTCCATGGGAGGCACCTCGGGAGGTCTCTACTCCATCTTCTTCTCCGGTCT
CGTGGTCGGTATCAAGGAGACCAAGGCCAAGGAGCTGTCTGTCGATGTGTTTGCCAAGG
CATGTGAGACTGCTCTGGAGACTCTTTCTAAGTACACCCAGGCCCGAGTCGGCGACCGAA
CCCTCATGGACGCACTTGTTCCCTTTGTAGAGACCCTCAGCAAGACCAAGGACTTCGCCA
AGGCCGTAGAGGCTGCTCGGAAGGGCGCCGACGAGACTTCCAAGCTGCCTGCCAATTTT
GGCCGTGCCTCGTATGTGAACGAGGAGGGATTGGAGAACATTCCTGACCCTGGAGCTCTT
GGACTGGCCGTCATTTTCGAAGGTCTTCTCAAGGCCTGGGAGAAGAAGTAG

DNA sequence of *fbp*

ATGGAAGCCAACCCCGAAGTCCAGACCGATATCATCACGCTGACCCGGTTCATTCTGCAG
GAACAGAACAAGGTGGGCGCGTCGTCCGCAATCCCCACCGGAGACTTCACTCTGCTGCT
CAACTCGCTGCAGTTTGCCTTCAAGTTCATTGCCCACAACATCCGACGATCGACCCTGGT
CAACCTGATTGGCCTGTCGGGAACCGCCAACTCCACCGGCGACGACCAGAAGAAGCTGG
ACGTGATCGGAGACGAGATCTTCATCAACGCCATGAAGGCCTCCGGTAAGGTCAAGCTG
GTGGTGTCCGAGGAGCAGGAGGACCTCATTGTGTTTGAGGGCGACGGCCGATACGCCGT
GGTCTGCGACCCCATCGACGGATCCTCCAACCTCGACGCCGGCGTCTCCGTCGGCACCAT
TTTCGGCGTCTACAAGCTCCCCGAGGGCTCCTCCGGATCCATCAAGGACGTGCTCCGACC
CGGAAAGGAGATGGTTGCCGCCGGCTACACCATGTACGGTGCCTCCGCCAACCTGGTGC
TGTCCACCGGAAACGGCTGCAACGGCTTCACTCTCGATGACCCTCTGGGAGAGTTCATCC
TGACCCACCCCGATCTCAAGCTCCCCGATCTGCGATCCATCTACTCCGTCAACGAGGGTA
ACTCCTCCCTGTGGTCCGACAACGTCAAGGACTACTTCAAGGCCCTCAAGTTCCCCGAGG
ACGGCTCCAAGCCCTACTCGGCCCGATACATTGGCTCCATGGTCGCCGACGTGCACCGAA
CCATTCTCTACGGAGGTATGTTTGCCTACCCCGCCGACTCCAAGTCCAAGAAGGGCAAGC
TCCGACTTTTGTACGAGGGTTTCCCCATGGCCTACATCATTGAGCAGGCCGGCGGTCTTG
CCATCAACGACAACGGCGAGCGAATCCTCGATCTGGTCCCCACCGAGATCCACGAGCGA
TCCGGCGTCTGGCTGGGCTCCAAGGGCGAGATTGAGAAGGCCAAGAAGTACCTTCTGAA
ATGA

DNA sequence of *fba1-2*

ATGCCTGTTACTGACGTCCTTAAGCGAAAGTCCGGTGTCATCGTCGGCGACGATGTCCGA
GCCGTGAGTATCCACGACAAGATCAGTGTCGAGACGACGCGTTTTGTGTAATGACACAA
TCCGAAAGTCGCTAGCAACACACACTCTCTACACAAACTAACCCAGCTCTTCGAGTACGC
CCGAGAGCACAAGTTCGCCCTCCCCGCCGTCAACGTGACCTCTTCGTCCACCGTTGTCGC
CGTTCTTGAGTCTGCCCGAGCCAACAAGTCCCCCGTCATCATCCAGATGTCCCAGGGTGG
CGCTGCCTACTTTGCTGGCAAGGGTGTCGACAACAAGGATCAGACCGCCTCCATCCAGG
GAGCCATTGCCGCTGCCCAGTTCATCCGAACCATTGCTCCCGTTTACGGCATTCCCGTCAT
CGTCCACACCGACCACTGTGCCCGAAAGCTGCTCCCCTGGCTCGACGGTATGCTCGACGC
CGATGAGGAGTACTTCAAGACTCACGGTGAGCCCCTCTTCTCTTCACACATGGTGGATCT
CTCCGAGGAGGAGCACCCCGAGAACATCGCCACCACCGCCGAGTACTTCAAGCGAGCCG
CCAAGATGAACCAGTGGCTCGAGATGGAGATTGGTGTCACCGGAGGTGAGGAGGATGGT
GTTGACAACACTGGTGTCGACAACTCCAAGCTCTACACCCAGCCCGAGGACATTTACGCC
GTCTACTCCGCCCTCGCTCCCATCTCCCCCAACTTCTCCATTGCCGCTGCCTTCGGTAACG
TGCACGGTGTCTACAAGGTCGGCAACGTCAAGCTGCACCCCGAGCTCCTCGAGAAGCAC
CAGGCTTACTCCGCCGAGAAGGTTGGCTCTCCCGAGAAGCACGGCAACGGAAAGCCTCT
CTTCCTCGTCTTCCACGGTGGATCCGGTTCTTCCGACTCCGACTACAAGATTGCCATTGAT
AACGGTGTTGTCAAGGTCAACCTCGATACTGATCTGCAGTACGCTTACCTTGTTGGTATC

AGAGACTACATTCTCTCCAAGAAGGACTACCTCATGCAGCAGGTCGGCAACCCCGAGGG
TGATGACAAGCCCAACAAGAAGTACTTCGACCCCCGTGTCTGGGTCCGAGAGGGTGAGA
AGACCATGGCCAAGCGACTCGACTCTGCCTTTGAGGTTTTCAACGCCAAGAACACCTTGT
AA